Solid-State Nuclear Magnetic Resonance of glasses: from basics to more advanced concepts

Dominique Massiot, Pierre Florian

CEMHTI-CNRS UPR3079 Orléans

http://www.cemhti.cnrs-orleans.fr/?nom=massiot

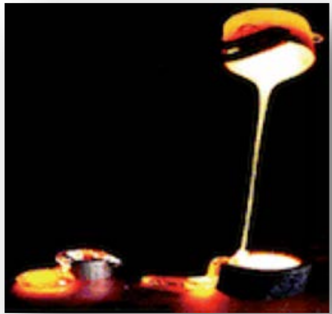
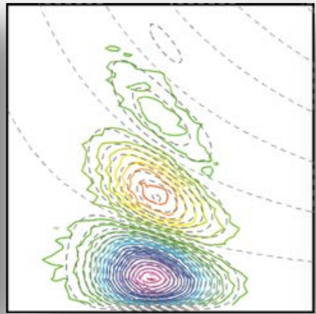
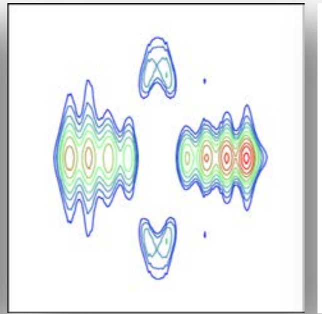
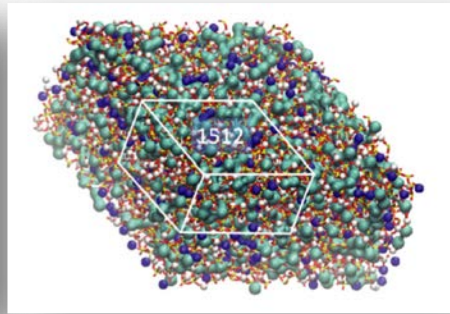

FIT DmFit

Google *dmfit nmr*

IR THC RMN

RESEARCH INFRASTRUCTURE

Magnetic Nuclear Resonance, Very High Fields

FR3050 CNRS

IR THC RMN

RESEARCH INFRASTRUCTURE
Magnetic Nuclear Resonance, Very High Fields
FR3050 CNRS

Since 2008 France has established a national network of flagship NMR facilities providing High-Resolution and High-Field capabilities, making available the latest cutting edge developments to a broad community of national and international users.

From 750 to 1000 MHz
1.2GHz to come 2020
Liquid & Solid State
Cryo-probes
Fast and ultra-fast MAS
DNP @800MHz
High & very High temperature

Open to national and international users upon proposals – constantly open on web

http://www.ir-rmn.fr/

Amorphous materials: Order within disorder

Philip S. Salmon

Nature Material **1**, 87 - 88 (2002)
doi:10.1038/nmat737

Geometrical & Chemical Order

Chemical order / Geometrical disorder

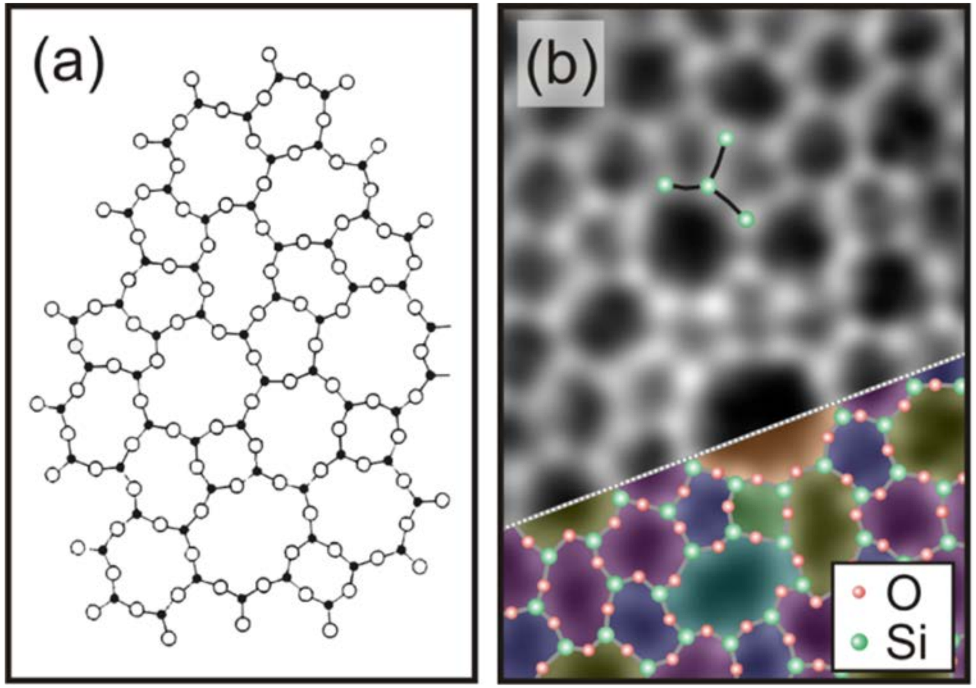

THE JOURNAL OF PHYSICAL CHEMISTRY C
Article
pubs.acs.org/JPCC

Atomic Arrangement in Two-Dimensional Silica: From Crystalline to Vitreous Structures

Leonid Lichtenstein, Markus Heyde,* and Hans-Joachim Freund

NANO LETTERS
Letter
pubs.acs.org/NanoLett

Direct Imaging of a Two-Dimensional Silica Glass on Graphene

Pinshane Y. Huang,[†,■] Simon Kurasch,[‡,■] Anchal Srivastava,[§,○] Viera Skakalova,[§,∥] Jani Kotakoski,[∥,⊥] Arkady V. Krasheninnikov,[⊥,¶] Robert Hovden,[†] Qingyun Mao,[†] Jannik C. Meyer,[‡,∥] Jurgen Smet,[§] David A. Muller,[*,†,□] and Ute Kaiser[*,‡]

Geometrical order / Chemical disorder

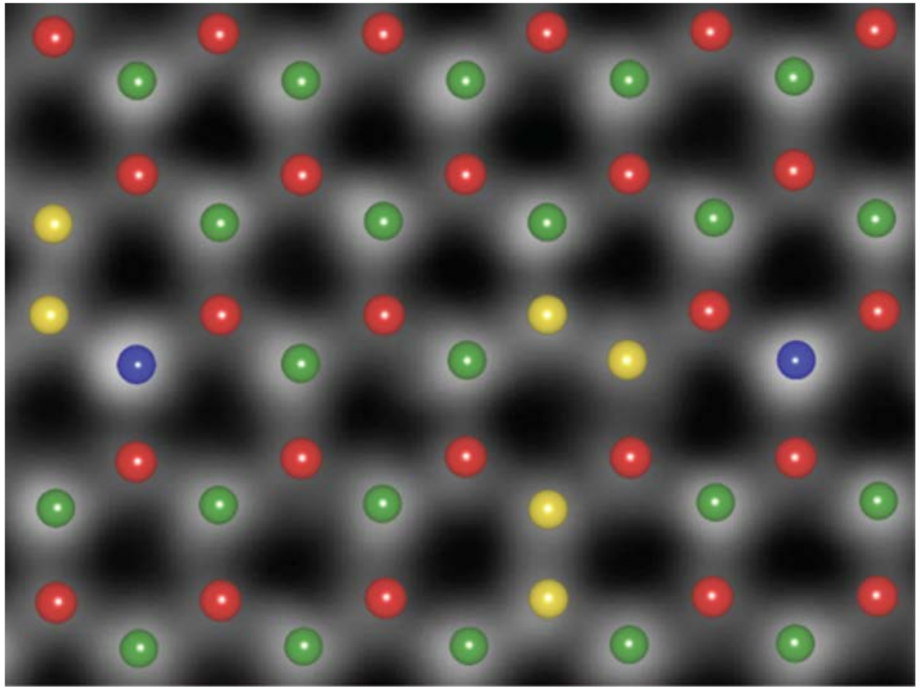

Vol 464 | 25 March 2010 | doi:10.1038/nature08879
nature
nature
LETTERS

Atom-by-atom structural and chemical analysis by annular dark-field electron microscopy

Ondrej L. Krivanek[1], Matthew F. Chisholm[2], Valeria Nicolosi[3], Timothy J. Pennycook[2,4], George J. Corbin[1], Niklas Dellby[1], Matthew F. Murfitt[1], Christopher S. Own[1], Zoltan S. Szilagyi[1], Mark P. Oxley[2,4], Sokrates T. Pantelides[2,4] & Stephen J. Pennycook[2,4]

Geometrical & Chemical Order

Chemical order

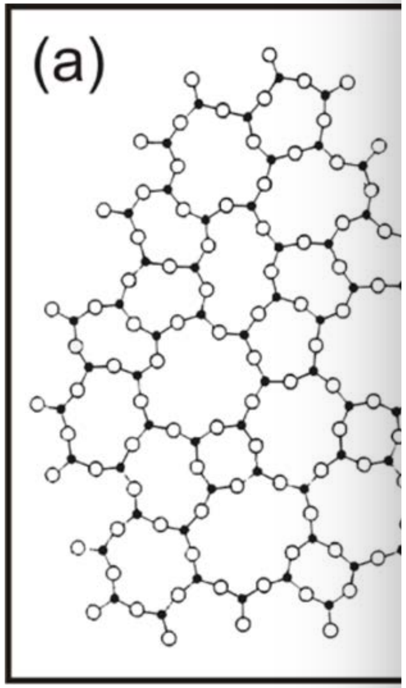

THE JOURNAL OF PHYSICAL CHEMISTRY C

Atomic Arrangement in Tw
Vitreous Structures

Leonid Lichtenstein, Markus Heyde,* an

NANO LETTERS

Direct Imaging of a Two-D

Pinshane Y. Huang, Simon Kurasch, Arkady V. Krasheninnikov, Robert Hc David A. Muller, and Ute Kaiser

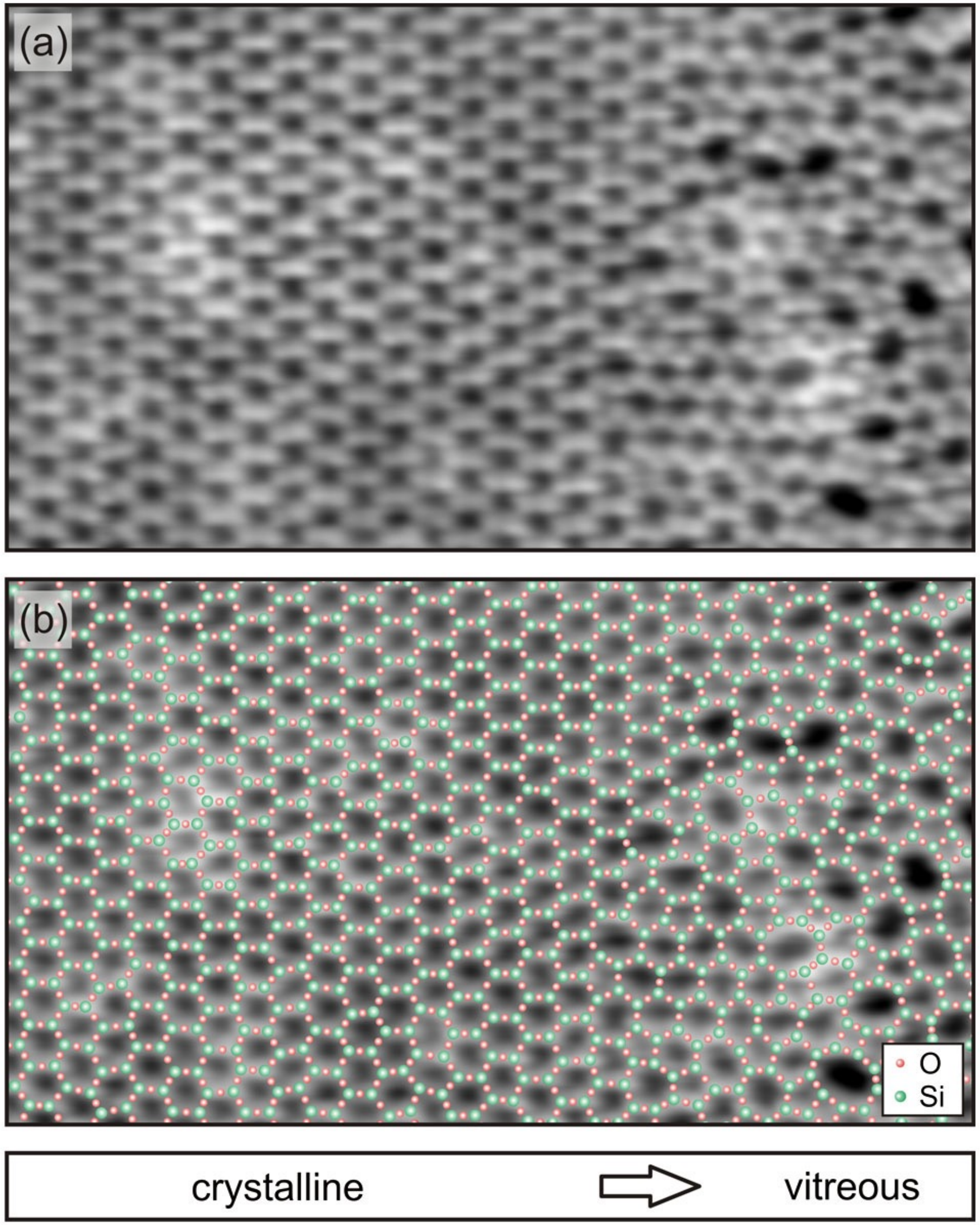

Chemical disorder

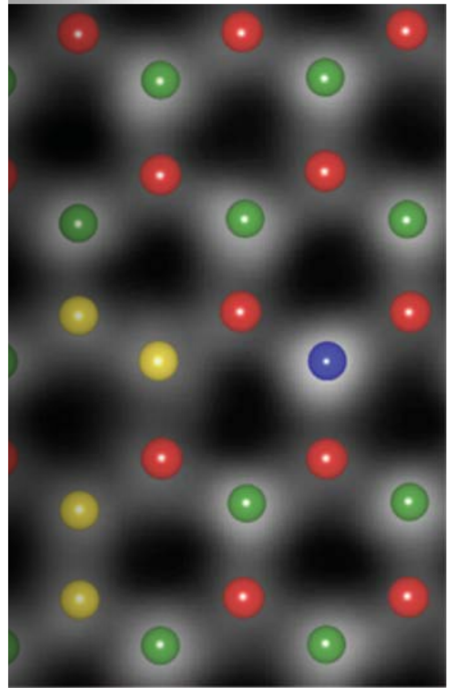

nature

LETTERS

nd chemical analysis by
microscopy

si[3], Timothy J. Pennycook[2,4], George J. Corbin[1], Zoltan S. Szilagyi[1], Mark P. Oxley[2,4],

Materials structure at different scales

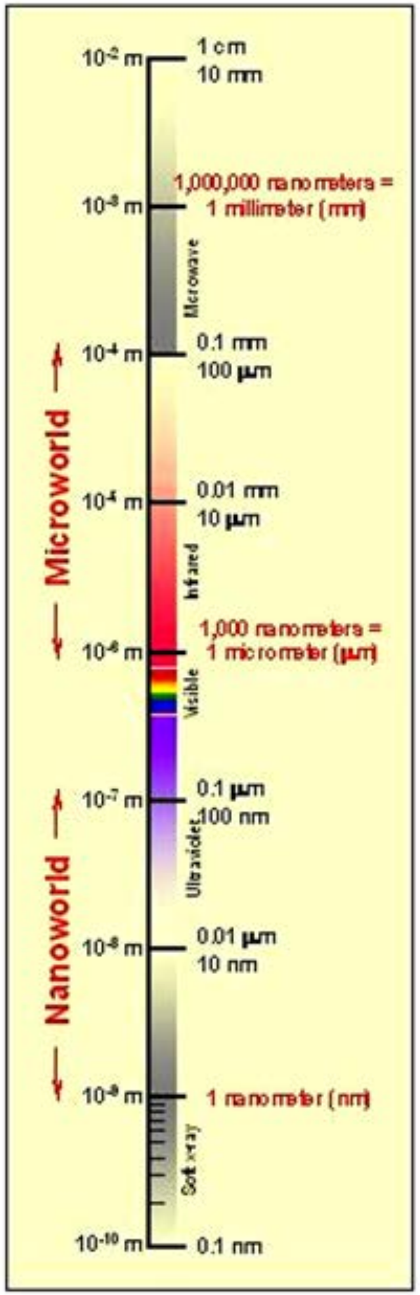

Diffraction X-Rays Neutrons e⁻

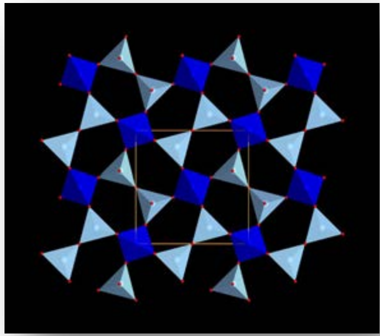

Order

Disorder

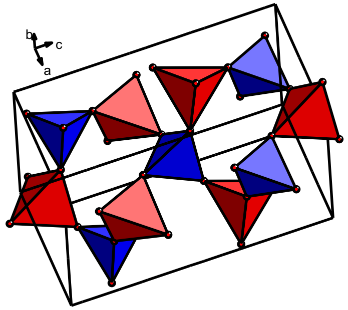

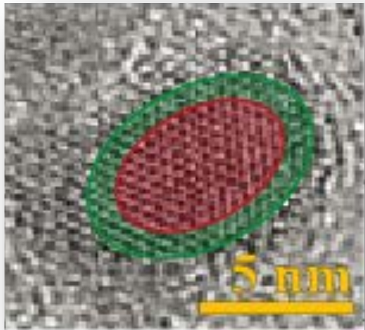

nm

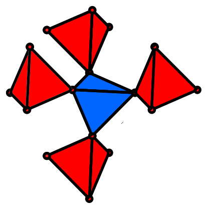

Local Order

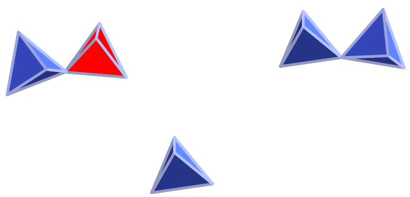

Å

NMR XAS Raman / IR

^{29}Si - Silica based materials

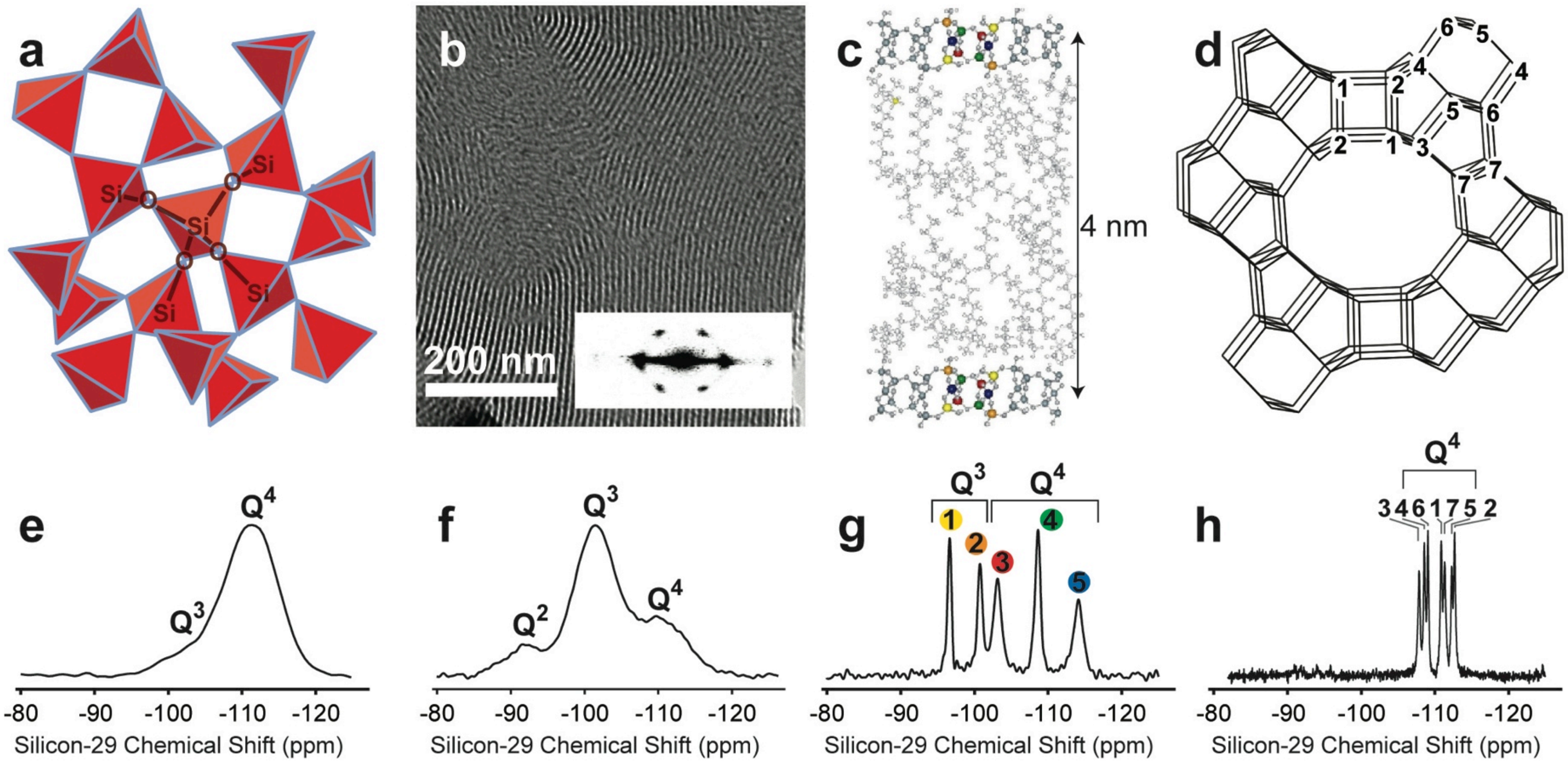

Glass | Mesoporous Silica | SiO_2-surfactant Mesophase | Zeolite

Resolution is gained by averaging out anisotropic signatures

Magic Angle Spinning MAS

D.Massiot, R.J.Messinger, S.Cadars, M.Deschamps, V.Montouillout, N.Pellerin, E.Veron, M.Allix, P.Florian, F.Fayon

Accounts Chem. Res. 46 1975–1984 2013

Structure & functions... Proteins / Glasses

Intrinsically Disordered Protein
IDPs

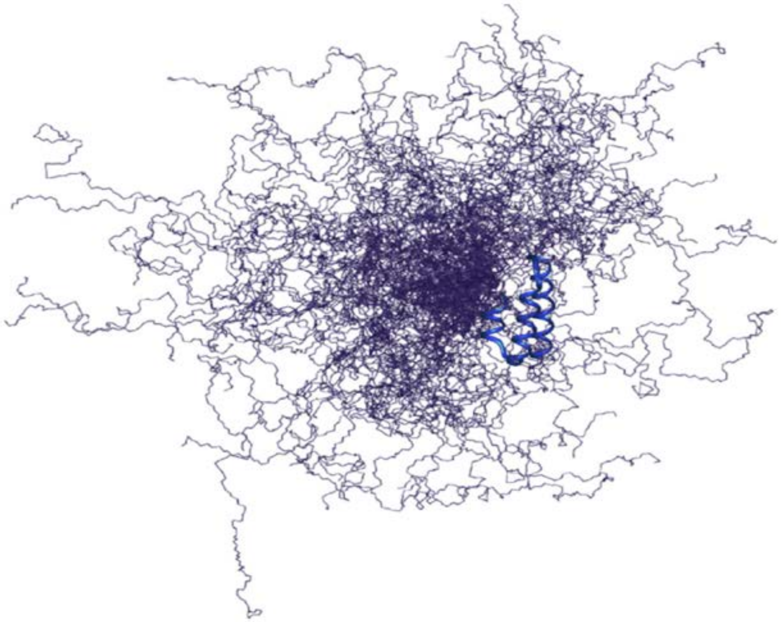

Macromolecules
secondary and ternary
Structure & dynamics
Constraints from identified spin pairs
Through-bond and through space
^{1}H / ^{13}C / ^{15}N

Glass
3D interconnected network

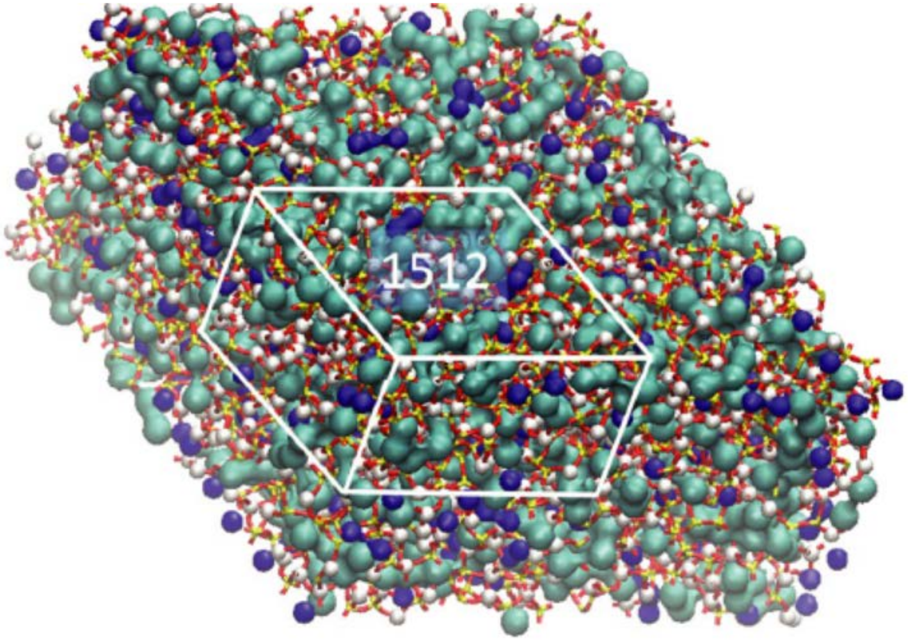

Multicomponent Glass SiO2-Al2O3 MO
Extended 3D *rigid* network of tetrahedral
Connectivity
Very similar information from
Dipolar and J-coupling
^{29}Si / ^{23}Na / ^{27}Al / ^{43}Ca / ^{17}O

Structure & functions... Proteins / Glasses

Intrinsincally Disordered Protein
IDPs

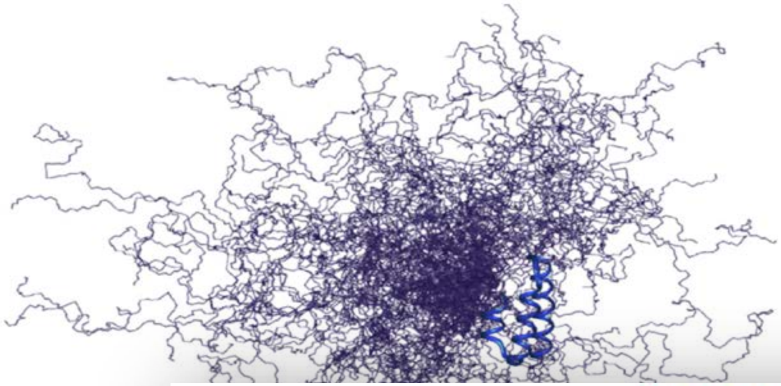

Glass
3D interconnected network

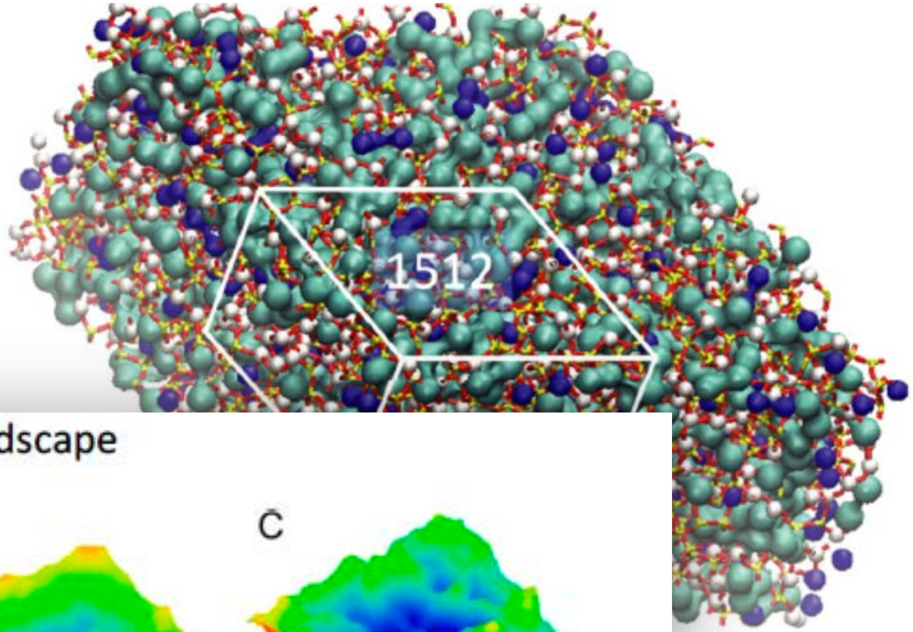

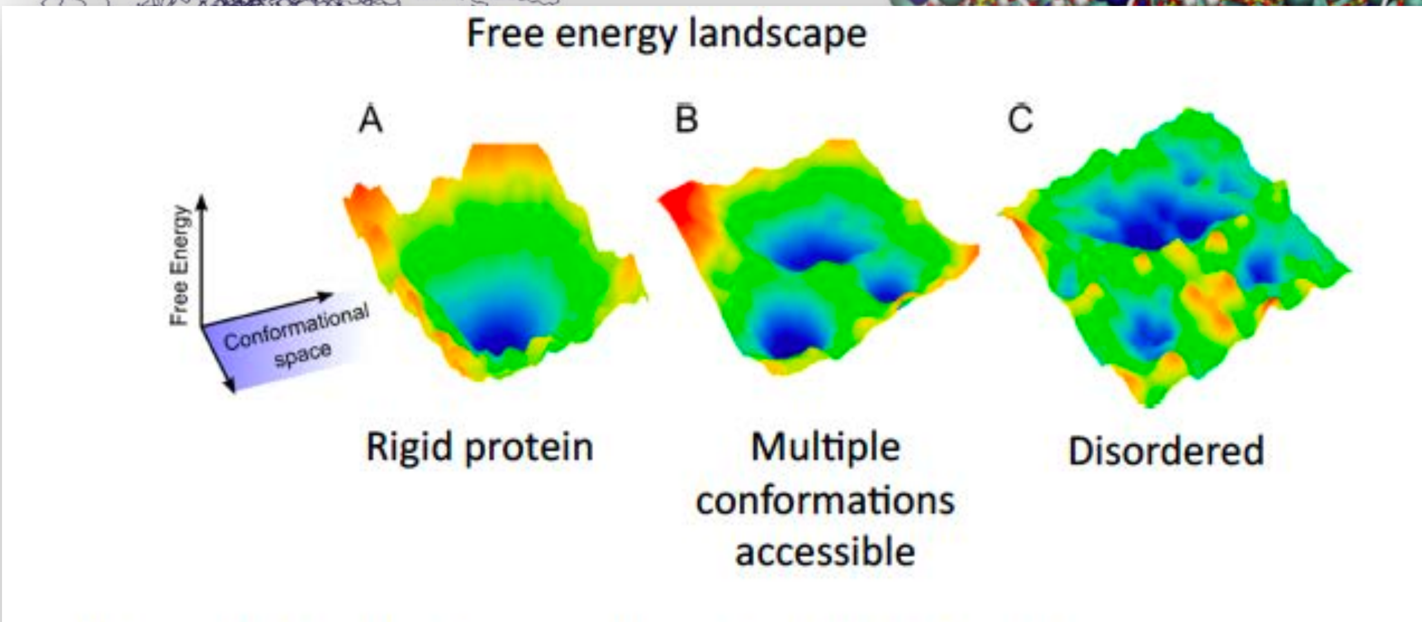

M. Brucale, B. Schuler, B. Samorì, Chem. Rev. **2014**, 114, 3281

NMR TimeLine

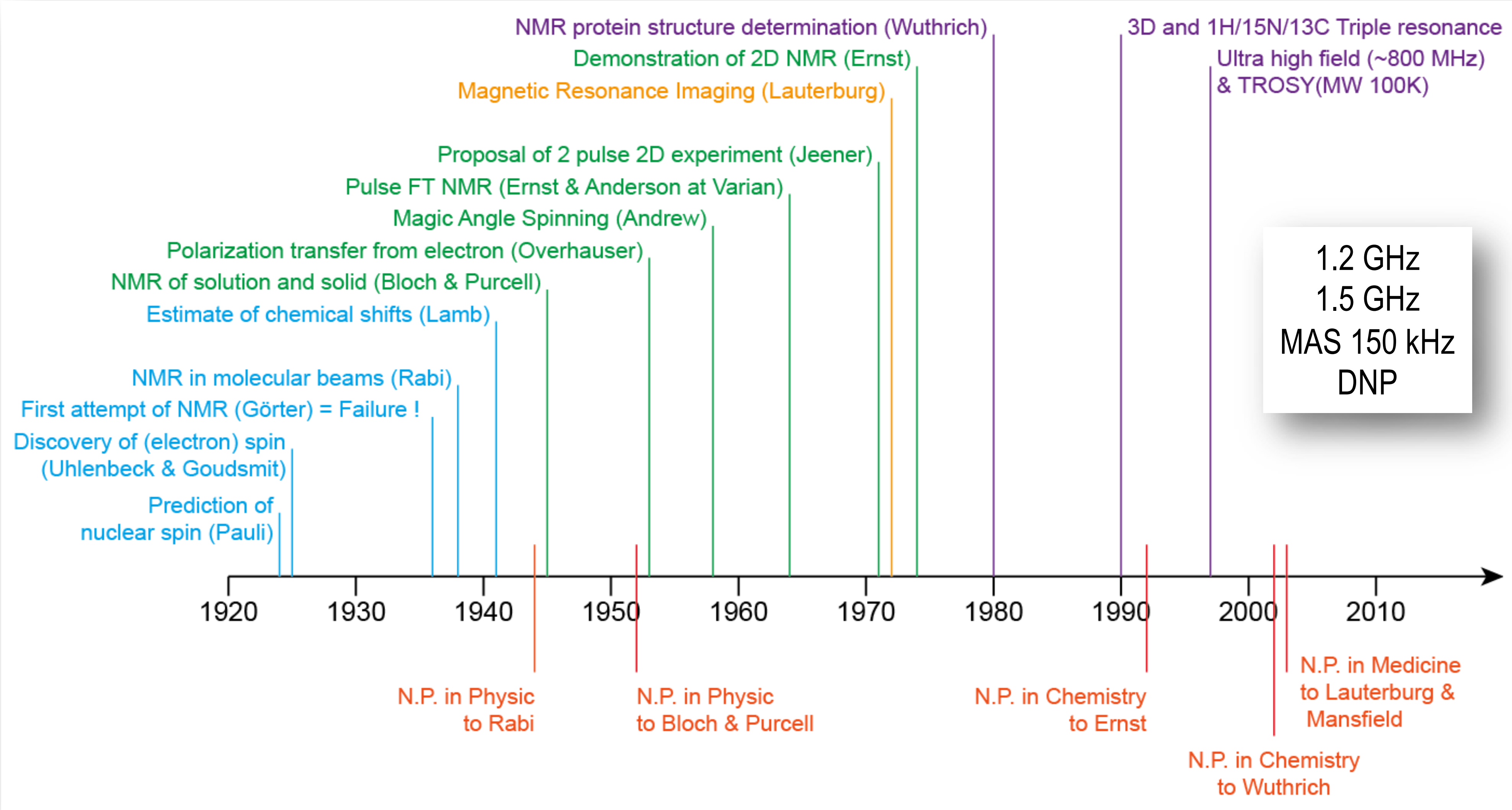

The Nuclear Magnetic Resonance

The Nobel Prize in Physics 1944
Isidor Isaac Rabi
by Professor E. Hulthén, Stockholm

Let us now for a moment touch upon Rabi's achievements in this field. Returning to the essential point of the problem, let us put the question: How does the atom react to the magnetic field? According to a theorem stated by the English mathematician Larmor, this influence may be ascribed to a relatively slow precession movement on the part of the electron and the atomic nucleus around the field direction - a gyromagnetic effect most closely recalling the gyroscopic movement performed by a top when it spins around the vertical line. If the strength of the magnetic field is known, the magnetic factor of the electron and of the atomic nucleus can also be estimated by this means, provided that we can observe and measure these precessional frequencies. Rabi solved the problem in a manner as simple as it was brilliant. Within the magnetic field was inserted a loop of wire, attached to an oscillating circuit the frequency of which could be varied in the same manner as we tune in our radio receiving set to a given wavelength. Now, when the atomic beam passes through the magnetic field, the atoms are only influenced on condition that they precess in time with the electric current in the oscillating circuit. This influence might perhaps be described graphically: the nucleus performs a vault (salto) - the technical term for which is a "quantum jump" - thereby landing in another positional direction to the field. But this means that the atom has lost all chance of reaching the detector and of being registered by it. The effect of these quantum jumps is observable by the fact that the detector registers a marked resonance minimum, the frequency position of the registration being determined with the extraordinary precision achievable with the radio frequency gauge. By this method Rabi has literally established radio relations with the most subtile particles of matter, with the world of the electron and of the atomic nucleus.

The Nuclear Magnetic Resonance

The Nobel Prize in Physics 1944
Isidor Isaac Rabi
by Professor E. Hulthén, Stockholm

Let us now for a moment tou … ng to the essential point of
the problem, let us put the q … c field? According to a
theorem stated by the Englis … scribed to a relatively slow
precession movement on th … nd the field direction - a
gyromagnetic effect most clo … d by a top when it spins
around the vertical line. If th … netic factor of the electron
and of the atomic nucleus ca … we can observe and measure
these precessional frequenci … as it was brilliant. Within the
magnetic field was inserted a … frequency of which could be
varied in the same manner a … elength. Now, when the
atomic beam passes through … on condition that they
precess in time with the elect … might perhaps be described
graphically: the nucleus perfo … s a "quantum jump" - thereby
landing in another positiona … m has lost all chance of
reaching the detector and of being registered by it. The effect of these quantum jumps is observable by the fact that the detector registers a marked resonance minimum, the frequency position of the registration being determined with the extraordinary precision achievable with the radio frequency gauge. By this method Rabi has literally established radio relations with the most subtile particles of matter, with the world of the electron and of the atomic nucleus.

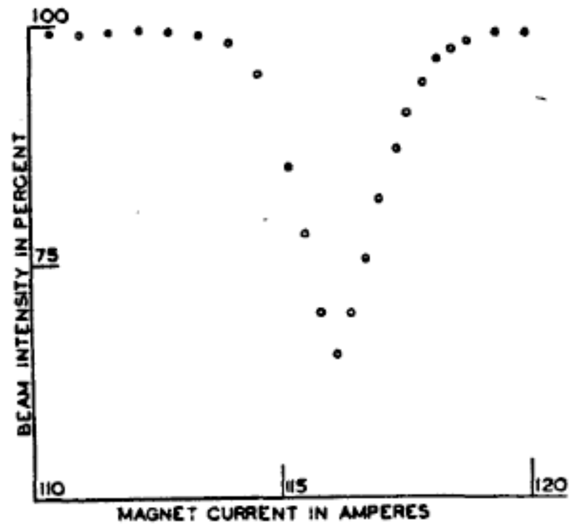

Resonance of LiCl from Rabi's 1938 paper.

The Magnetic *Nuclear Induction* approach

E.M. Purcell et F. Bloch, Nobel of Physics 1952 for the discovery of NMR

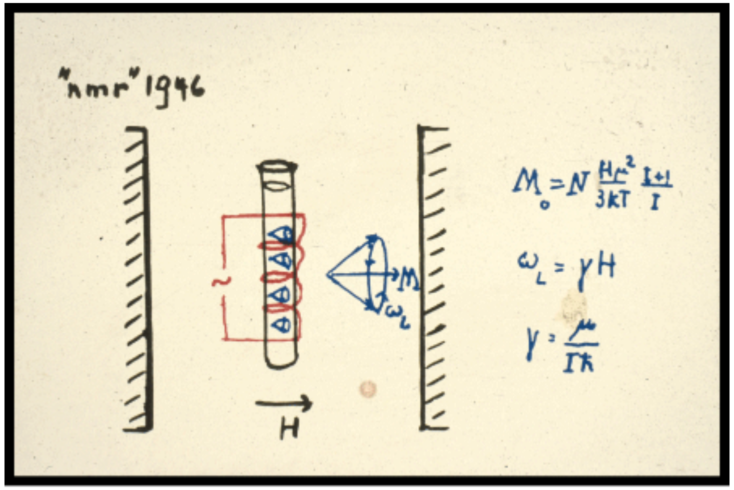

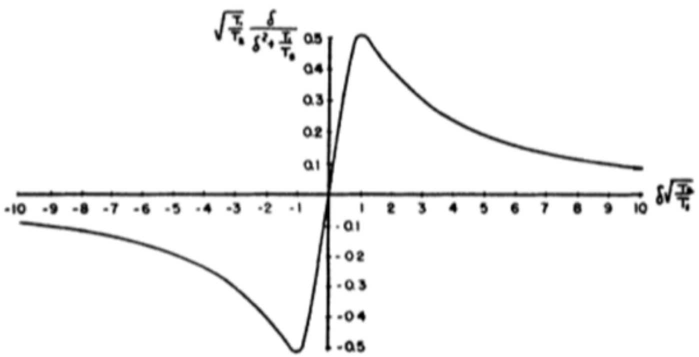

FIG. 2. Schematic representation of the voltage amplitude in the case of slow passage. T_1 and T_2 are the longitudinal and transversal relaxation times, respectively, and the scale is chosen such as to make the plot independent of their values. The significance of abscissa and ordinate is otherwise the same as in Fig. 1.

Nuclear Induction

F. Bloch, W. W. Hansen, and Martin Packard
Stanford University, Stanford University, California

January 29, 1946

THE nuclear magnetic moments of a substance in a constant magnetic field would be expected to give rise to a small paramagnetic polarization, provided thermal equilibrium be established, or at least approached. By superposing on the constant field (z direction) an oscillating magnetic field in the x direction, the polarization, originally parallel to the constant field, will be forced to precess about that field with a latitude which decreases as the frequency of the oscillating field approaches the Larmor frequency. For frequencies near this magnetic resonance frequency one can, therefore, expect an oscillating induced voltage in a pick-up coil with axis parallel to the y direction. Simple calculation shows that with reasonable apparatus dimensions the signal power from the pick-up coil will be substantially larger than the thermal noise power in a practicable frequency band.

We have established this new effect using water at room temperature and observing the signal induced in a coil by the rotation of the proton moments. In some of the experiments paramagnetic catalysts were used to accelerate the establishment of thermal equilibrium.

Phys. Rev., **69**, 127 (1946)

Sensitivity / Observability

H 2																	*He*
Li 6,7	**Be** 9											**B** 10,11	*C*	**N** 14	**O** 17	*F*	**Ne** 21
Na 23	**Mg** 25											**Al** 27	*Si*	*P*	**S** 33	**Cl** 35,37	Ar
K 39,41	**Ca** 43	**Sc** 45	**Ti** 47,49	**V** 50,51	**Cr** 53	**Mn** 55	*Fe*	**Co** 59	**Ni** 61	**Cu** 63,65	**Zn** 67	**Ga** 69,71	**Ge** 73	**As** 75	*Se*	**Br** 79,81	**Kr** 83
Rb 85,87	**Sr** 87	*Y*	**Zr** 91	**Nb** 93	**Mo** 97	Tc	**Ru** 99,101	*Rh*	**Pd** 105	*Ag*	*Cd*	**In** 113-5	*Sn*	Sb 121-3	*Te*	**I** 127	**Xe** 129-31
Cs 133	**Ba** 135-7	**La** 138-9	**Hf** 177-9	**Ta** 181	*W*	**Re** 185-7	**Os** 187-9	**Ir** 191-3	*Pt*	**Au** 197	**Hg** 201	*Tl*	*Pb*	*Bi*	Po	At	Rn
Fr	Ra	Ac															

Ce	**Pr** 141	**Nd** 143-5	Pm	**Sm** 147-9	**Eu** 151-3	**Gd** 155-7	**Tb** 159	**Dy** 161-3	**Ho** 165	**Er** 167	*Tm*	**Yb** 173	**Lu** 175-6
Th	Pa	**U** 235	Np	Pu	Am	Cm	Bk	Cf	Es	Fm	Md	No	Lr

Element n'ayant que des isotopes de spin I=1/2

Element ayant des isotopes de spin quadripolaire (I>1/2)

- **Observability**
  - **abundance**
  - **Gyromagnetic ratio**
  - **Quadrupolar momentum**

Numerous possibly sensitive nuclei but fewer easily observed

The most usually observed are *«light»* nuclei

- **I=1/2 : ^{1}H, ^{29}Si, ^{31}P, ^{13}C,**
- **I=3/2 : ^{23}Na, ^{11}B**
- **I=5/2 : ^{27}Al, ^{17}O (isotopic enrichment)**

Larmor Frequency

$$\nu_0 = \gamma B_0 \mid \Delta E = h\nu_0$$

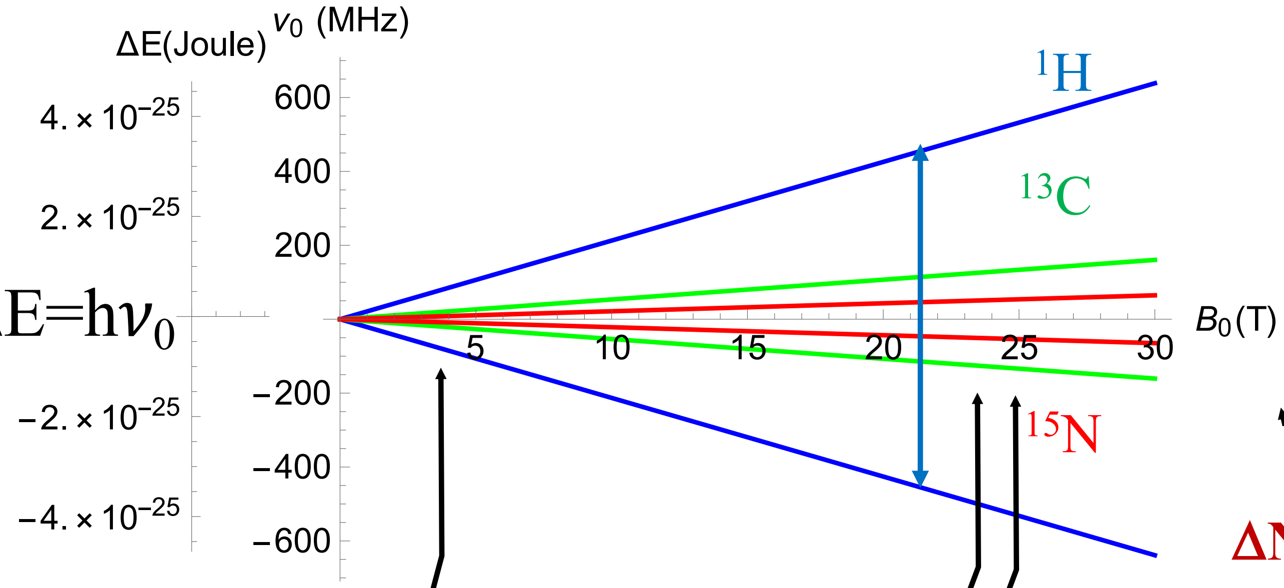

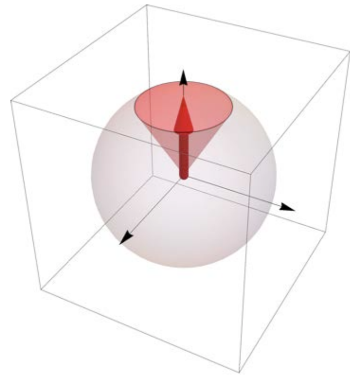

NMR signal

$\Delta N \; \alpha \; \exp(-\Delta E/kT)$

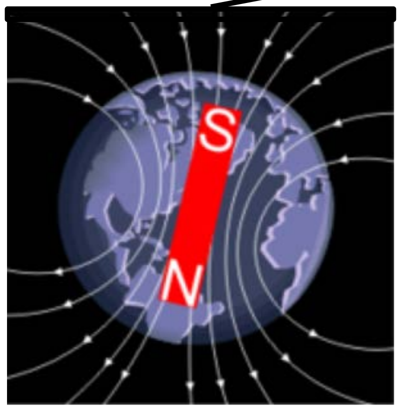

Earth Field
~50μT (0.5G)
magnetometer

3T [128MHz]
Whole body (Philips)

23.4T
1GHz (Lyon)
1.2GHz Bruker 2019

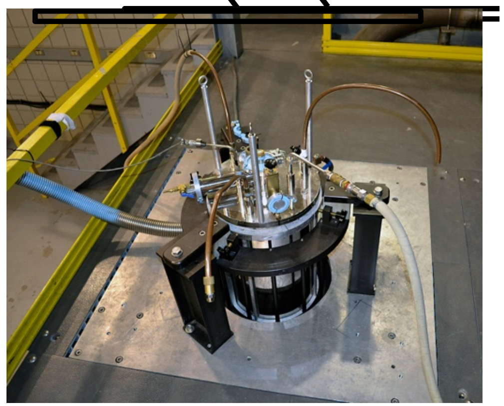

35 T
1.5 GHz (Thallahassee)
40T inhomogeneous

Precession – Rotating Frame

Top in a Gravitational field

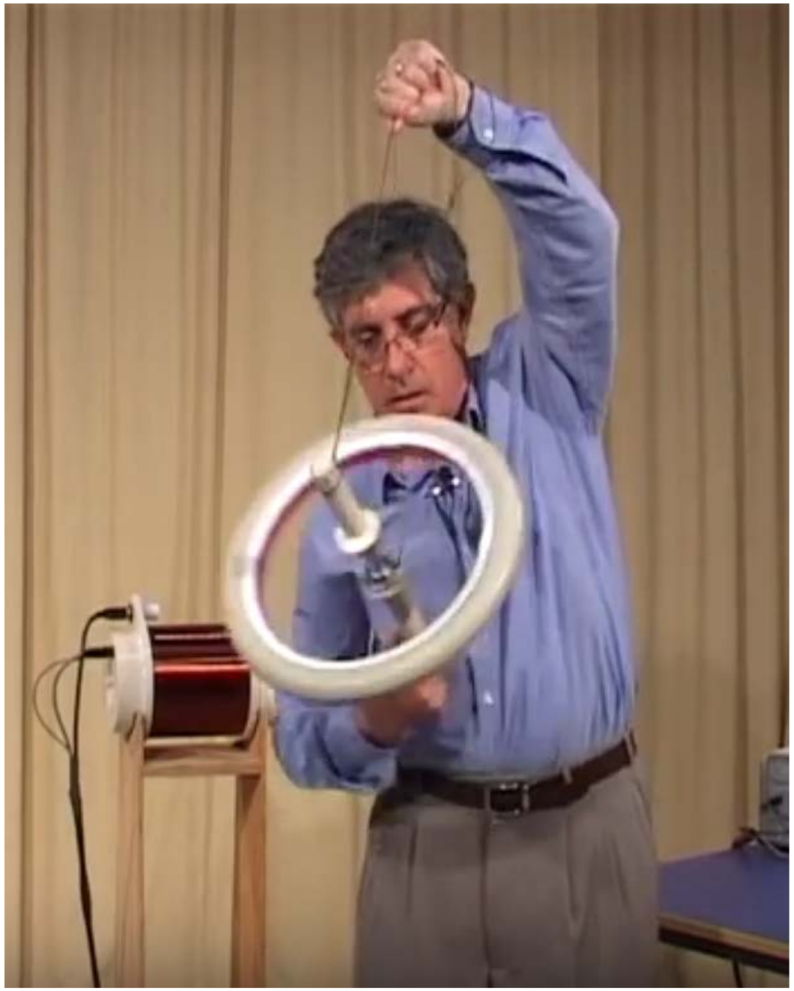

Paul Callaghan applying a pulse in the gravitational field
https://www.youtube.com/watch?v=7aRKAXD4dAg

"Spin" in Magnetic Field

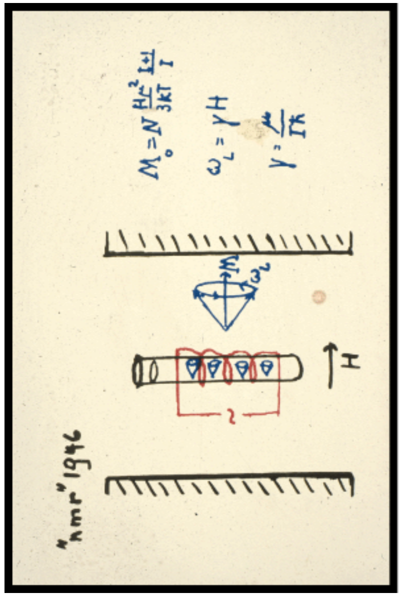

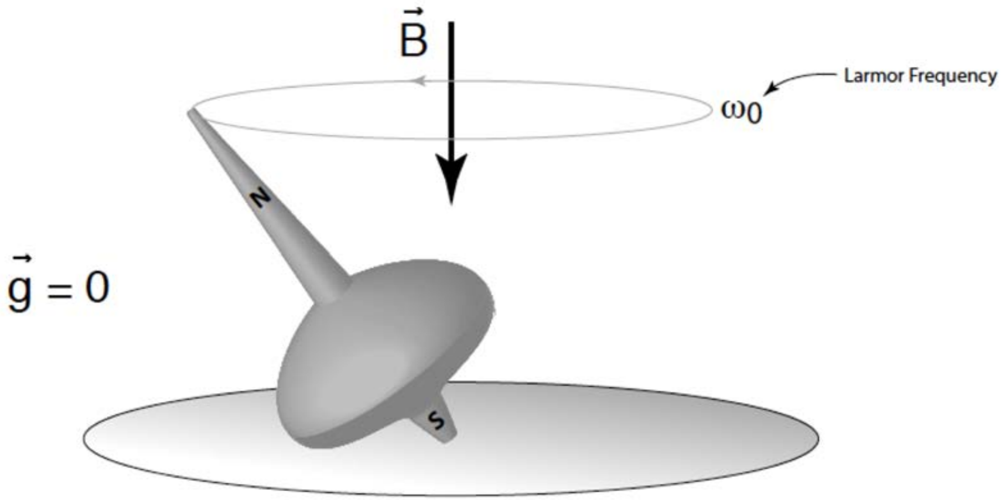

Rotating Frame

Bloch Equations – with B_1 on - Pulses

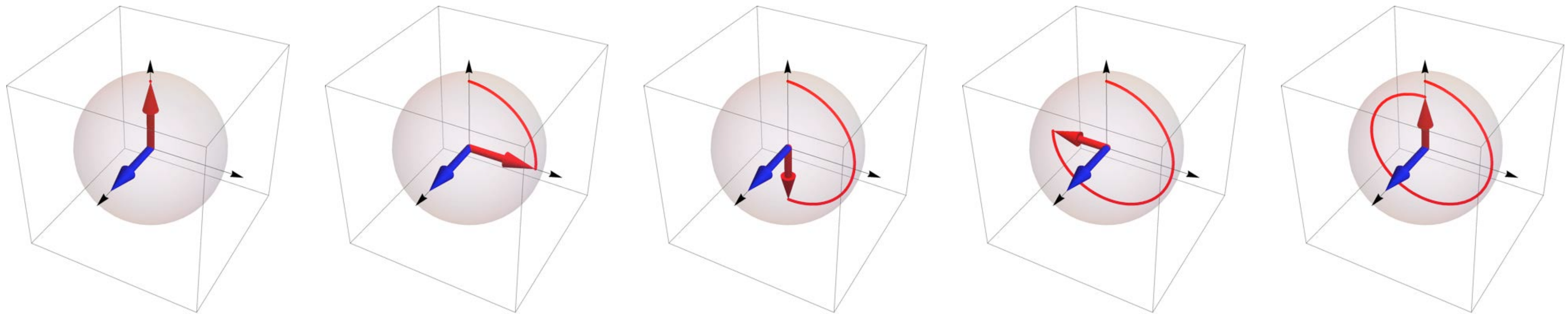

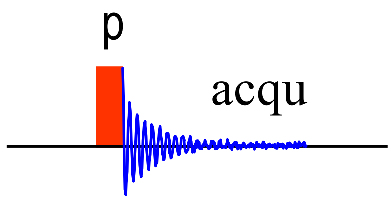

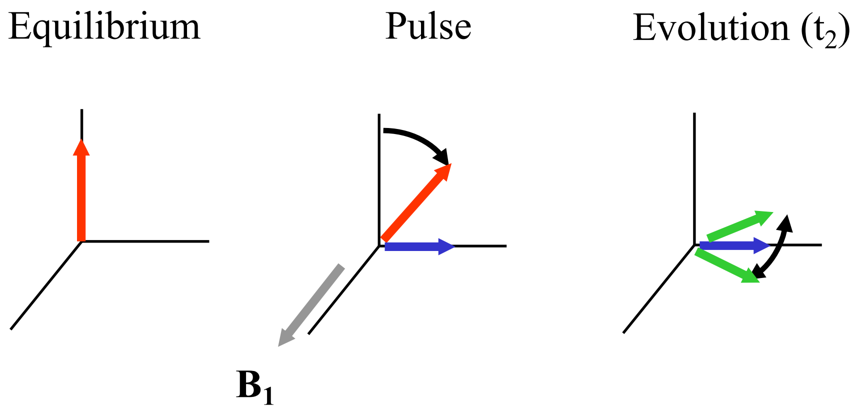

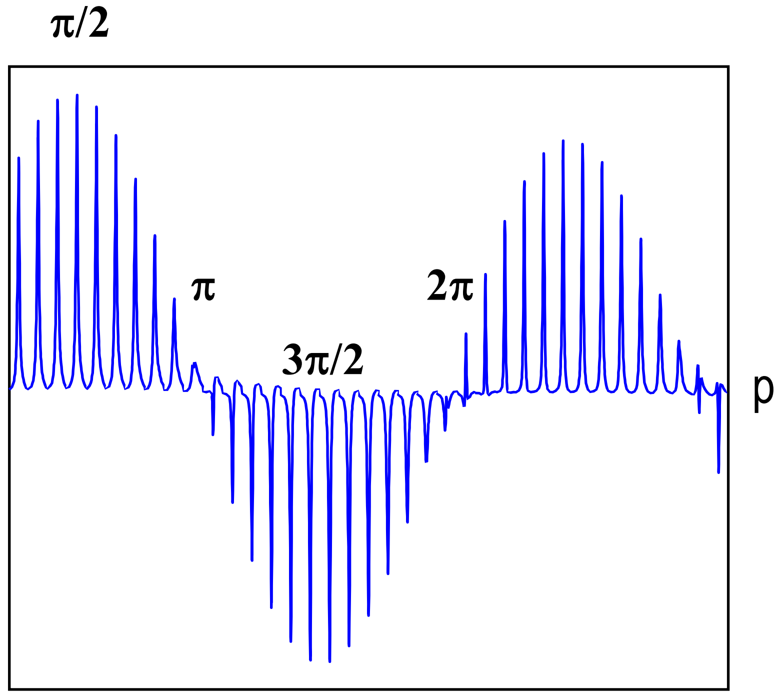

Precession in the B1 field [$\nu_1 = \gamma B_1$] – remaining far from thermal equilibrium

Pulsed NMR – long lasting coherence

Bloch Equations

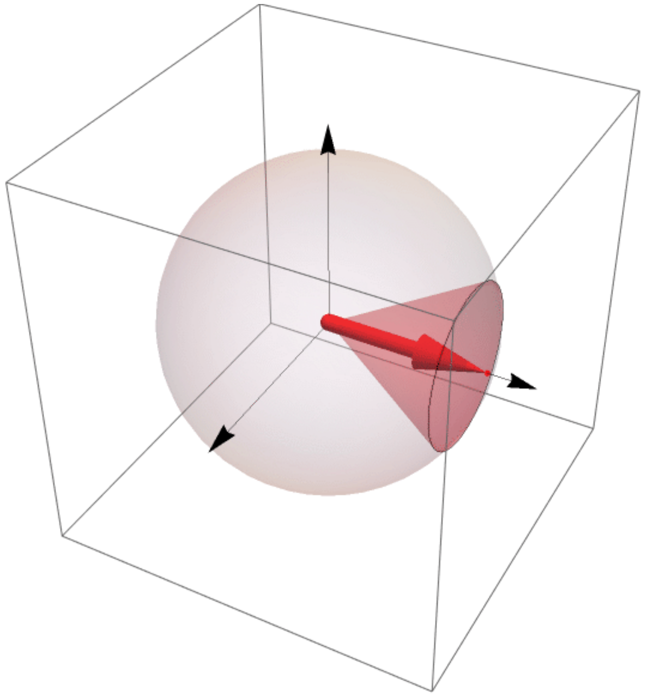

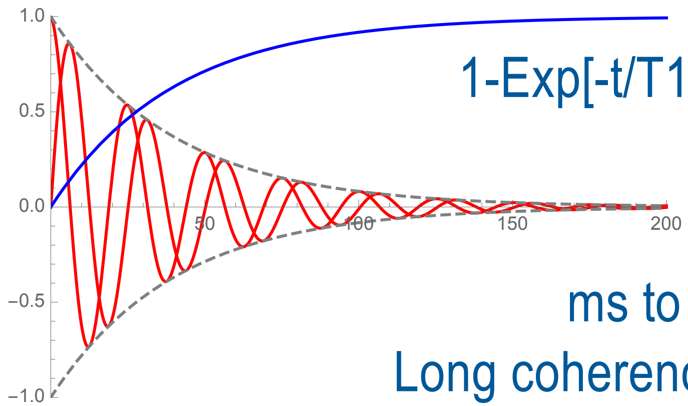

ms to s

Long coherence lifetime

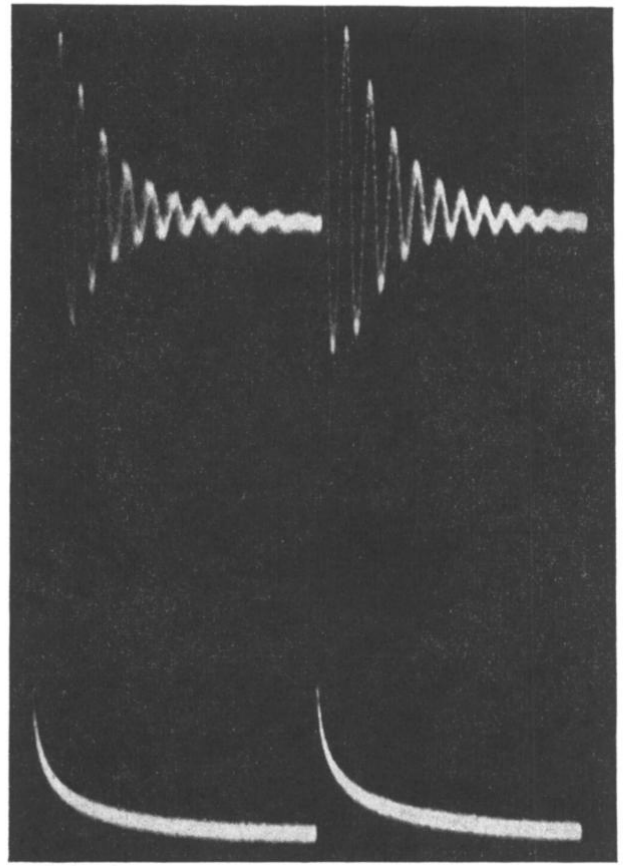

FIG. 2. The top trace indicates a beat note between an external r-f signal generator (near the Larmor frequency, loosely coupled to the inductive coil) and the nuclear signal shown alone (after detection) on the bottom trace. This beat note is identical in principle with the "wiggle effect" (see reference 5) except that H_0 is held constant in this case.

E.L. Hahn, *Phys. Rev.*, **77**, 297 (1950)

T1 measurement – Inversion Recovery

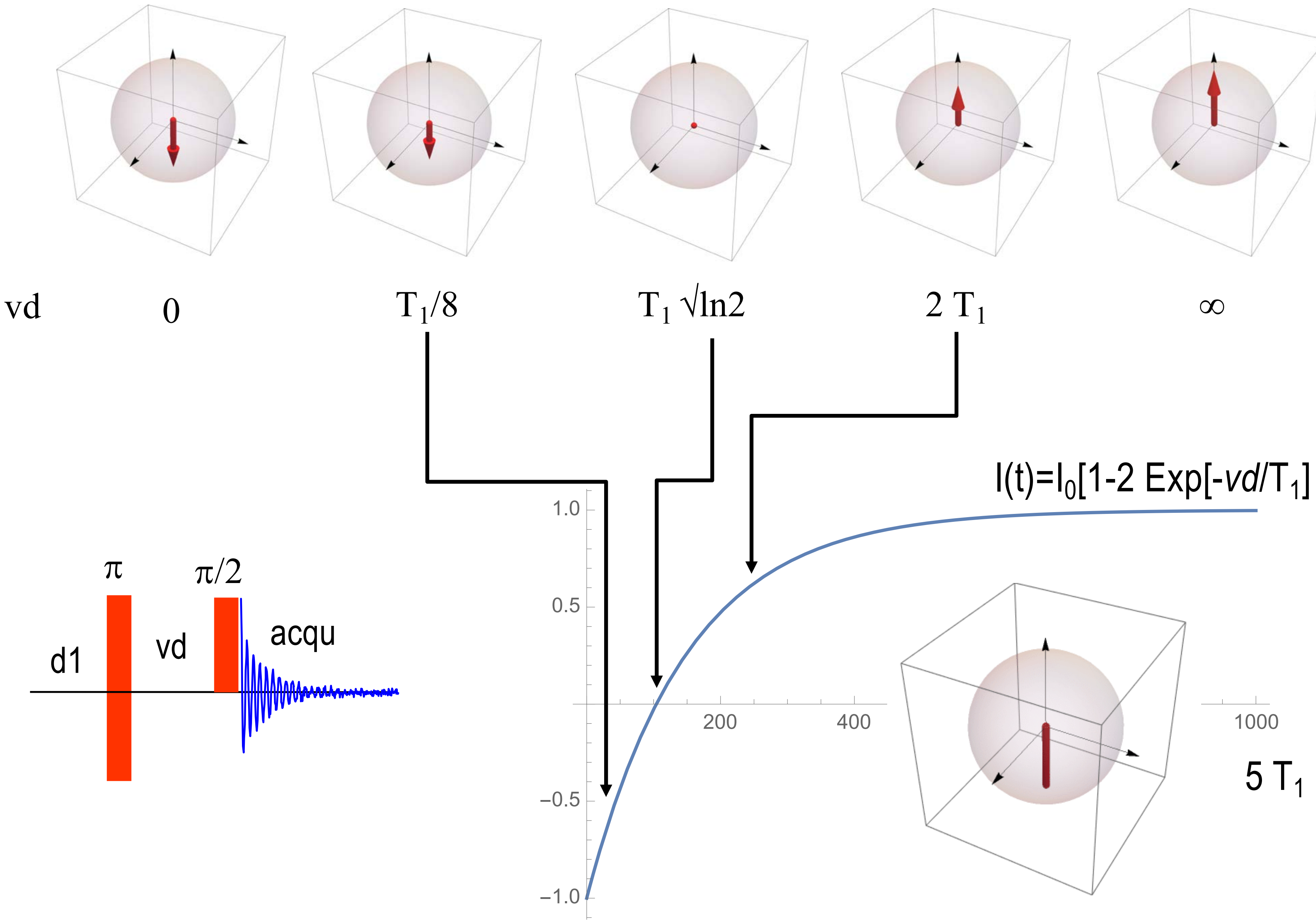

Spin Echo – signal can be refocused

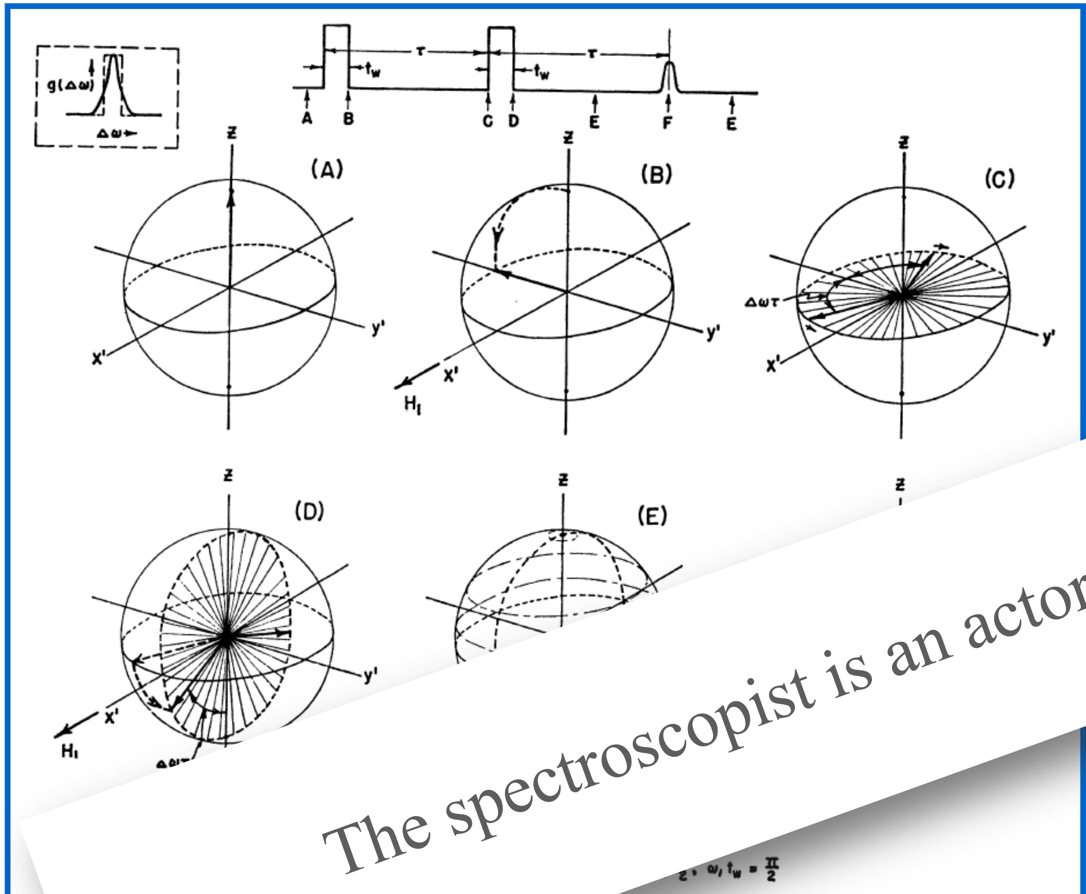

F... at a... pulse ... -ball echo pattern is shown in the coordinate system rotating ... allowed to ravel completely in a time $\tau \gg 1/(\Delta\omega)_i$ before the second ... ude at $\omega_1 t_w = 2\pi/3$.

The spectroscopist is an actor of the experiment

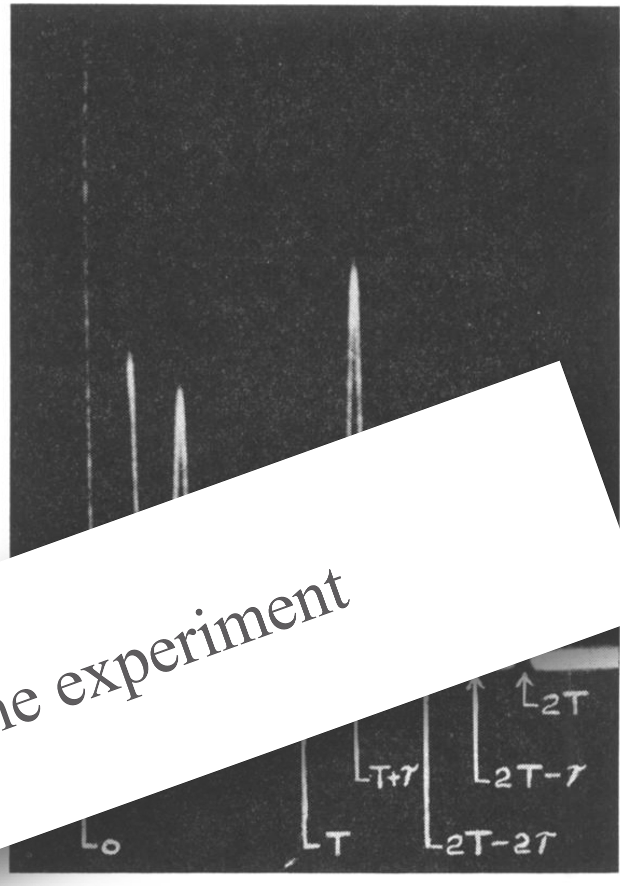

c

FIG. 5. Proton echo patterns in H_2O resulting from three applied r-f pulses. The pulses are visible in the upper two traces, and have a width $t_w \sim 0.5$ msec. In the upper trace $\tau = 0.008$ sec., $T = 0.067$ sec., and for the second trace $\tau = 0.046$ sec. and $T = 0.054$ sec. The bottom photograph shows a similar pattern for the case $T > 2\tau$ where induction decay signals can be seen following very short invisible r-f pulses. Saturation of a narrow band communications receiver, used in the case of the upper two traces, prevents the observation of these signals, whereas a wide band i.f. amplifier makes this observation possible in the bottom photograph.

E.L. Hahn, *Phys. Rev.*, **80**, 580 (1950)

Hahn Echo – Spin Echo

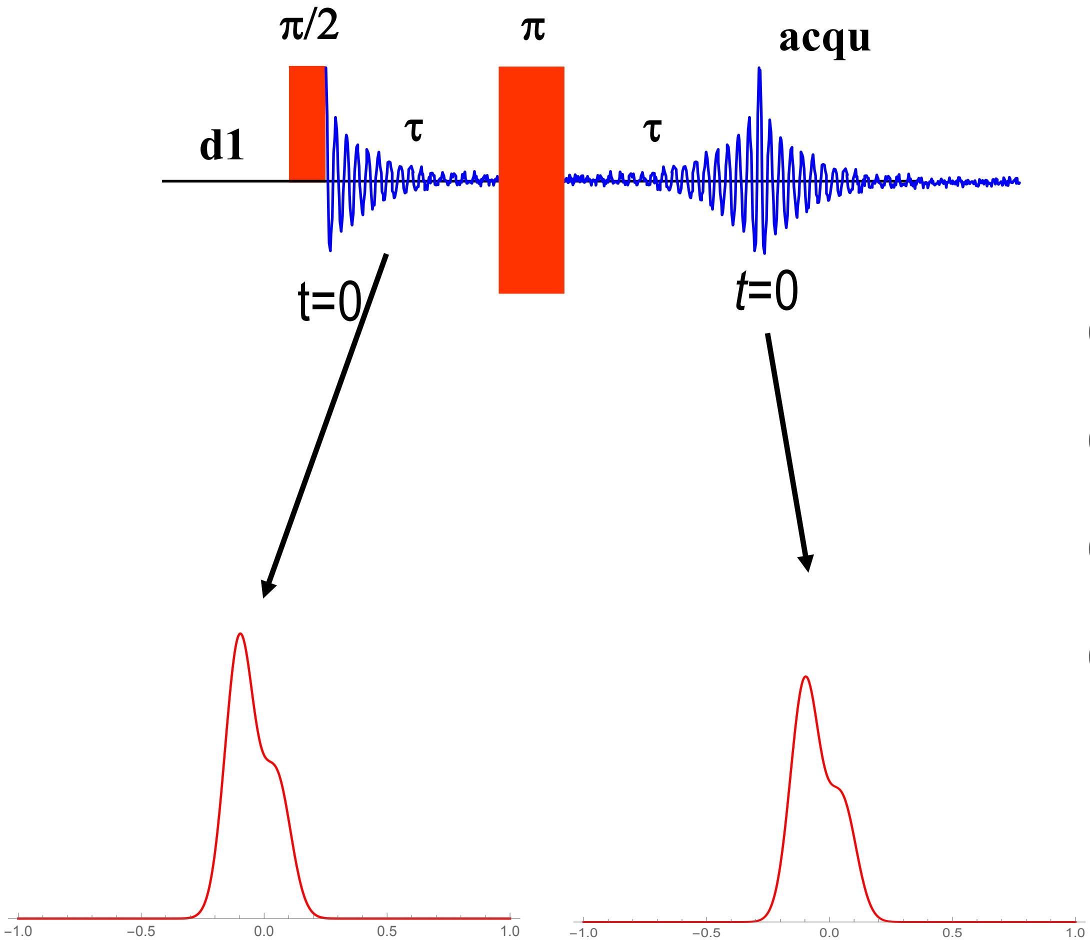

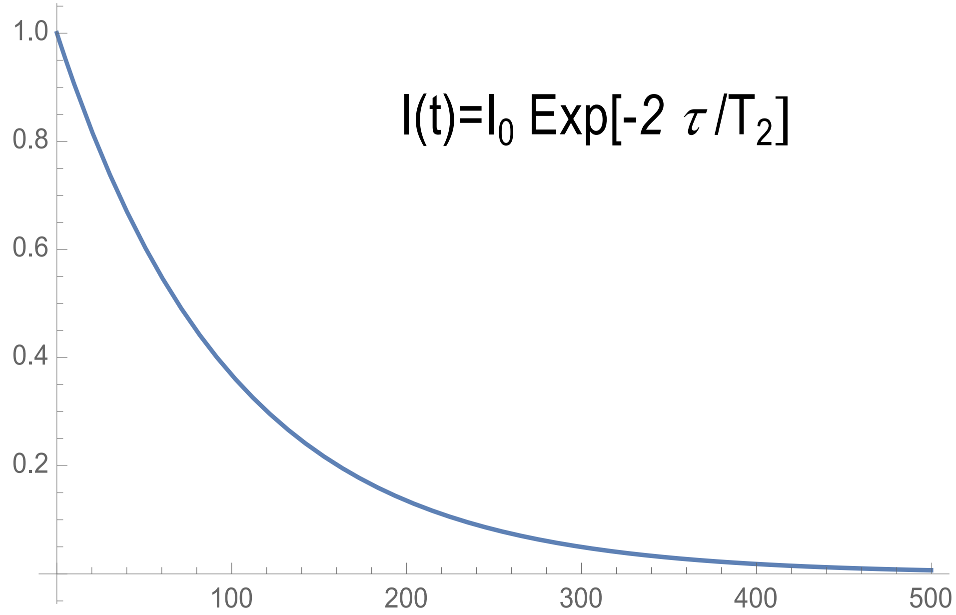

Measurement of T_2

the life time of the coherence

in the XY [transverse] plane

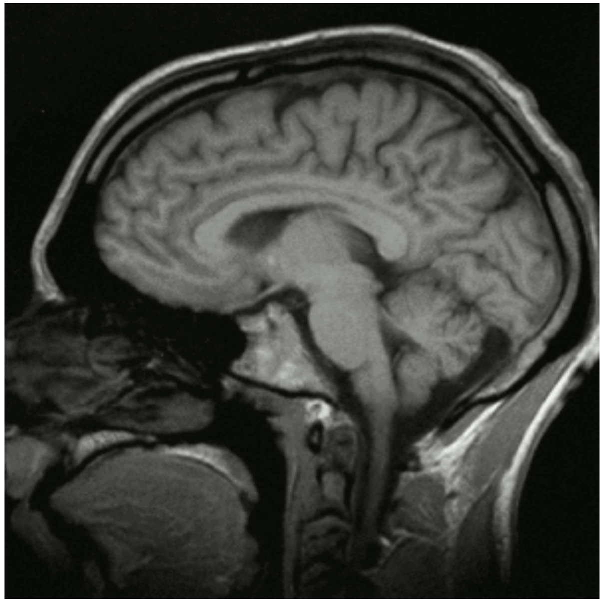

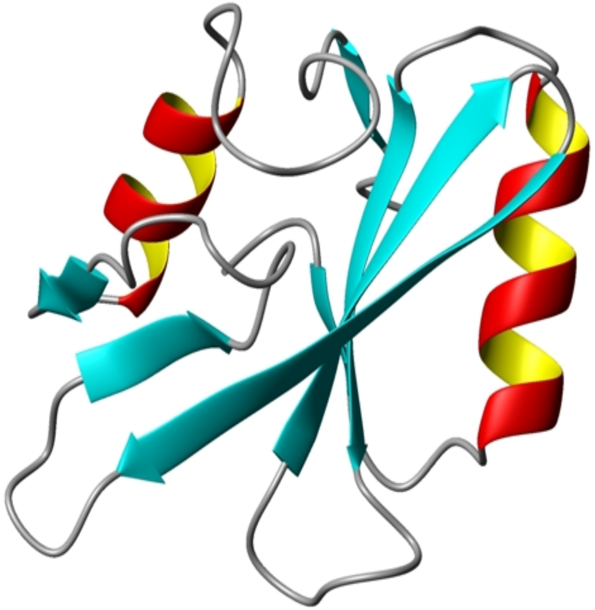

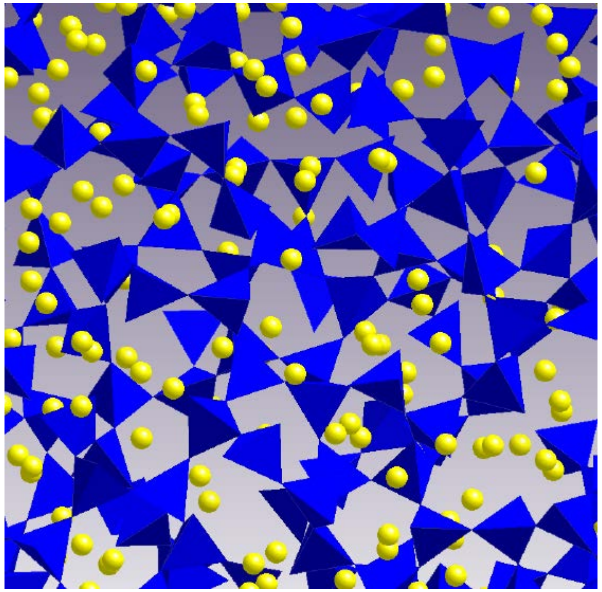

Spatial Encoding
Field Gradients

Imaging
anatomy / function
Diffusion / Rheology

Local Field
Homogeneous Principal Field (<ppm)

Spectroscopy

Chemistry

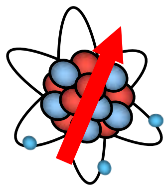

In a magnetic field - $\nu 0 = \gamma\ B0/2\pi$

Coding of position - Imaging

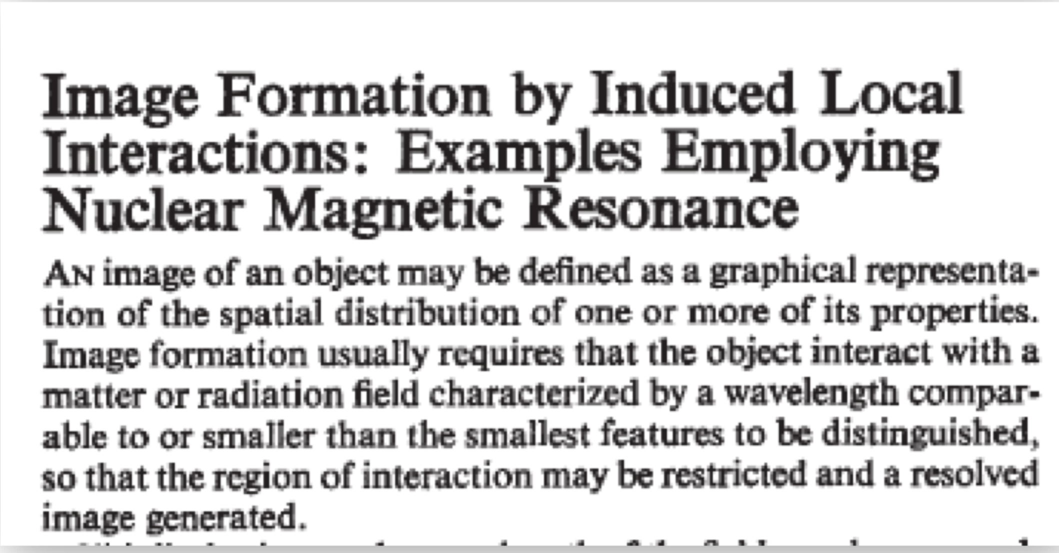

Image Formation by Induced Local Interactions: Examples Employing Nuclear Magnetic Resonance

An image of an object may be defined as a graphical representation of the spatial distribution of one or more of its properties. Image formation usually requires that the object interact with a matter or radiation field characterized by a wavelength comparable to or smaller than the smallest features to be distinguished, so that the region of interaction may be restricted and a resolved image generated.

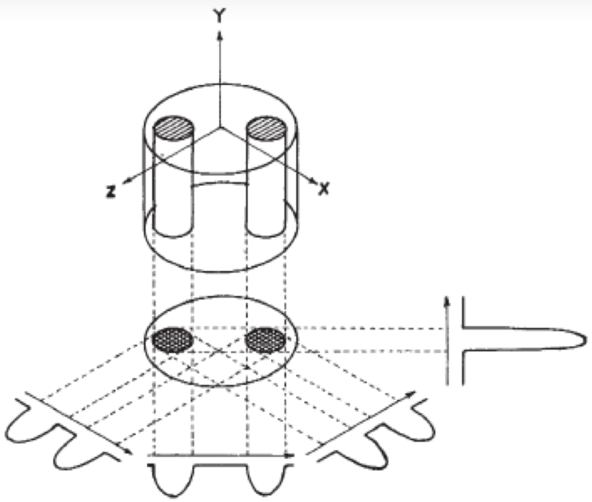

Fig. 1 Relationship between a three-dimensional object, its two-dimensional projection along the Y-axis, and four one-dimensional projections at 45° intervals in the XZ-plane. The arrows indicate the gradient directions.

Paul C. Lauterbur – Nature 1973
Nobel Physiology & Medecine 2003

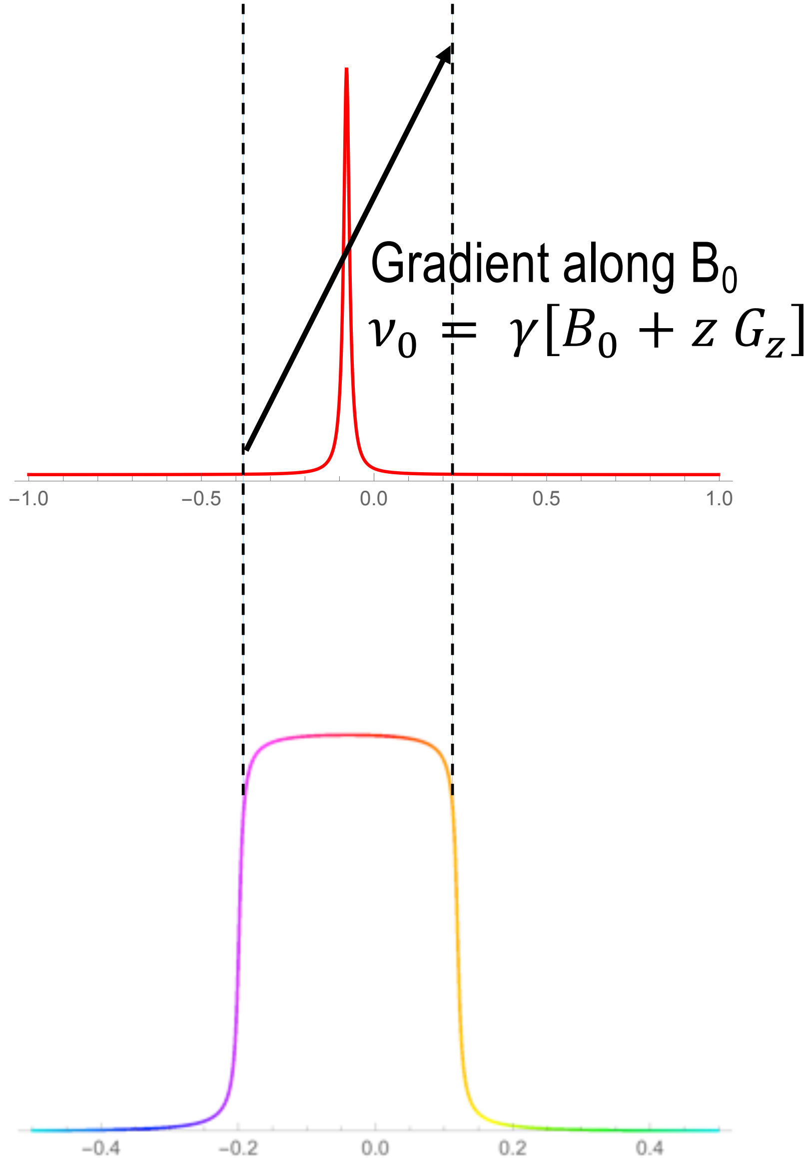

Projection on the Field Gradient

The Discovery of Chemical Shift

The Dependence of a Nuclear Magnetic Resonance Frequency upon Chemical Compound*

W. G. Proctor and F. C. Yu
Department of Physics, Stanford University, Stanford, California
January 18, 1950

IN the course of measurements on N^{14}, mentioned in the previous letter, we made the surprising observation that its frequency of resonance, in liquid samples, depended strongly upon the chemical compound in which it was contained.[1,2] This effect is strikingly demonstrated by the appearance of two resonances, separated by 1.6 kc in the neighborhood of 3300 kc, corresponding to a field of 10,500 gauss, using a solution of NH_4NO_3 in 2.0-molar $MnSO_4$ as a sample. These resonances presumably arise from the NH_4^+ and NO_3^- complexes, since samples of $NH_4C_2H_3O_2$ and HNO_3 separately give rise to two different resonances whose frequencies approximate those from the above sample. The separation is four times greater than the line widths measured between points of maximum slope.

Phys. Rev., **77**, 716 (1950)

Dependence of the F^{19} Nuclear Resonance Position on Chemical Compound*

W. C. Dickinson
Research Laboratory of Electronics, Massachusetts Institute of Technology, Cambridge, Massachusetts
January 9, 1950

MOST unexpectedly, it has been found that for F^{19} the value of the applied magnetic field H_0 for nuclear magnetic resonance at a fixed radiofrequency depends on the chemical compound containing the fluorine nucleus. The assumption has generally been made that the time average of all internal magnetic fields is zero, excluding of course the small diamagnetic field at the nucleus due to the Larmor precession of its atomic electrons in H_0. Nuclear resonance shifts in metals,[1] interpreted as being due to the conduction electrons, are larger by about an order of magnitude than those reported here.[2]

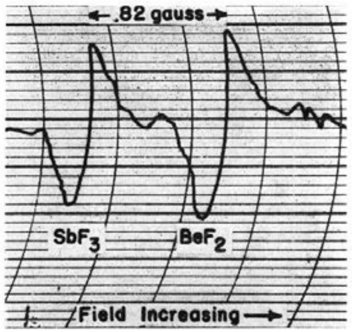

Fig. 2. The nuclear resonances of F^{19} in a single sample containing a half and half mixture of SbF_3 and BeF_2 (saturated aqueous solutions). The applied resonance magnetic field is about 7000 gauss at a radiofrequency of 28.0 megacycles.

Phys. Rev., **77**, 736 (1950)

Visibility of each family of nuclei

Zn O_3P C_2H_4 CO_2H - 0.5 $C_6H_5NH_2$

Phosphonate (B.Bujoli – Nantes)

^{13}P I=1/2
100% ab.
162MHz

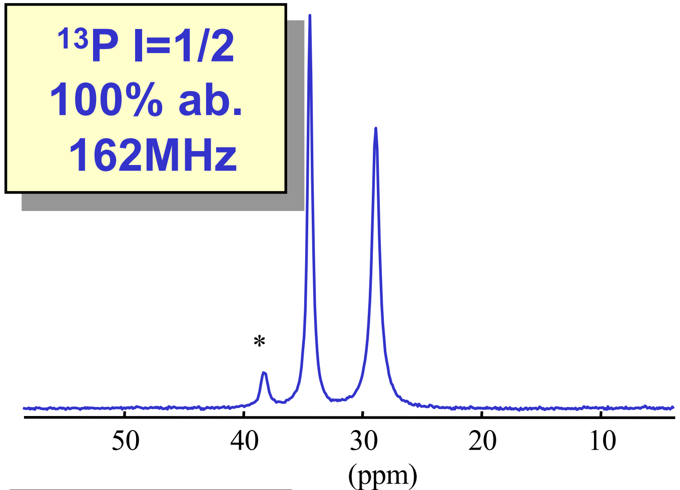

^{1}H I=1/2
99.9% ab.
400MHz

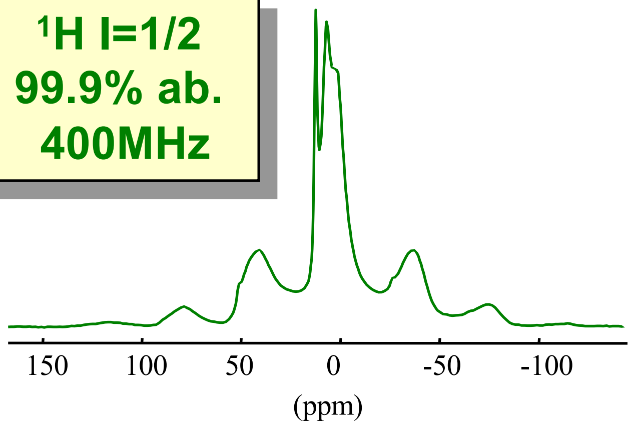

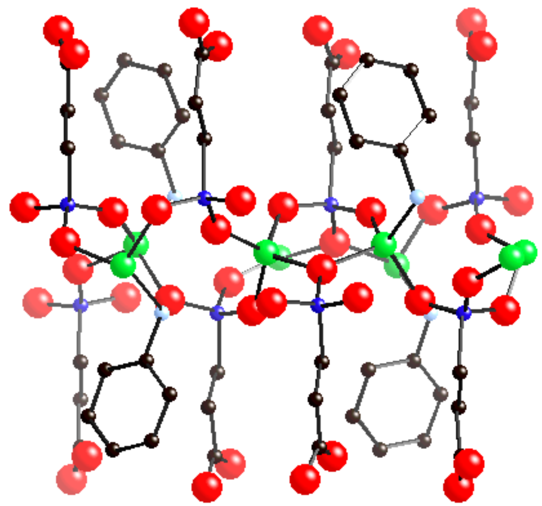

^{13}C I=1/2
1.18% ab.
100MHz

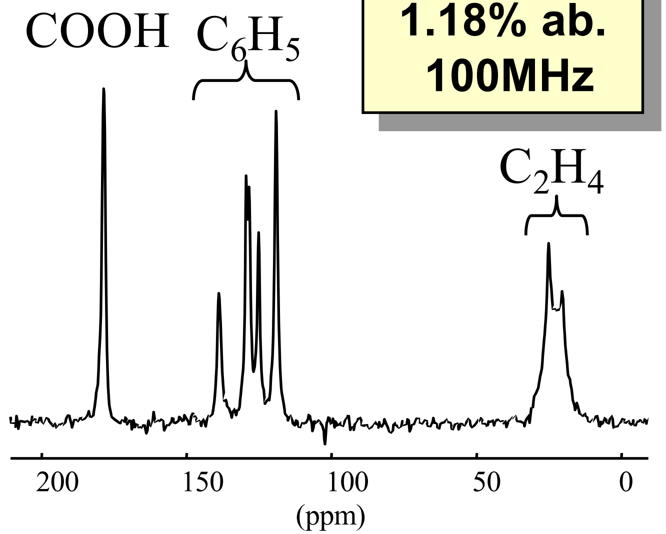

^{17}O I=5/2
0.037% ab.
54 MHz

^{14}N I=1
99.6 % ab.
29 MHz

^{67}Zn I=5/2
4.11% ab.
25 MHz

^{31}P / ^{1}H MAS MRI

$^{1}H/^{31}P$ CPMAS

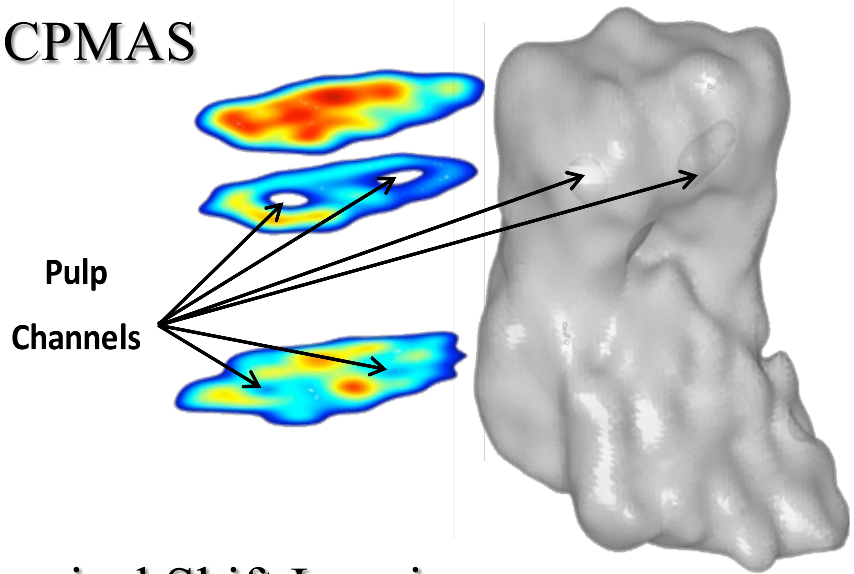

^{1}H Chemical Shift Imaging

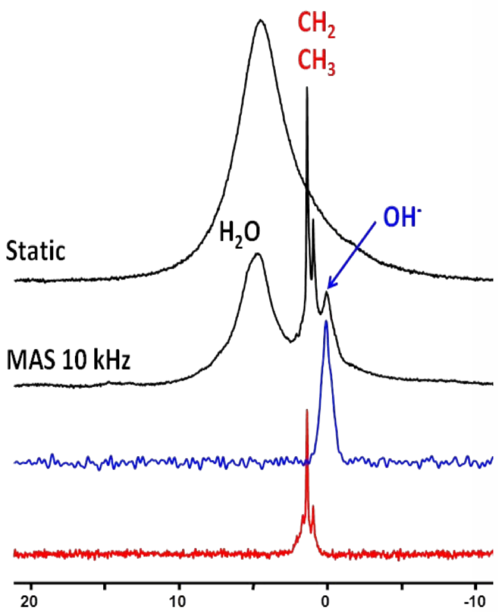

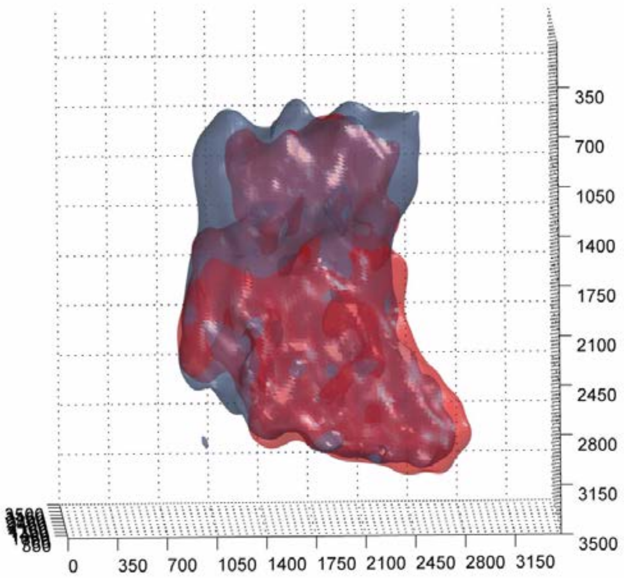

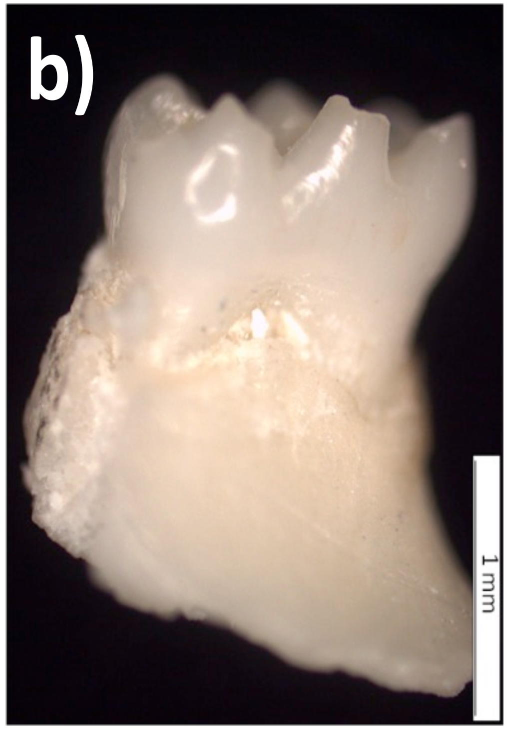

V.Sarou-Kanian *et al.*, Scientific Report 5, 9872 (2015)

The different perturbating interactions

Chemical Shift Anisotropy
electronic shielding
first shells, coordinence and geometry

~10s of kHz

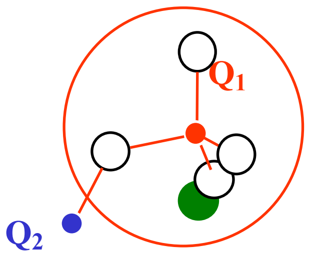

Dipolar interaction
neighboring spins
Distances

~kHz $1/r^3$

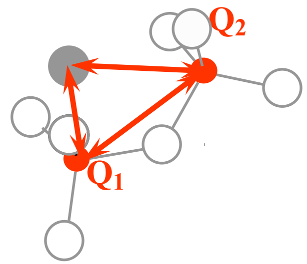

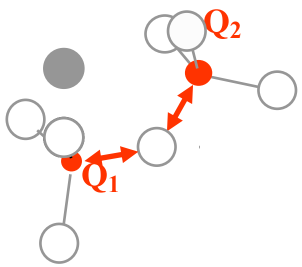

< 100s of Hz

Indirect J Coupling
chemical bonding
Connectivity

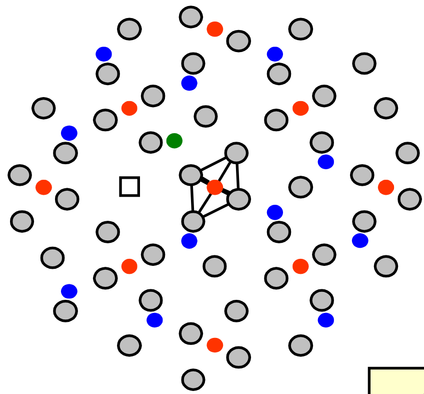

I>1/2 up to MHz

Quadrupolar interaction
Electric Field Gradient
Surrounding Charges,
electrons and nuclei
geometry

Powder Pattern

Interactions are ansiotropic and take the following form (at 1st order):

$$\nu=\nu_0+A\left(\frac{3\cos^2\beta-1}{2}-\frac{\eta}{2}\sin^2\beta\cos2\alpha\right)$$

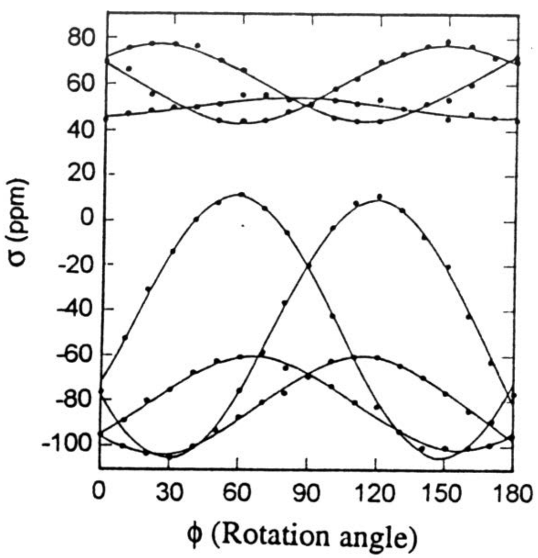

Single Crystal rotation pattern

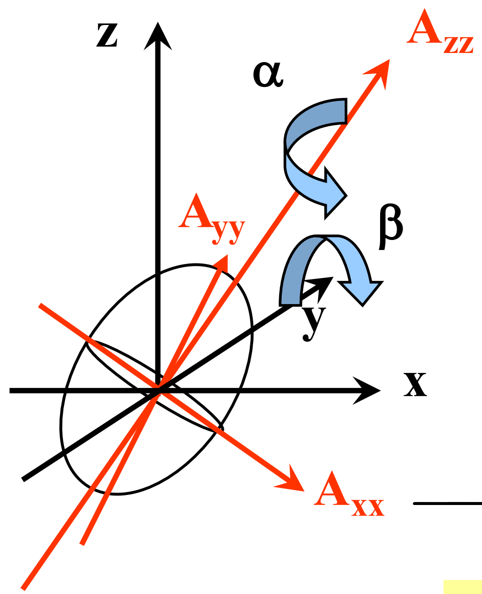

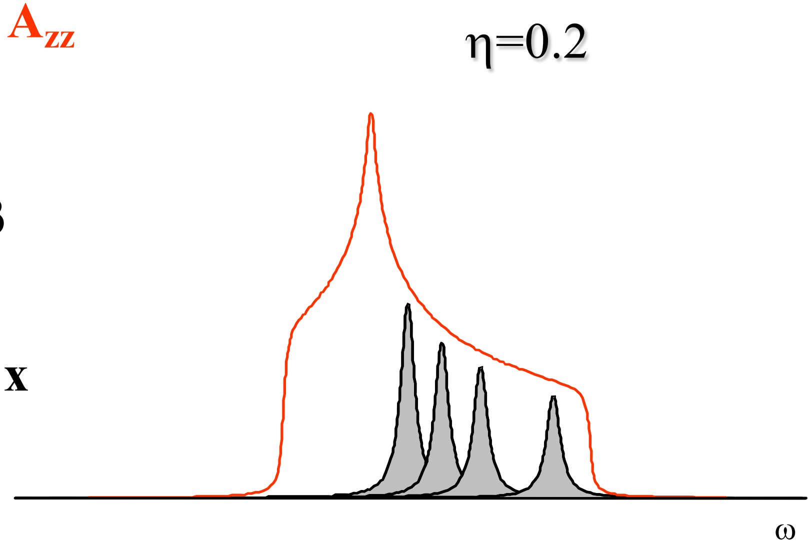

Crystalline Powder overlapping Broad lines

Magic Angle Spinning

^{31}P Spin 1/2 CSA

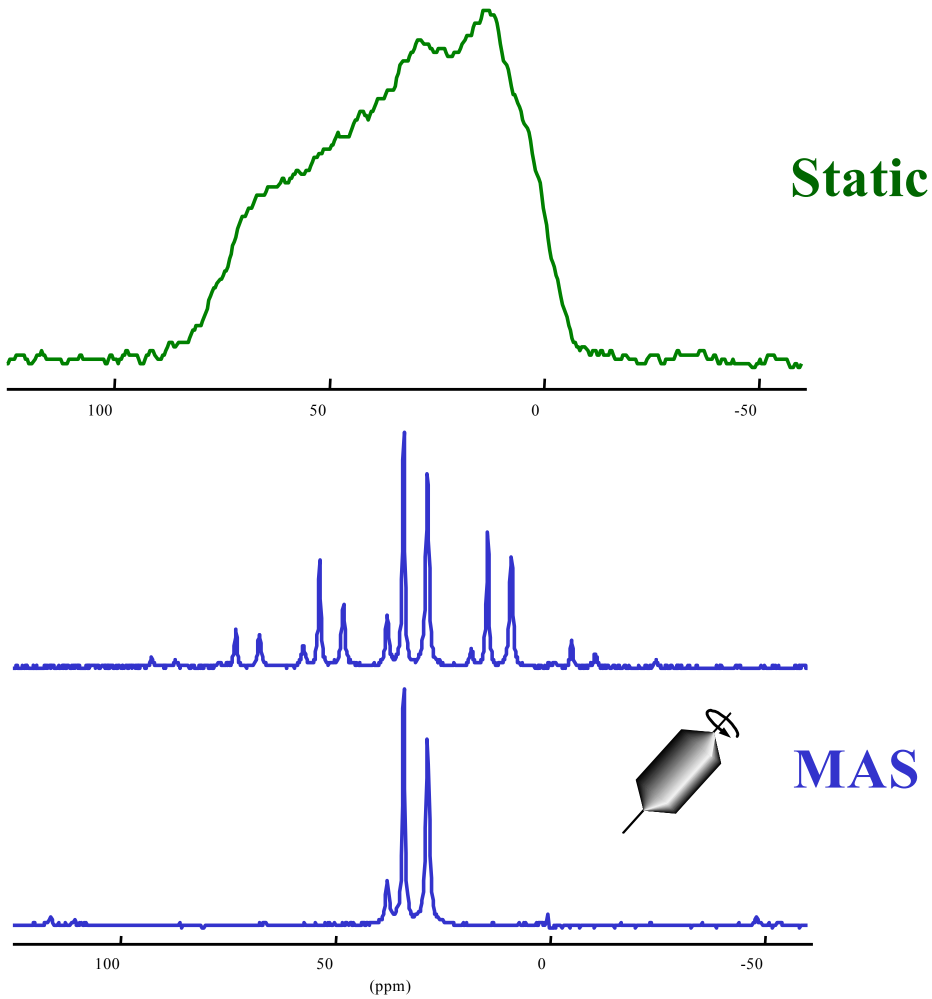

Modulation into sharp lines

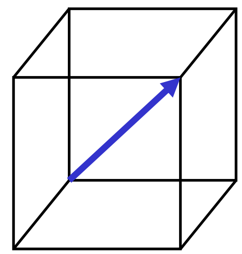

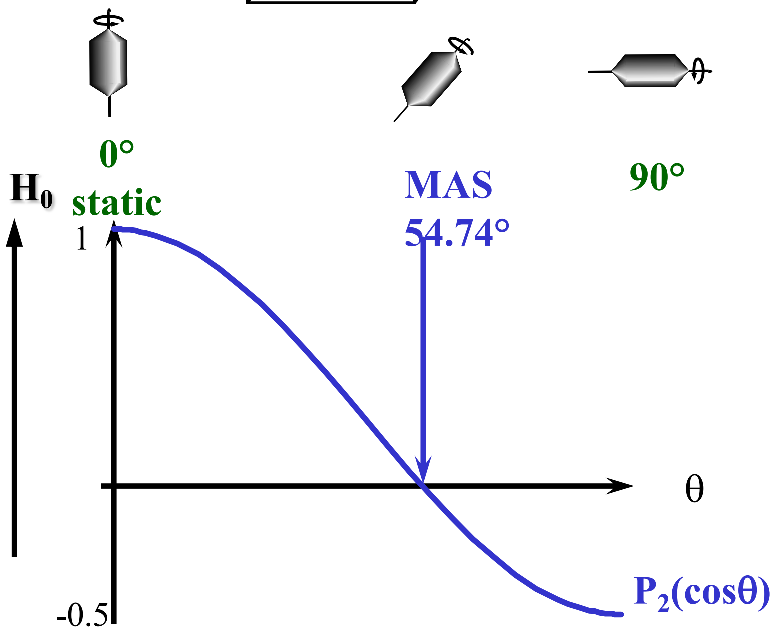

Dipolar -> 0
Chem. Shift -> δ_{iso}
Jcoupling

Quad 1st -> 0
Quad 2^{nd} -> δ^{2nd}

Getting to High Resolution

^{31}P

high speed MAS spinning attenuate dipolar coupling and modulates chemical shift anisotropy

unresolved spectrum
CSA + Dipolar

Static

MAS

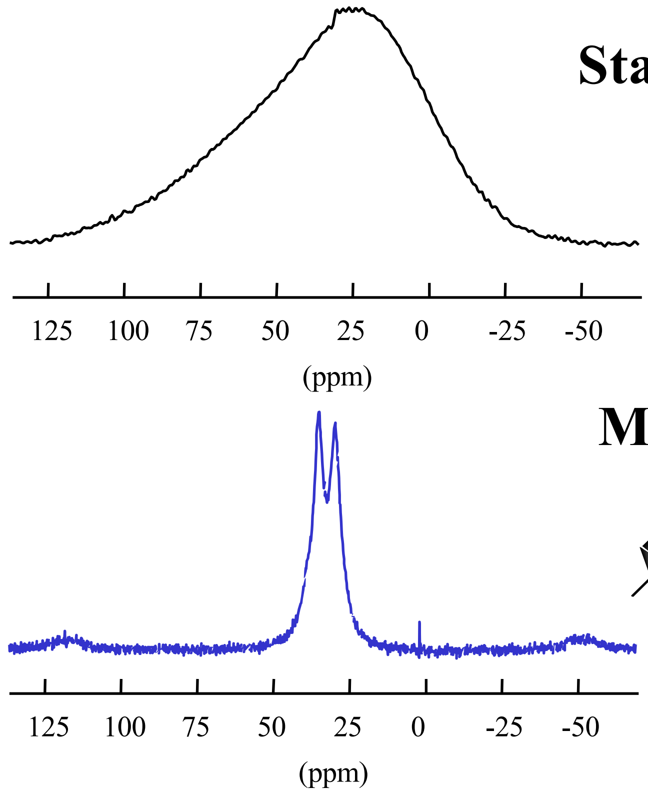

~~CSA~~ **+ Dipolar**

$Zn\ O_3P\ C_2H_4\ CO_2H - 0.5\ C_6H_5NH_2$

Phosphonate (B.Bujoli – Nantes)

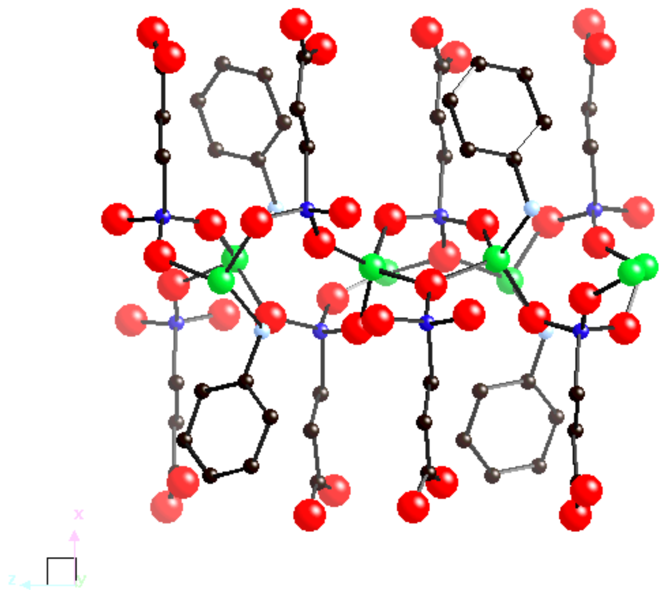

Getting to High Resolution

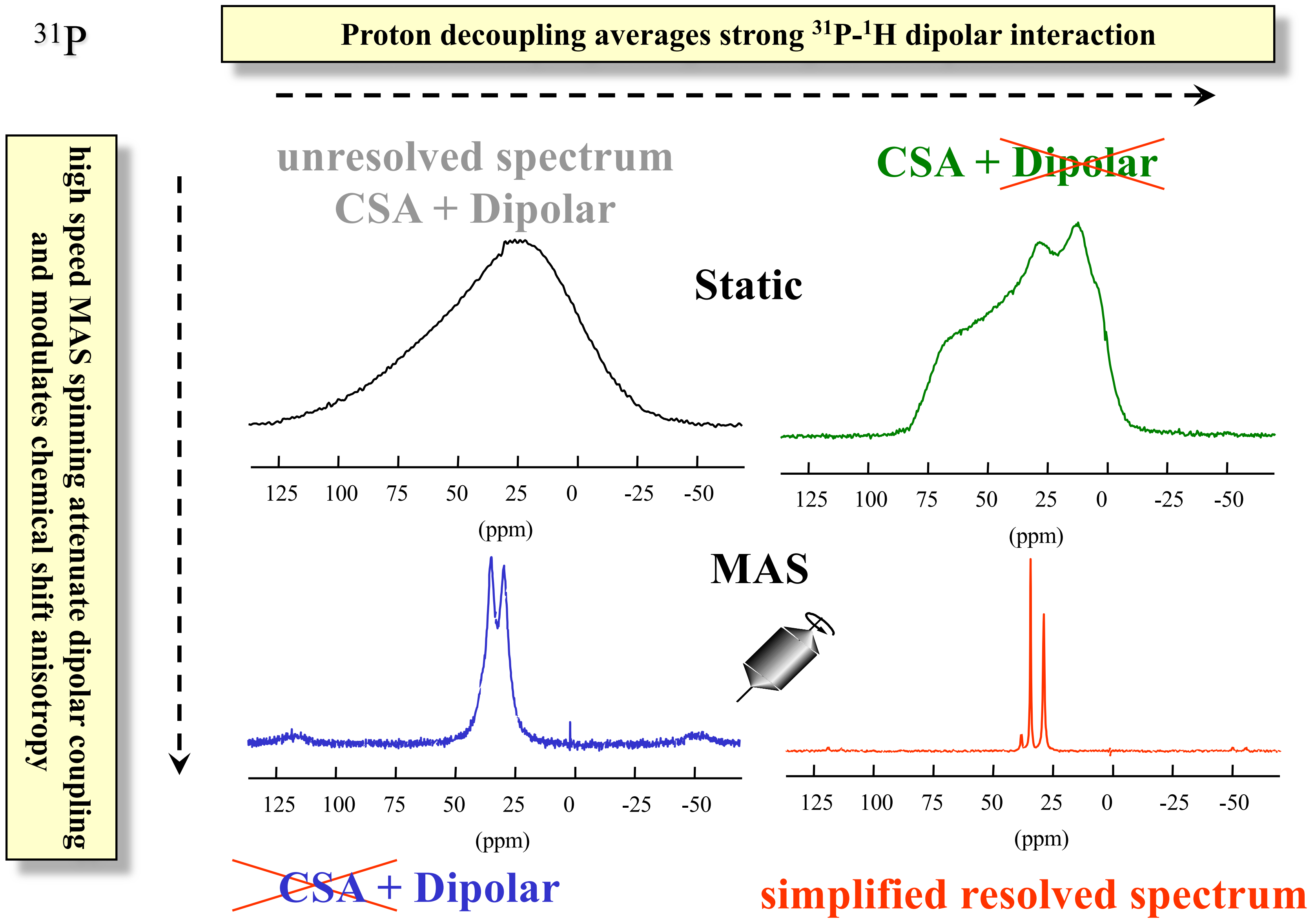

Magic Angle Spinning ^{13}C

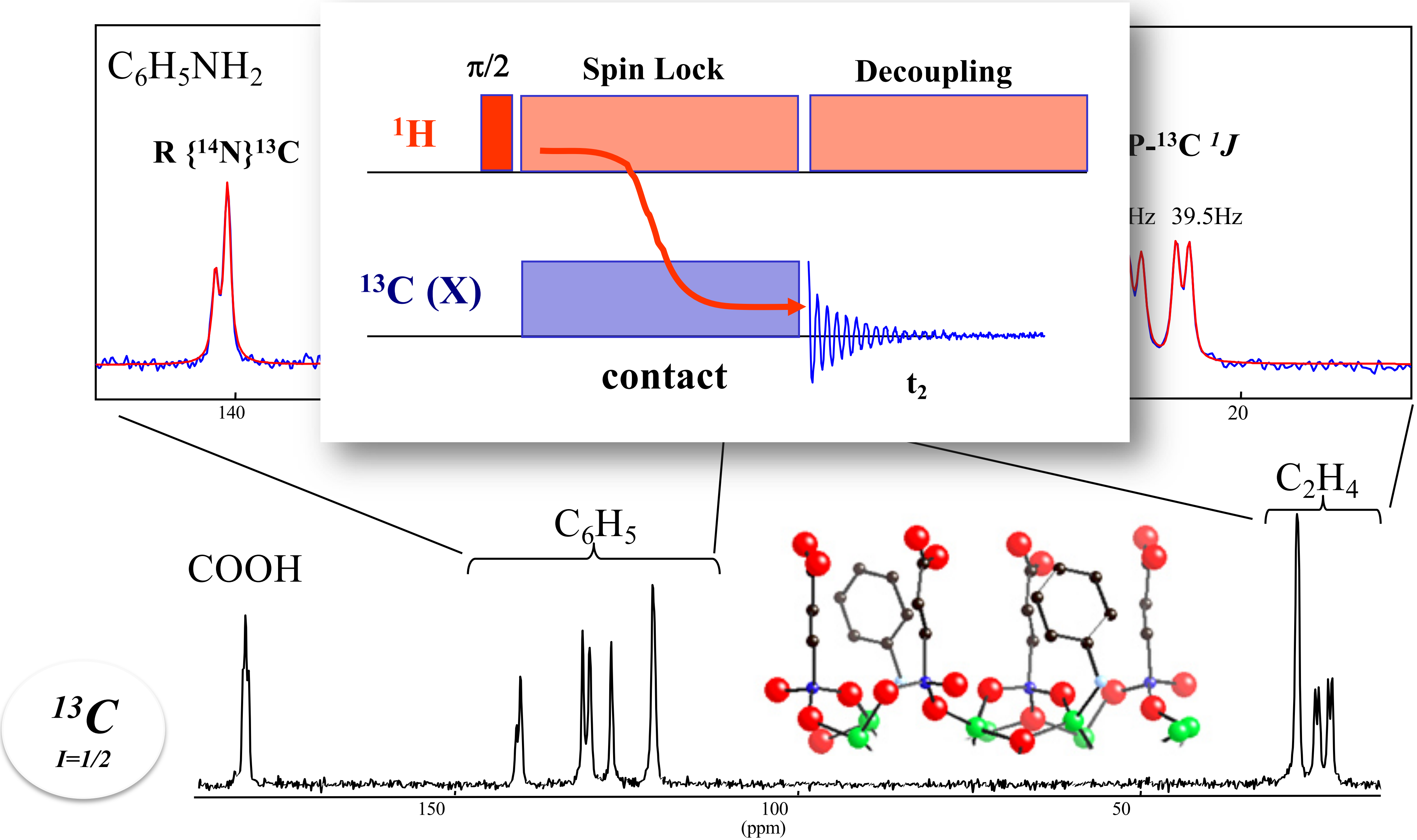

D.Massiot, F.Fayon, M.Deschamps, S.Cadars, P.Florian, V.Montouillout, N.Pellerin, J.Hiet, A.Rakhmatullin, C.Bessada
'Detection and use of small J couplings in solid state NMR experiments.'
Comptes Rendus de Chimie 13 117-129 ***2010***

Solid State NMR Concepts & Methods tool box

Zeeman Interaction
100s of MHz
Sensitivity & spectral resolution (CSA)

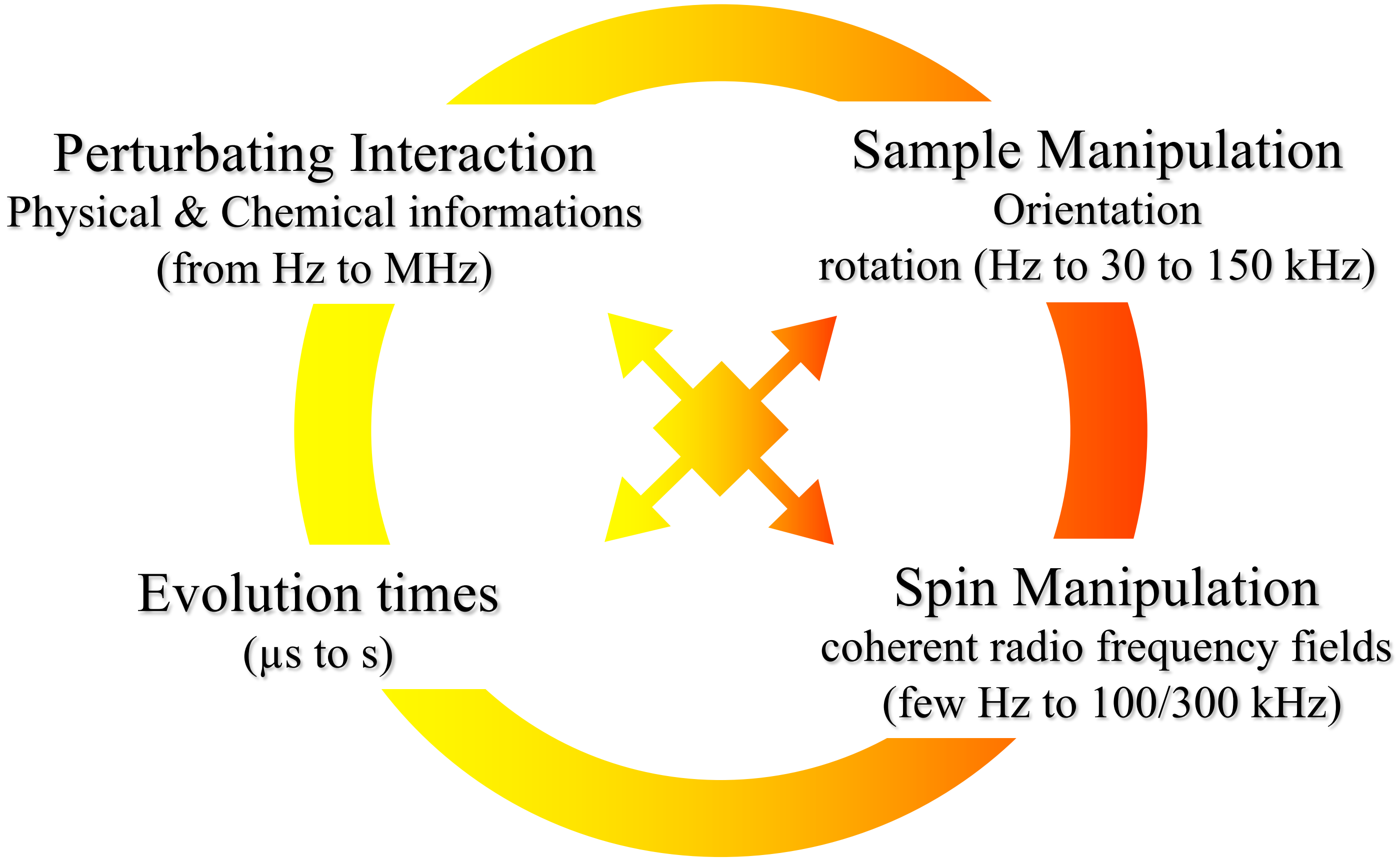

Long lasting relaxation times T1 up to 100s sec – T2 up to 100s ms

^{29}Si - Silica based materials

Chemical Shift Anisotropy
electronic shielding
first shells, coordinence and geometry

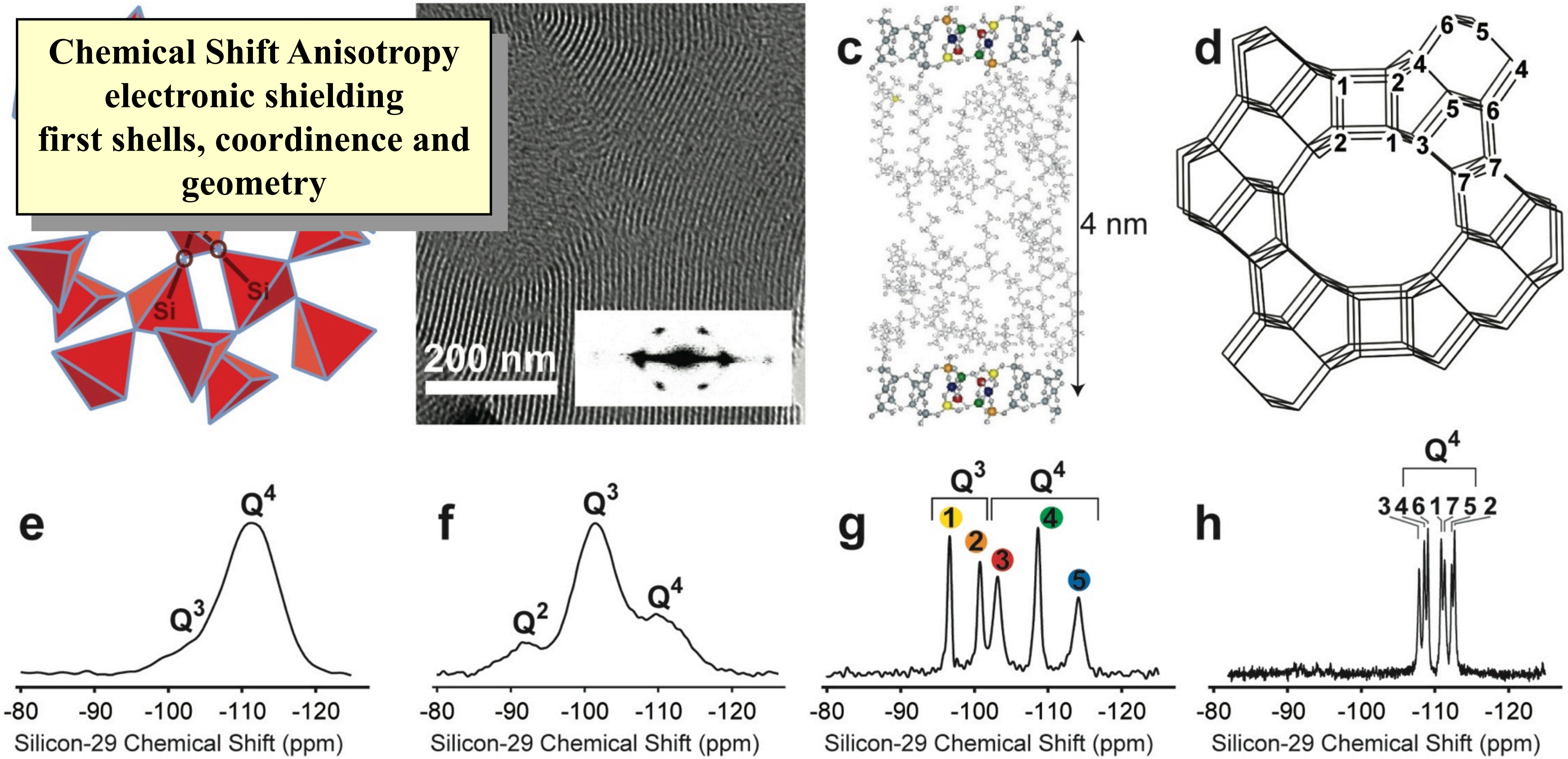

Glass | Mesoporous Silica | SiO_2-surfactant Mesophase | Zeolite

Average Chemical Shift ~ local field
electronic shielding α B_0 -> first shells, coordinence and geometry

D.Massiot, R.J.Messinger, S.Cadars, M.Deschamps, V.Montouillout, N.Pellerin, E.Veron, M.Allix, P.Florian, F.Fayon
Accounts Chem. Res. 46 1975–1984 2013

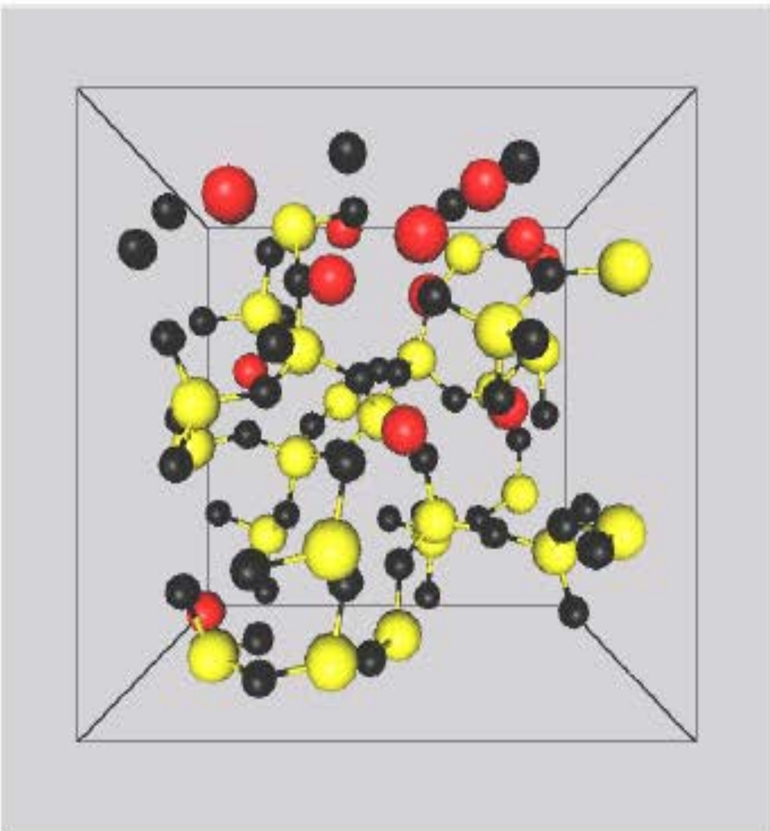

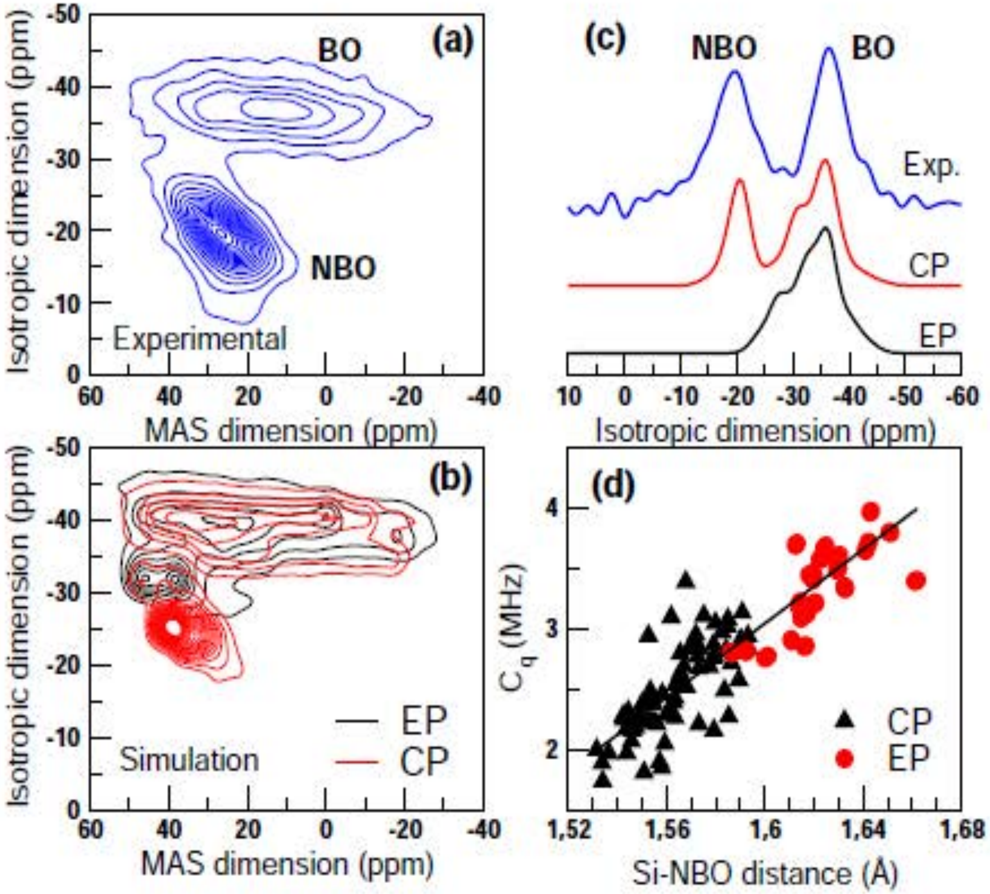

The combination of molecular dynamics simulations with first-principles (or *ab initio*) calculations with density functional theory (DFT) enable the prediction of NMR spectra from a structural model (here oxygen-17 MQMAS). Two spectra are compared, the first from classical molecular dynamics (EP, Effective Potential) and the second from ab-initio molecular dynamics (CP, Car-Parinello). Differences between the two models in Si-NBO distances induce a difference in the position of isotropic peaks of non-bridging oxygens. This can be explained by the high sensitivity of the quadrupole interaction (C_Q) to the Si-NBO distance

S.Ispas, T.Charpentier, F.Mauri, D.Neuvllle – Solid State Science 2010 12 183

T.Charpentier, D.Massiot, in *From glass to crystal phase separation, nucleation and growth, from research to applications*, EDP Sciences, 2017

Diffusion / Model / NMR : local order

B_2O_3 Glass

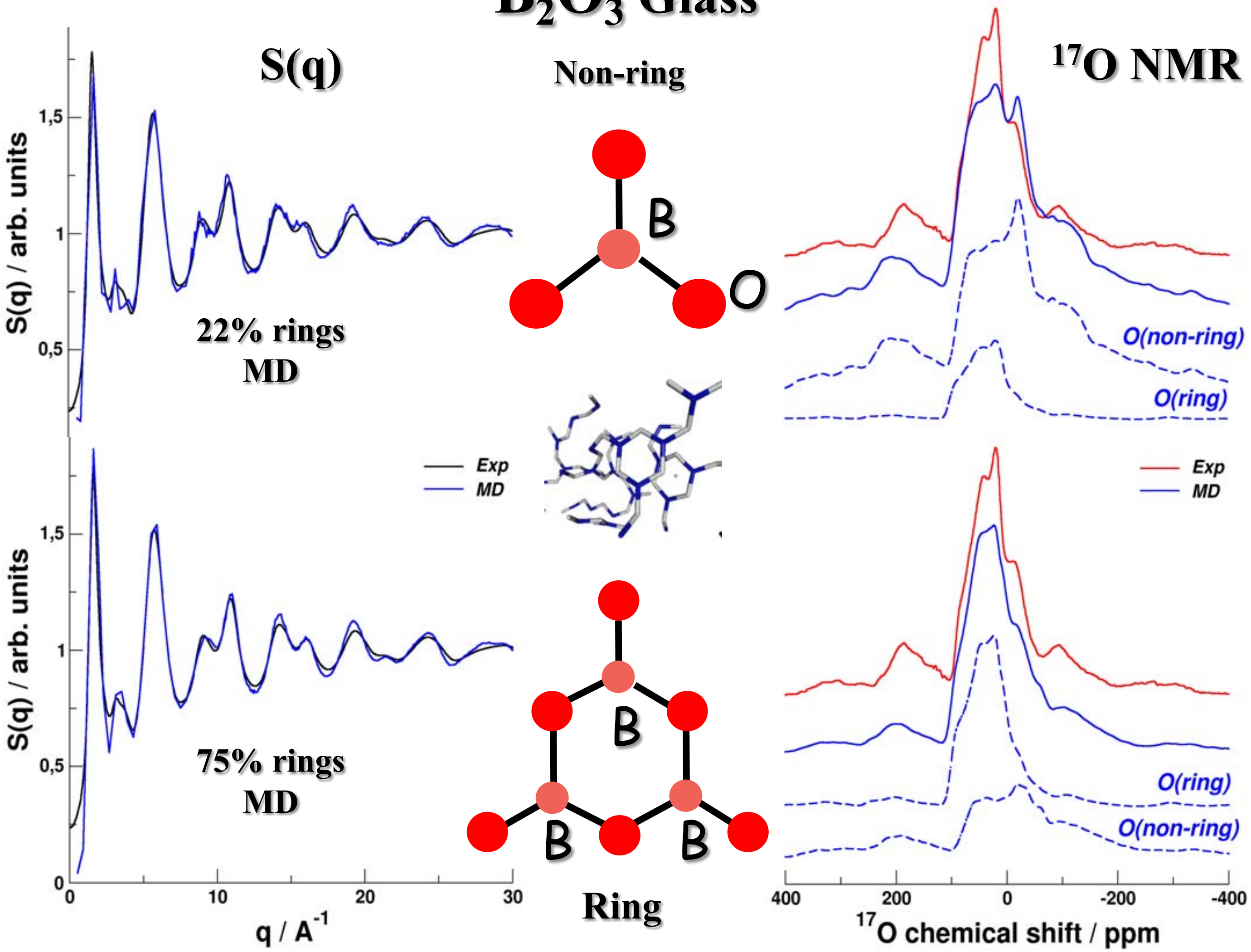

G.Ferlat, T.Charpentier, A.P.Seitsonen, A.Takada, M.Lazzeri, L.Cormier, G.Calas, F.Mauri
"*Boroxol Rings in Liquid and Vitreous B2O3 from First Principles*"
Phys. Rev. Lett. 101 065504 ***2008***

Computing NMR parameters

^{29}Si MAS NMR

$Q^{(n)}$: $Si(OSi)_n(O^-)_{(4-n)}$

^{29}Si MAS NMR:
Direct access to silicon $Q^{(n)}$ speciation

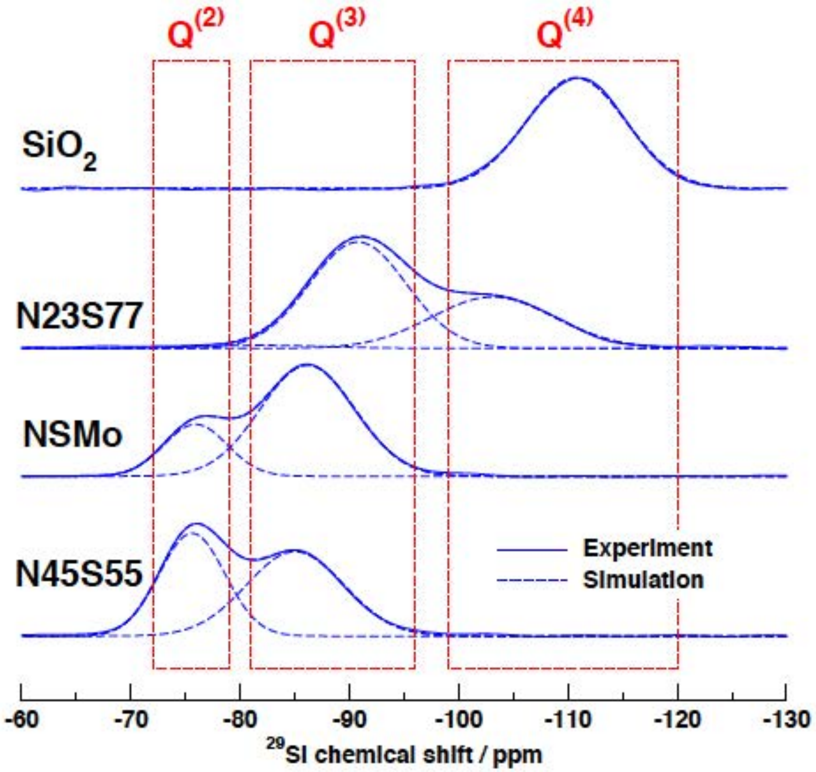

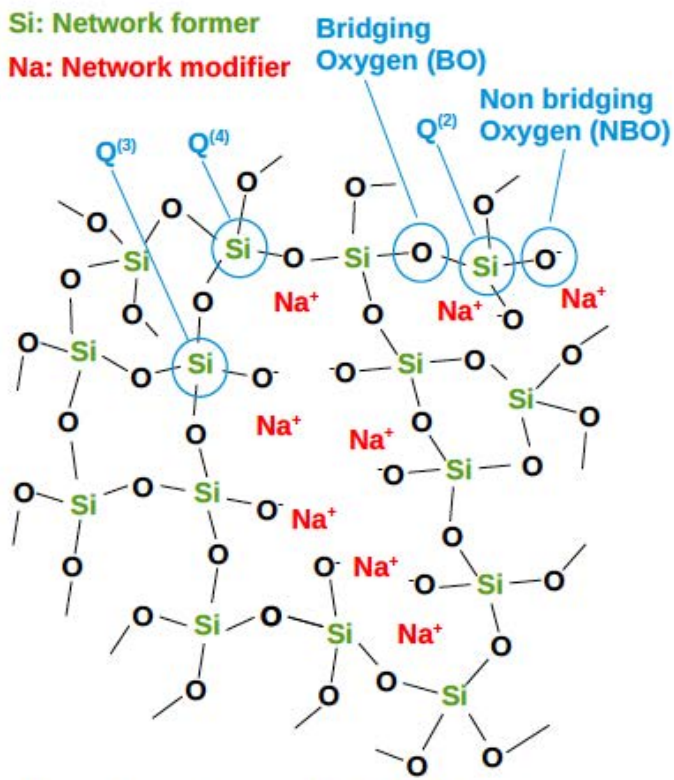

NMR peaks reflective of a Gaussian distribution of δ_{iso} (I=1/2)

Note: $\delta_{iso} = -(\sigma_{ref} - \sigma_{iso})$

Angeli F., *et al.* Geochim. Cosmochim. Acta, 75, 2453-2469, 2011 - Ispas S., *et al.* Solid State Sci., 12, 183-192, 2010

Computing NMR parameters

^{29}Si MAS NMR: Direct access to silicon $Q^{(n)}$ speciation

$Q^{(n)}$: $Si(OSi)_n(O^-)_{(4-n)}$

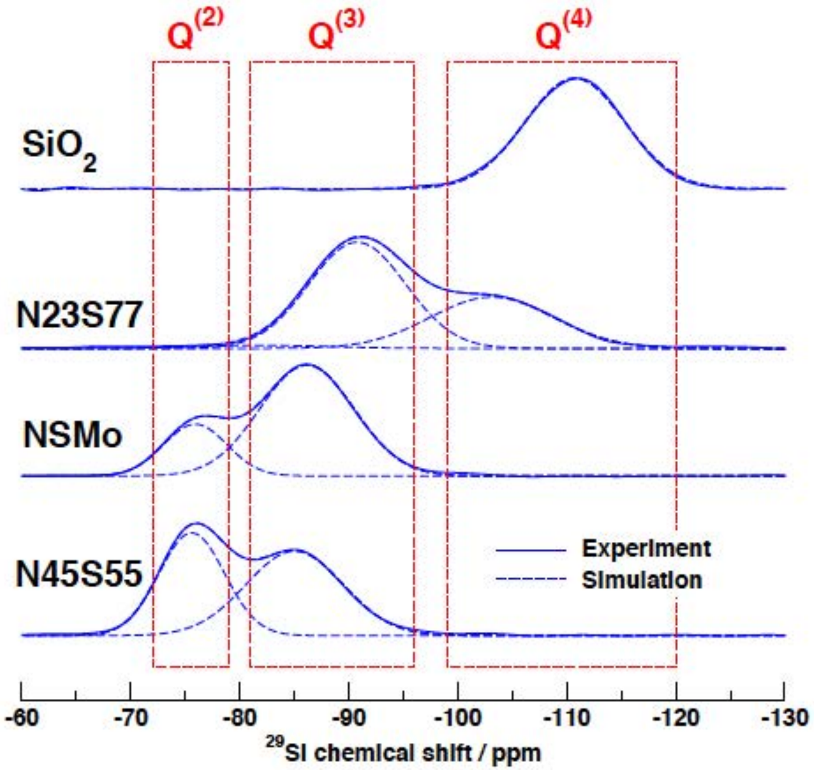

Binary Na_2O - SiO_2 glasses
NSMo: N39S60 + 1 MoO_3

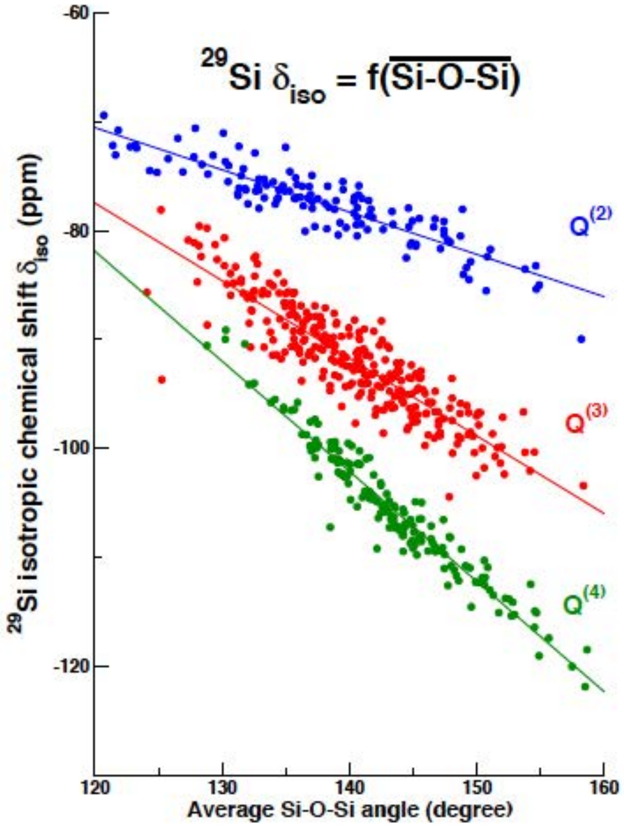

The NMR response of $Q^{(n)}$ species to disorder (bond angle distribution) is different.

Angeli F., *et al.* Geochim. Cosmochim. Acta, 75, 2453-2469, 2011 - Ispas S., *et al.* Solid State Sci., 12, 183-192, 2010

Structure of CaO-SiO_2-P_2O_5 Bioglasses

Silicate (phosphate) network: Q^n units

(SiO_4, PO_4 tetrahedra with n bridging oxygen atoms)

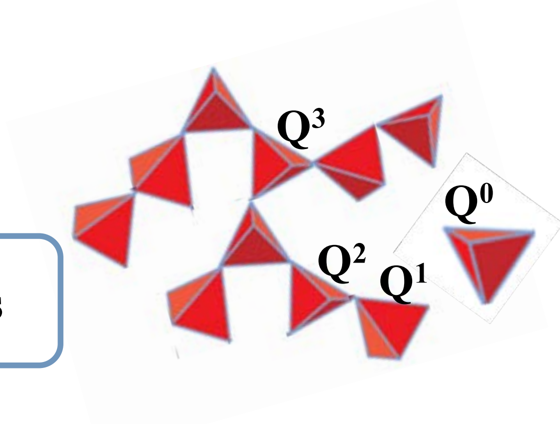

1D MAS spectra of CaO-SiO_2-P_2O_5 glasses

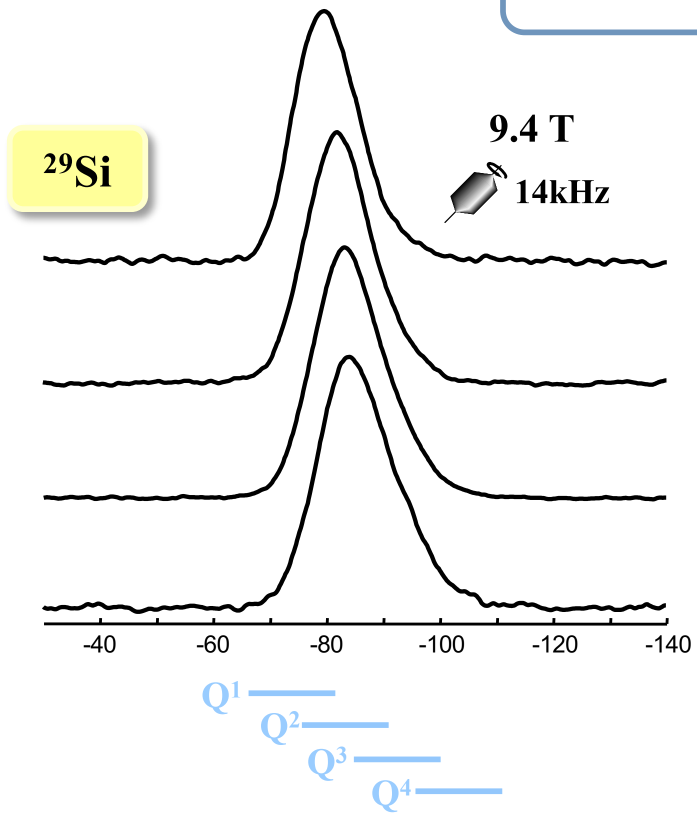

Broad chemical shift distribution (disordered materials)

Ca/Si = 1.11

P_2O_5 ↓

2.6 P_2O_5

3.8 P_2O_5

5.0 P_2O_5

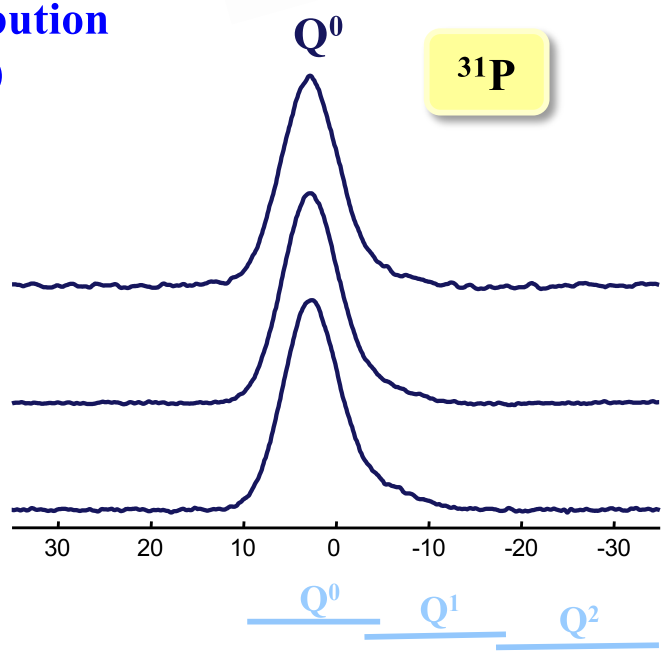

Lack of resolution: Q^n units quantification ?

Mainly orthophosphate units (Q^0 : PO_4^{3-})

F.Fayon, C.Duée, T.Poumeyrol, M.Allix, D.Massiot, J. Phys. Chem. 117 2283-2288 **2013**

Distribution of PO_4^{3-} units in bioactive glasses

Chemical homogeneity ?
(Random distribution)

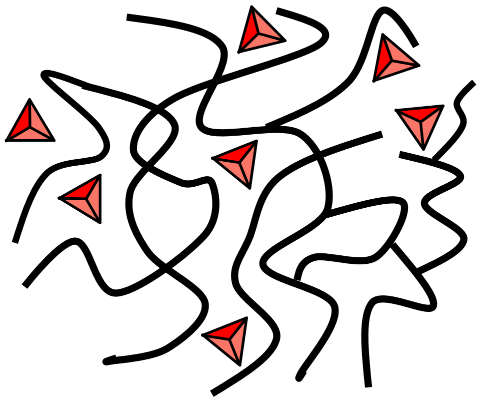

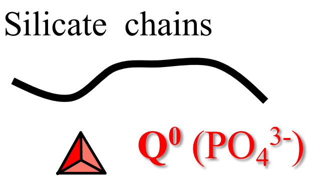

Phosphate clusters ?

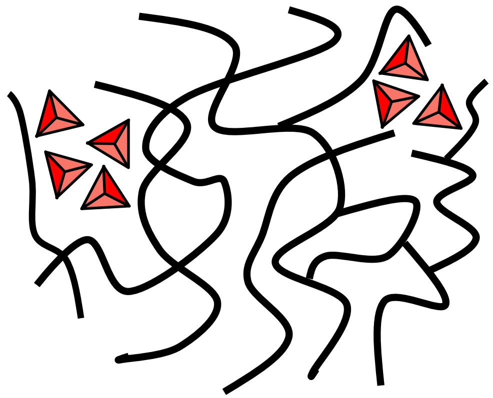

$CaO-SiO_2-P_2O_5$

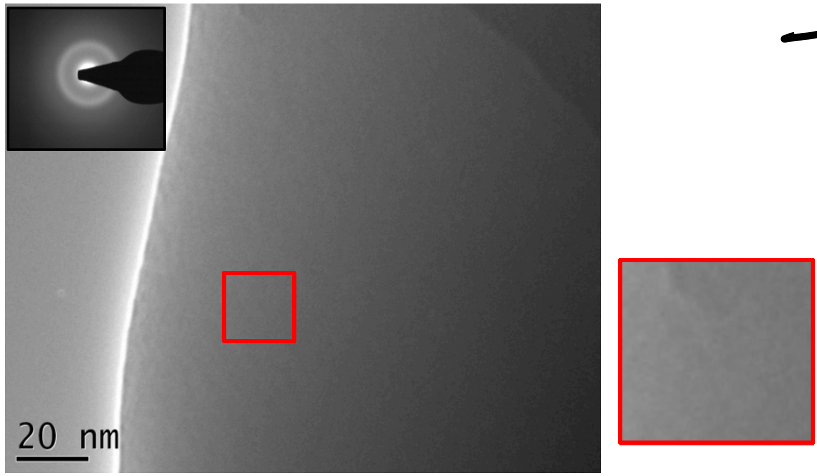

TEM (5.0 mol.% P_2O_5)

- **Very weak Z-contrast** between **Si and P:** **No information from SAXS and TEM**

Counting ^{31}P neighbors by spin-counting dipolar NMR ?

F.Fayon, C.Duée, T.Poumeyrol, M.Allix, D.Massiot, J. Phys. Chem. 117 2283-2288 **2013**

Counting neighboring ^{31}P spins

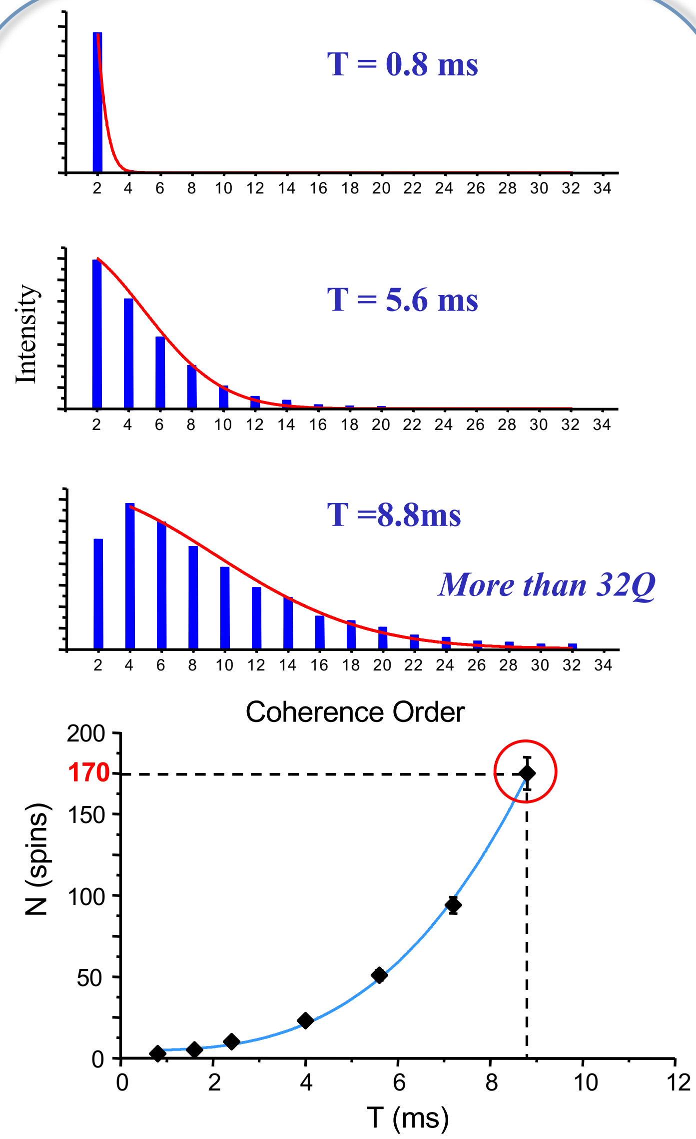

$Ca_4P_2O_9$

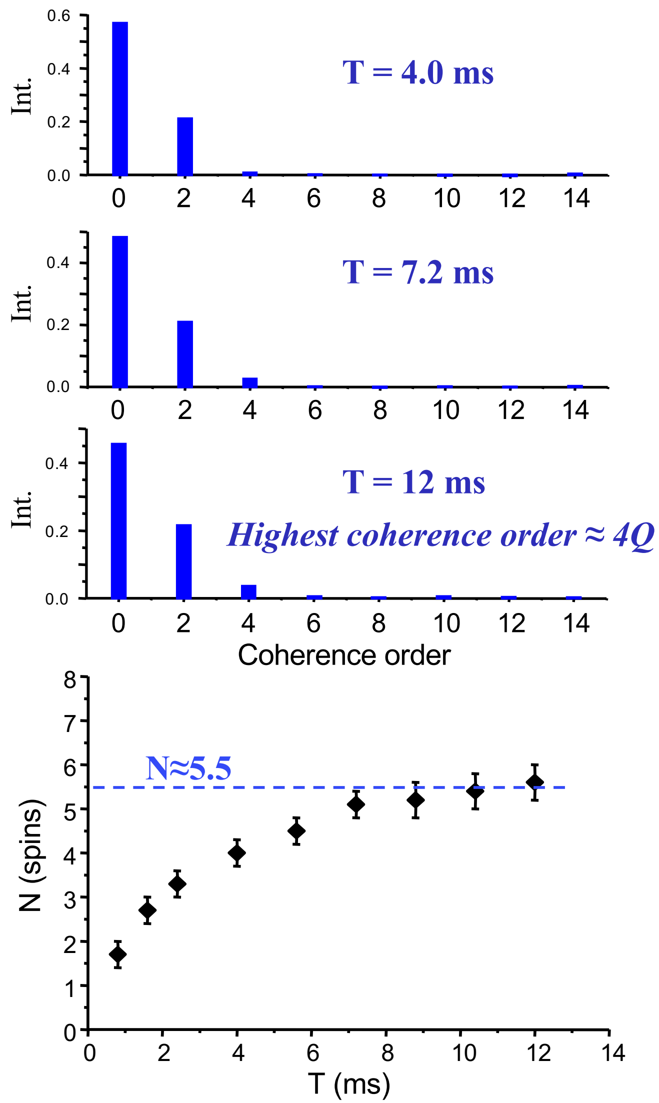

BioGlass – 2.6%P_2O_5

F.Fayon, C.Duée, T.Poumeyrol, M.Allix, D.Massiot, J. Phys. Chem. 117 2283-2288 **2013**

Static ^{31}P-^{31}P Dipolar network

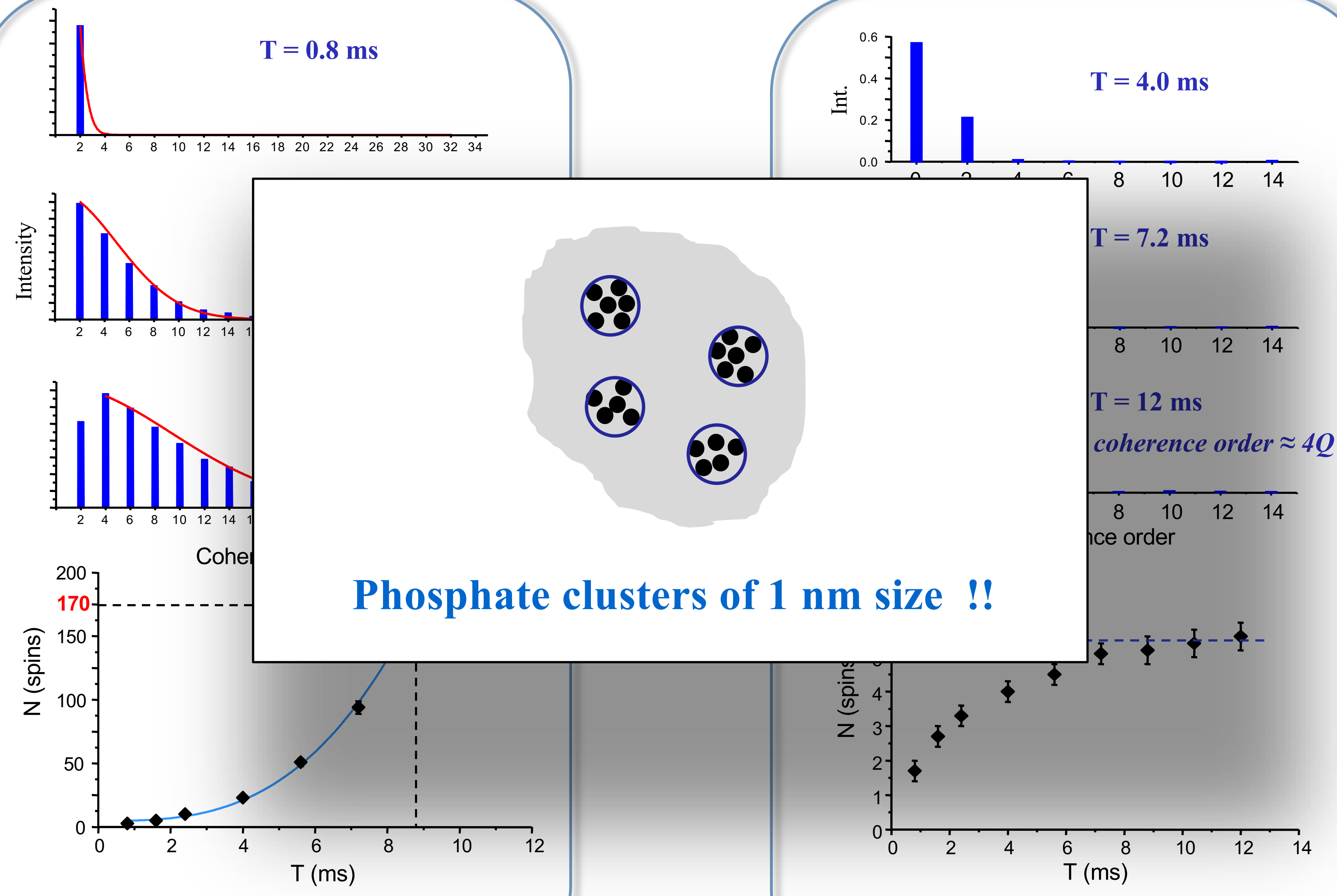

$Ca_4P_2O_9$

BioGlass – 2.6%P_2O_5

F.Fayon, C.Duée, T.Poumeyrol, M.Allix, D.Massiot, J. Phys. Chem. 117 2283-2288 **2013**

^{207}Pb / ^{31}P NMR in PbO-P_2O_5 glasses

Fayon et al., *JACS* **119** (1997), *JNCS* **232-234** (1998)., *JNCS* **243** (1999), *JMR* **137** *(1999), Inorg. Chem.* **38** *(1999)* .

^{31}P MAS NMR spectra

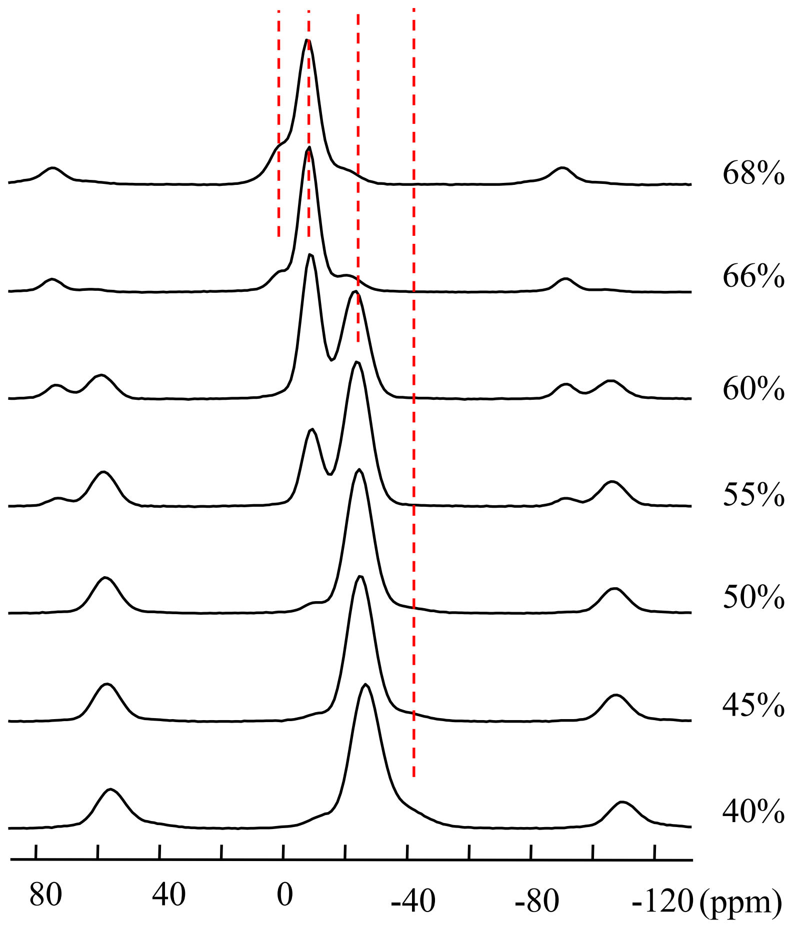

^{207}Pb static NMR spectra

NMR static or MAS

XAFS

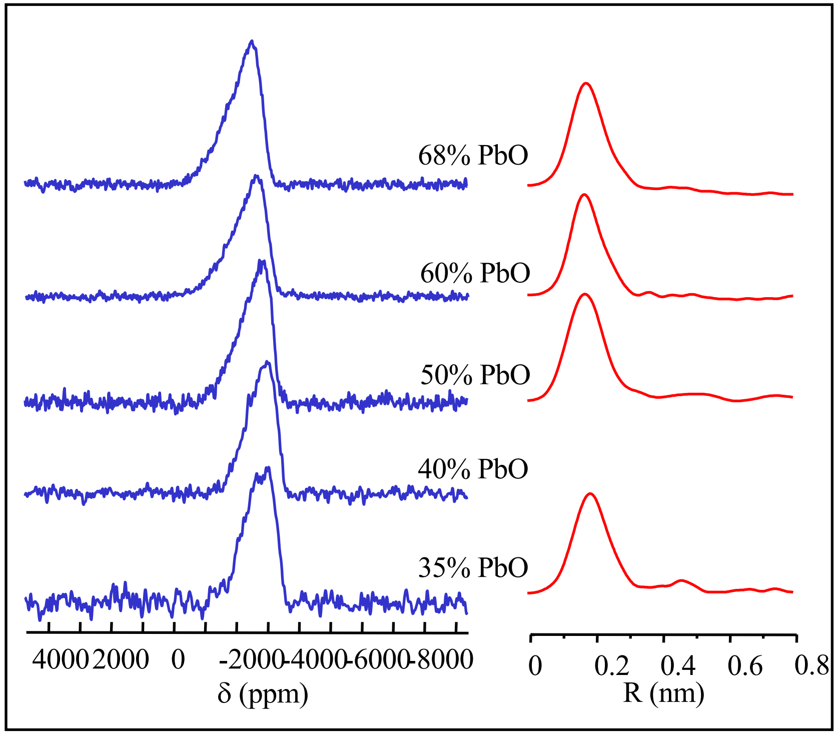

P_2O_5-PbO

- CN ~ 9 to 7
- d(Pb-O) ~ 0.26-7nm

CSA : ^{207}Pb NMR in PbO-P_2O_5 glasses

Fayon et al., *JACS* **119** (1997), *JNCS* **232-234** (1998)., *JNCS* **243** (1999), *JMR* **137** *(1999), Inorg. Chem.* **38** *(1999)* .

NMR
static or MAS

XAFS

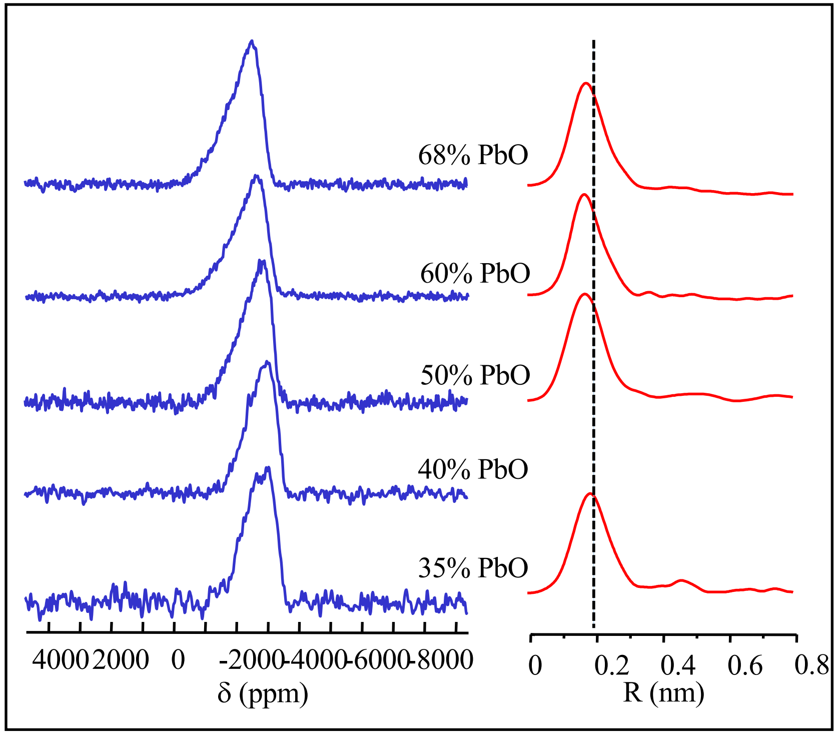

P_2O_5-PbO
- CN ~ 9 to 7
- d(Pb-O) ~ 0.26-7nm

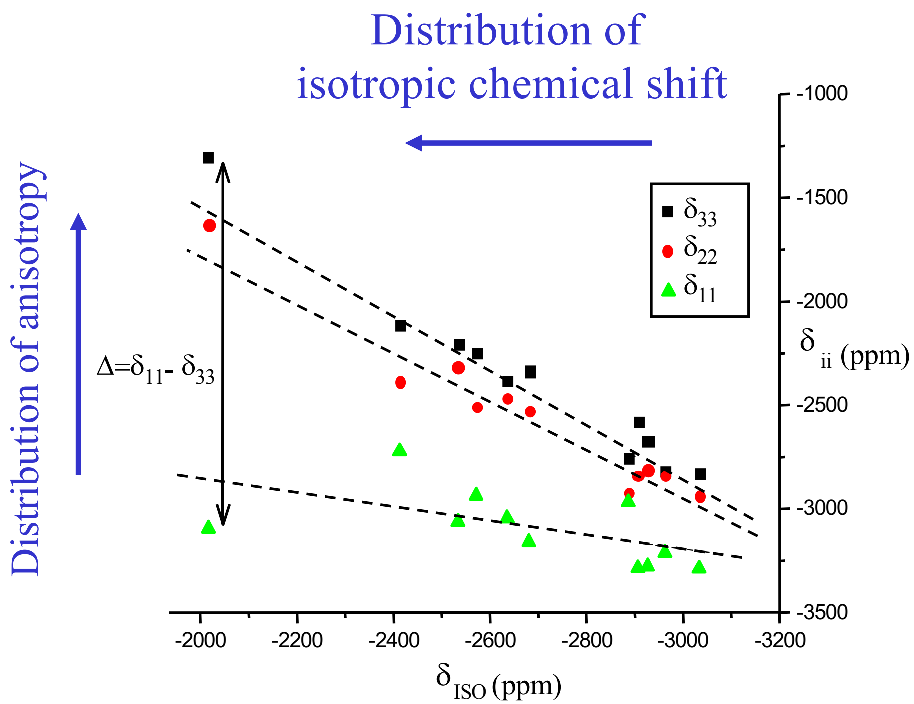

Distribution of ionic to covalent chemical binding of Pb in the network

^{31}P NMR in $PbO-P_2O_5$ glasses

Fayon et al., *JACS* **119** (1997), *JNCS* **232-234** (1998)., *JNCS* **243** (1999), *JMR* **137** *(1999), Inorg. Chem.* **38** *(1999)*.

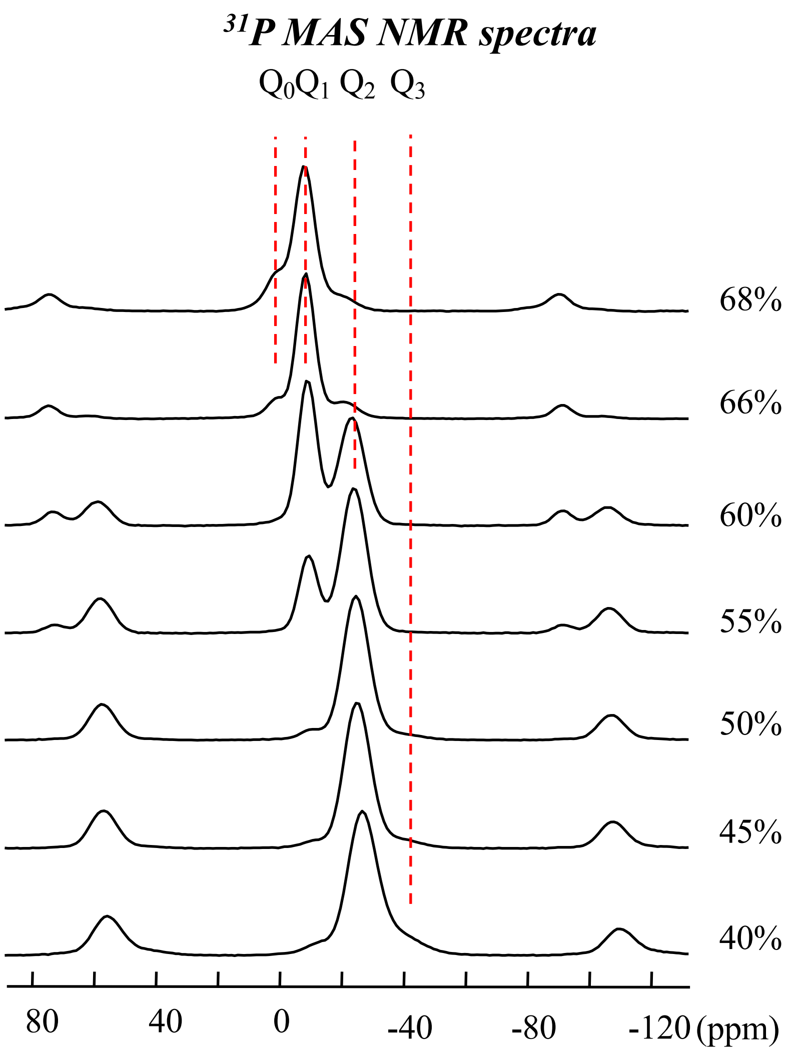

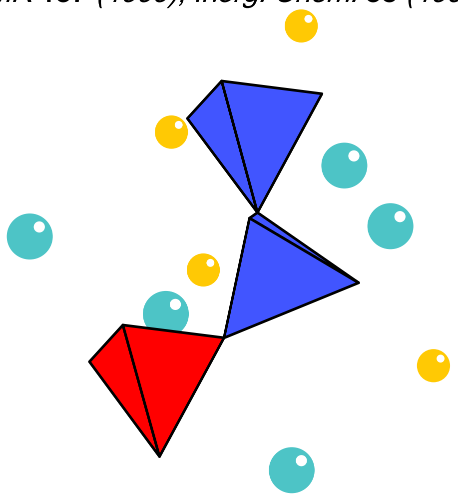

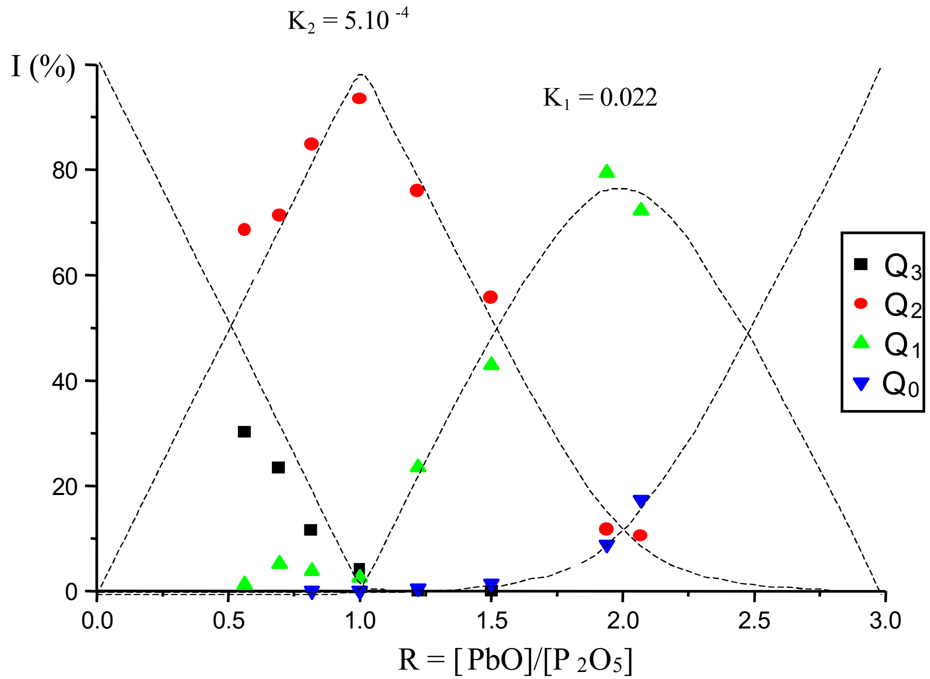

Phosphate Glasses : ^{31}P MAS NMR

$(PbO)_{0.61}(P_2O_5)_{0.39}$ glass

Q^1 (end of chain)
750 Hz

Q^2 (middle of chain)
1200 Hz

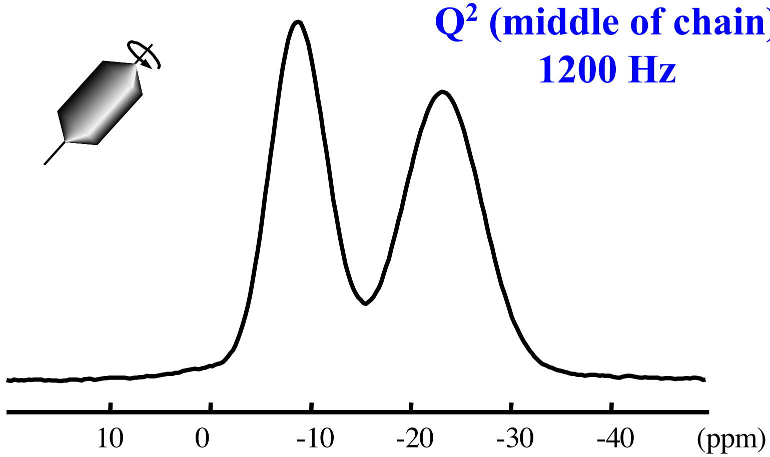

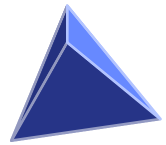

$[Q^1] = [Q^2]$

Average chain length
$N_{av.} \sim 4$

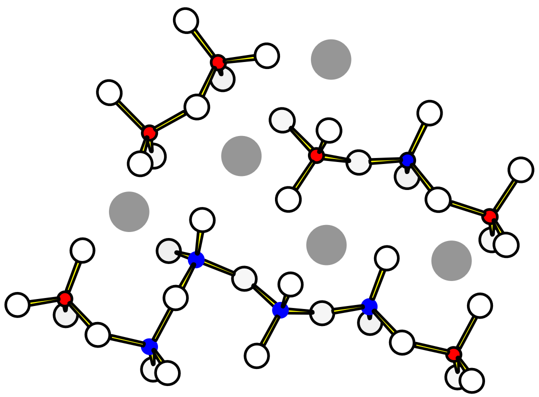

? Nature
of disorder at
the nanometric
scale ?

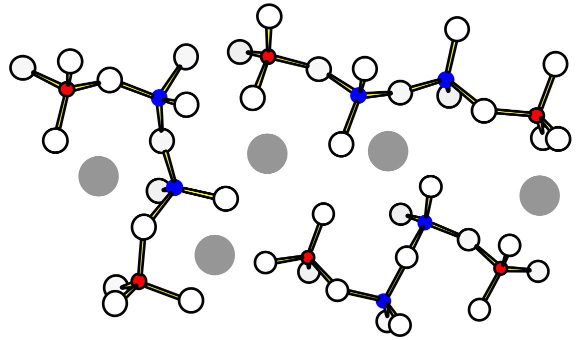

Chain length distribution?
Chemical disorder

Chain geometries?
Topological or geometrical disorder

P-O-P chemical bonds can be viewed from J based P-P experiments

2D NMR

The unpublished Baško Polje (1971) lecture notes about two-dimensional NMR spectroscopy

J. Jeener

Faculté des Sciences (CPI-232), Campus Plaine, Université Libre de Bruxelles, B-1050 Brussels, Belgium

Abstract. — The main part of this paper is a reproduction of (previously unpublished) lecture notes, which were circulated in 1971, and which are often cited as the initiation of two-dimensional NMR spectroscopy. A brief discussion follows, about the way of handling dates and durations in time-dependent quantum mechanics, and about the use of diagrams in NMR pulse spectroscopy in the usual or the superoperator formalisms.

In « *NMR and More* », M. Goldman et M. Porneuf Eds (1994)

Two-dimensional spectroscopy. Application to nuclear magnetic resonance

W. P. Aue, E. Bartholdi, and R. R. Ernst

Laboratorium für physikalische Chemie, Eidgenössische Technische Hochschule, 8006 Zürich, Switzerland

(Received 13 November 1975)

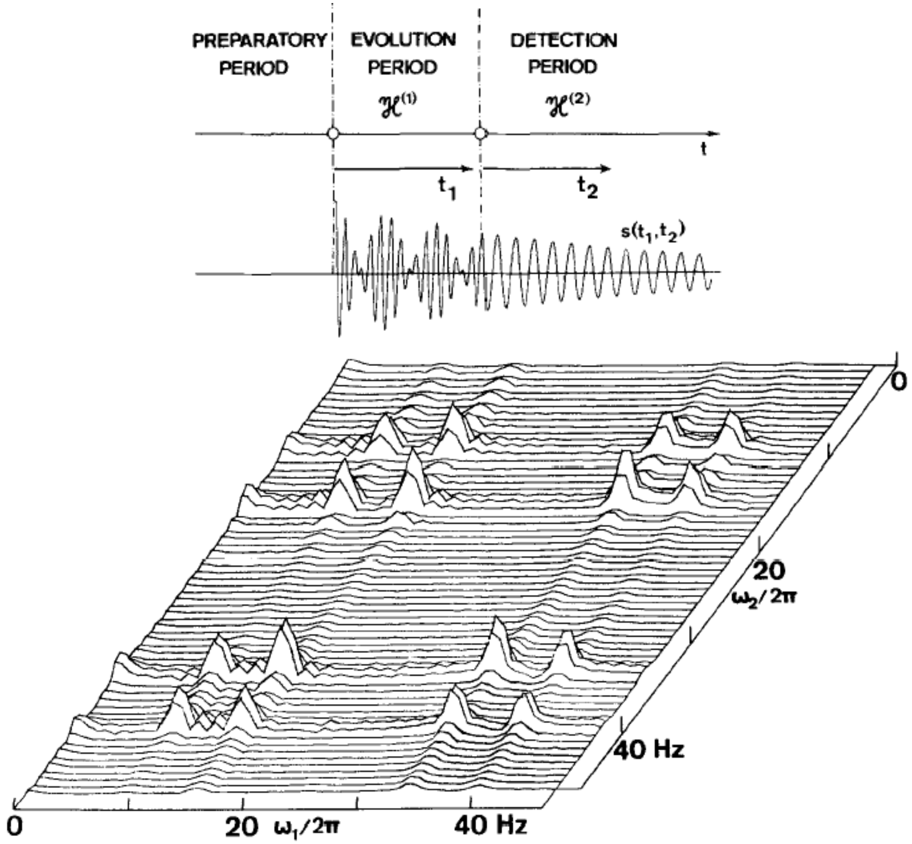

J. Chem. Phys., **64**, 2229 (1974)

Hahn Echo – Spin Echo

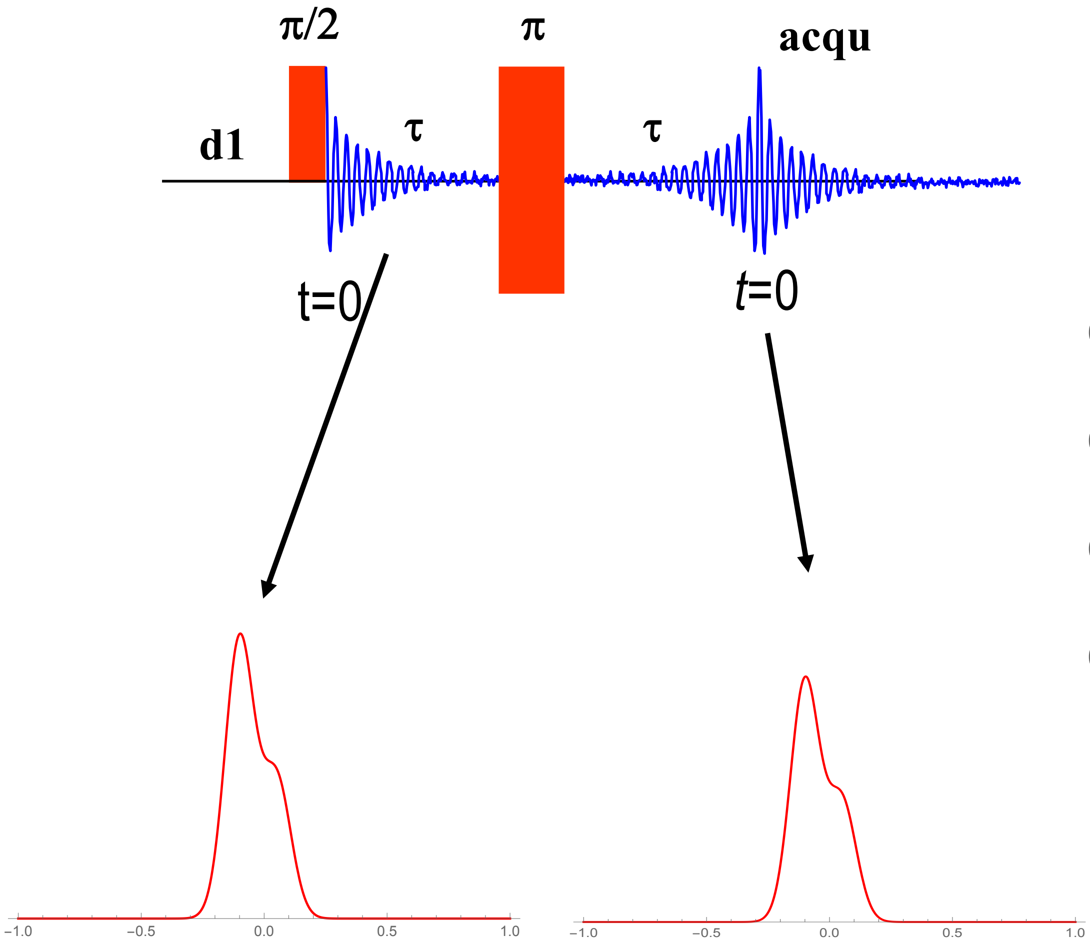

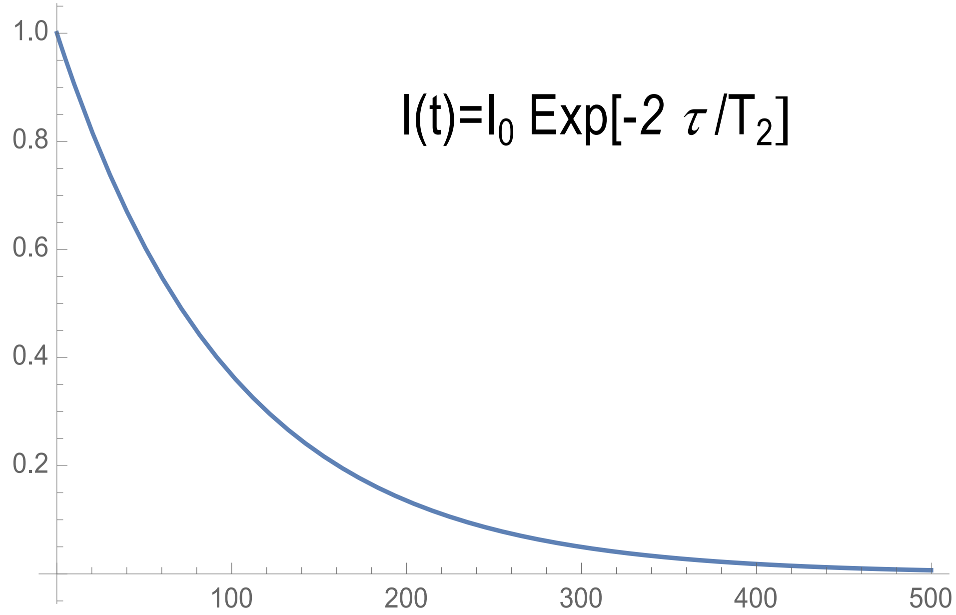

$$I(t)=I_0\ \mathrm{Exp}[-2\ \tau/T_2]$$

Measurement of T_2
the life time of the coherence
in the XY [transverse] plane

2D Exchange (NOESY - EXSY)

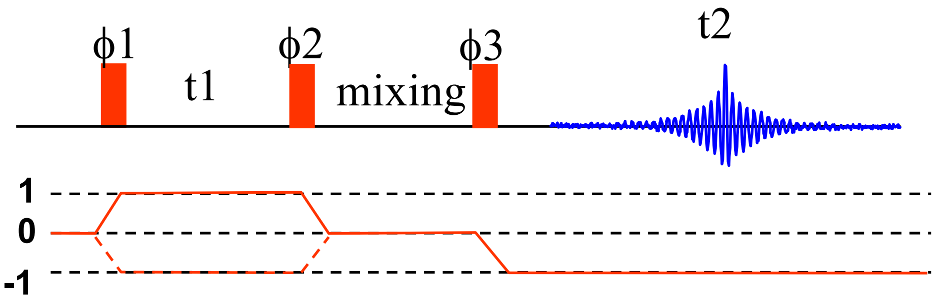

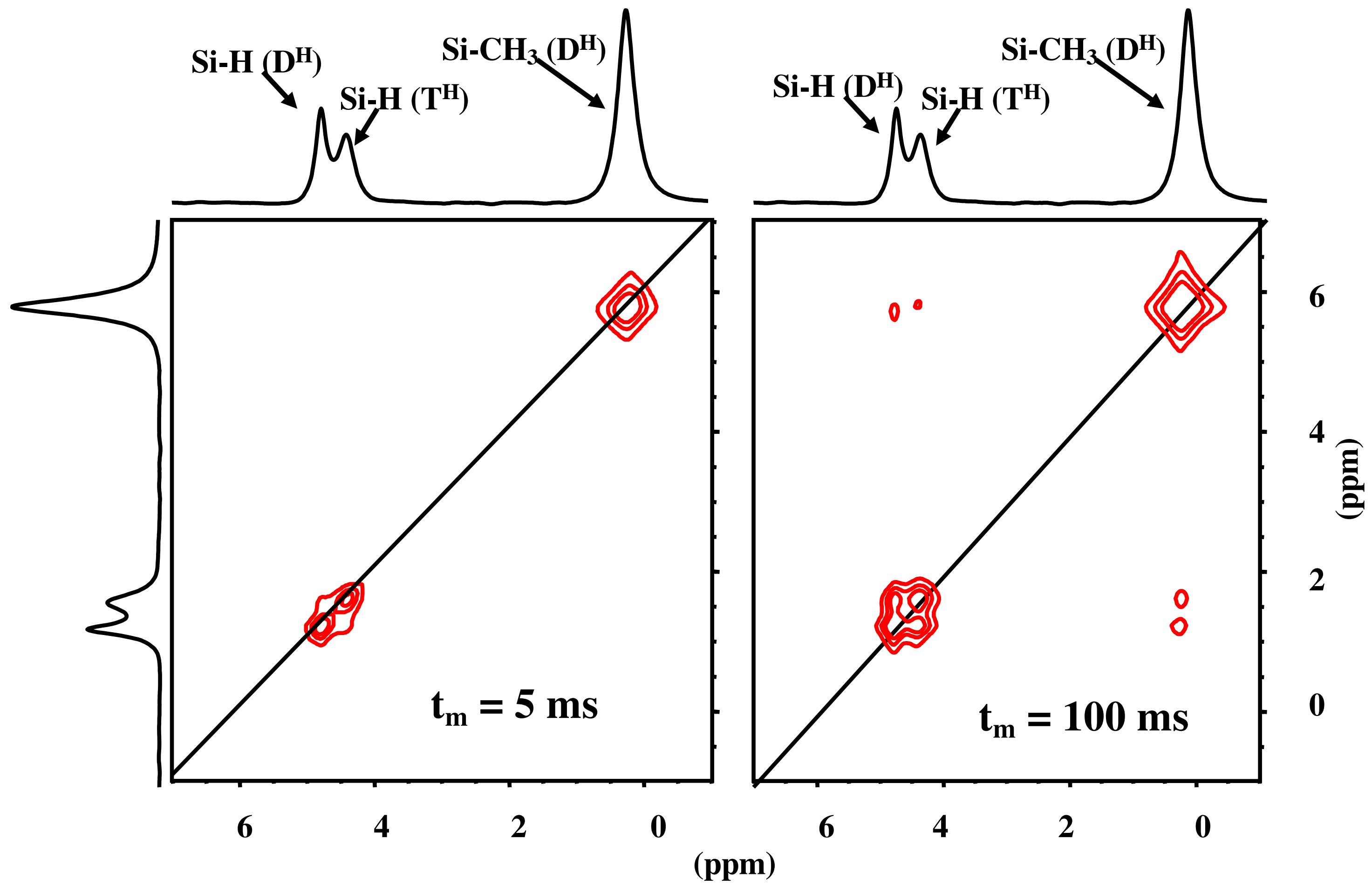

Principle of a 2D homonuclear experiment

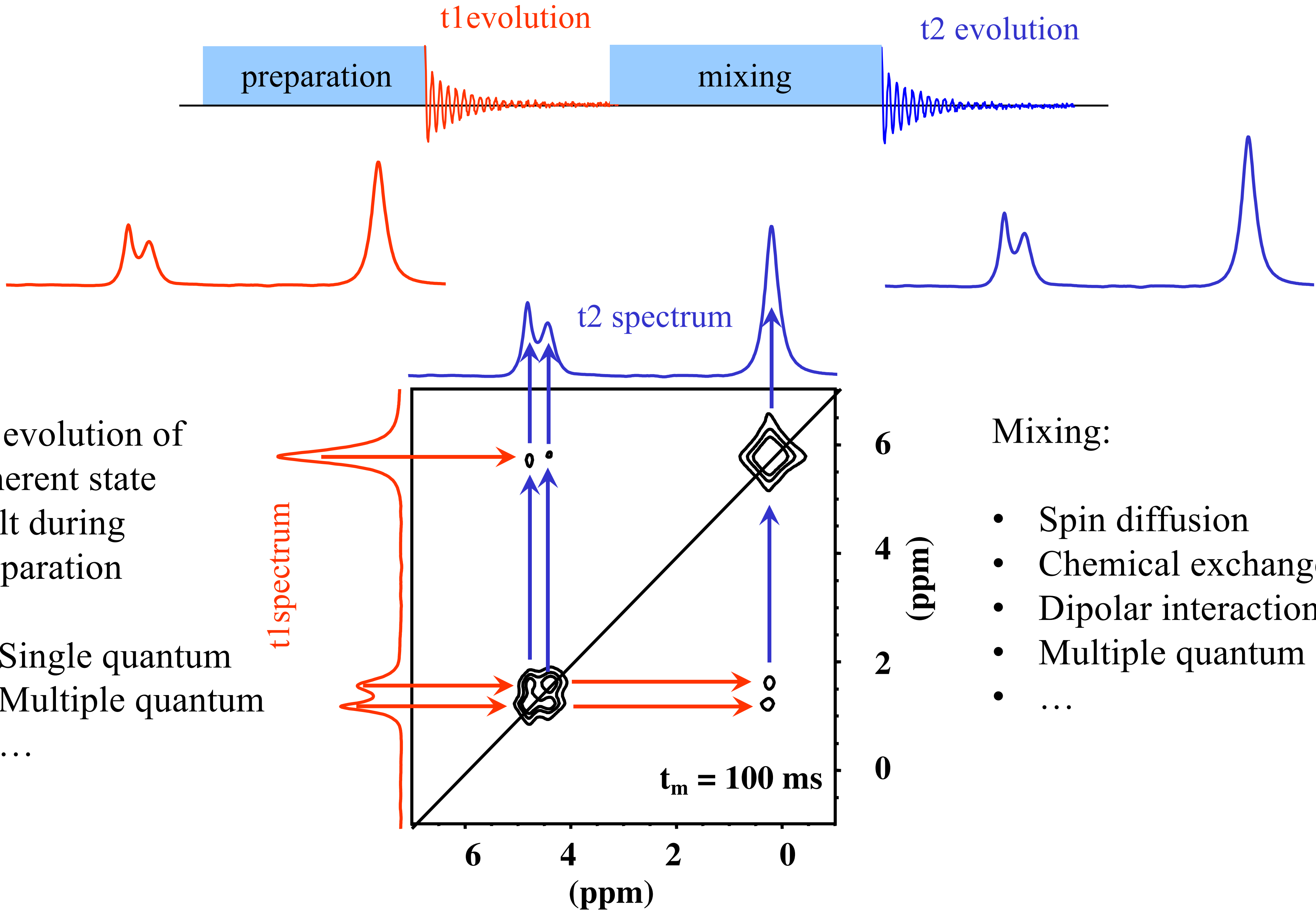

t_1 : evolution of coherent state built during Preparation

- Single quantum
- Multiple quantum
- …

Mixing:

- Spin diffusion
- Chemical exchange
- Dipolar interaction
- Multiple quantum filter
- …

Anisotropic nature of local structure

^{29}Si MAF Spectrum of K_2O-$2SiO_2$

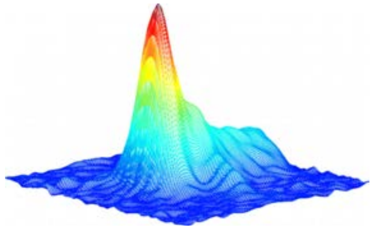

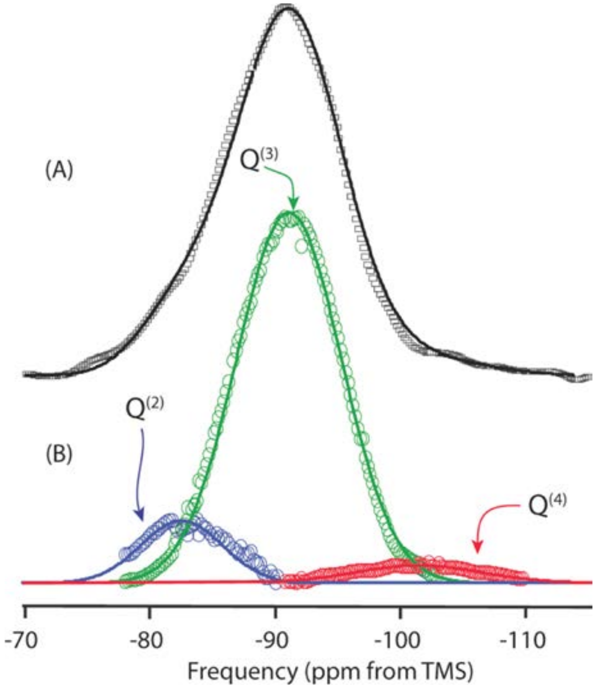

Isotropic MAS

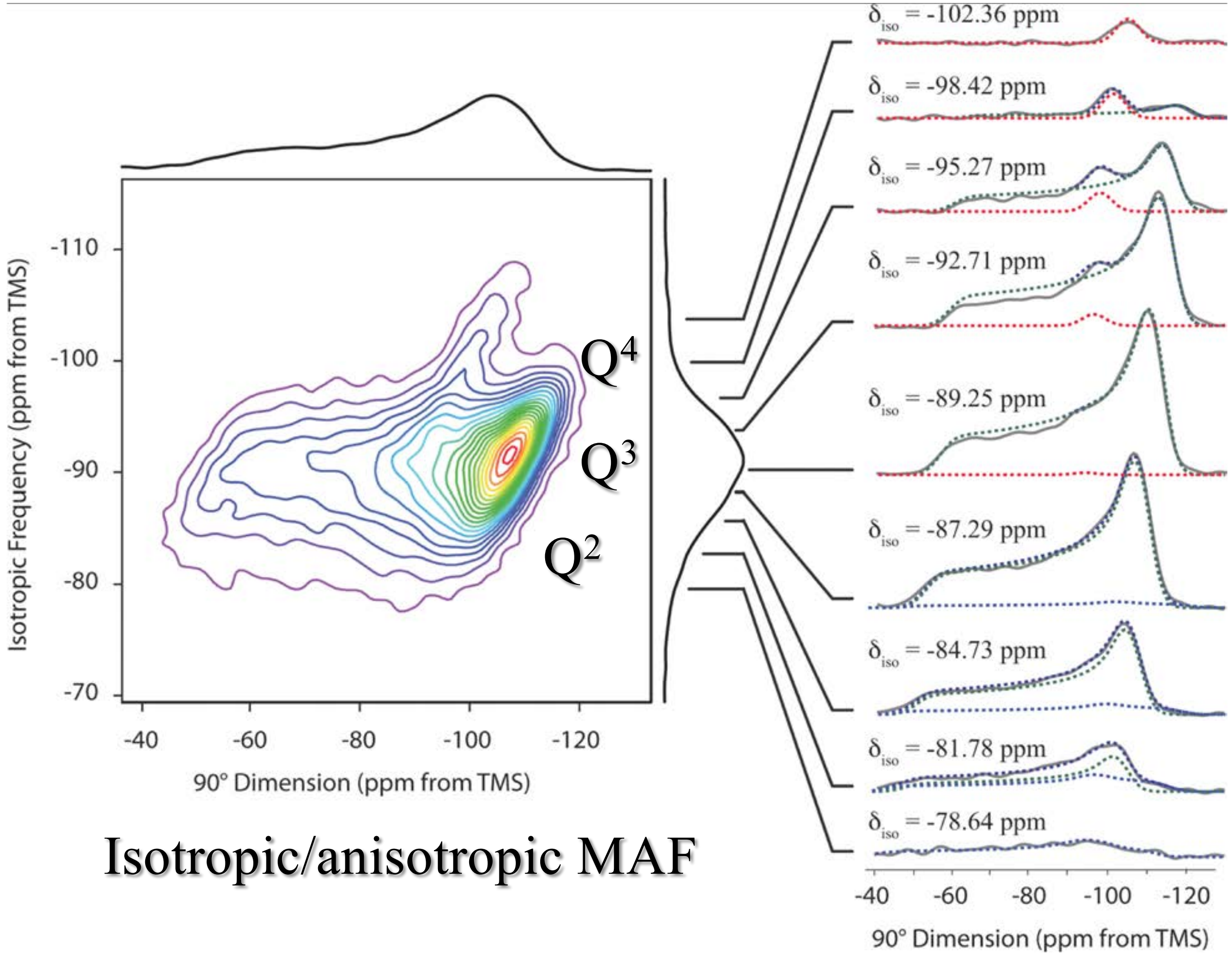

Isotropic/anisotropic MAF

M.Davis, D.Kaseman, S.Parvani, K.Sanders, P.J.Grandinetti, P.Florian, D.Massiot
Q(n)-Species Distribution in K2O • 2 SiO2 Glass by 29Si Magic Angle Flipping NMR
J. Phys. Chem. A 114 5503–5508 (2010)

Phosphate Glasses : ^{31}P MAS NMR

$(PbO)_{0.61}(P_2O_5)_{0.39}$ glass

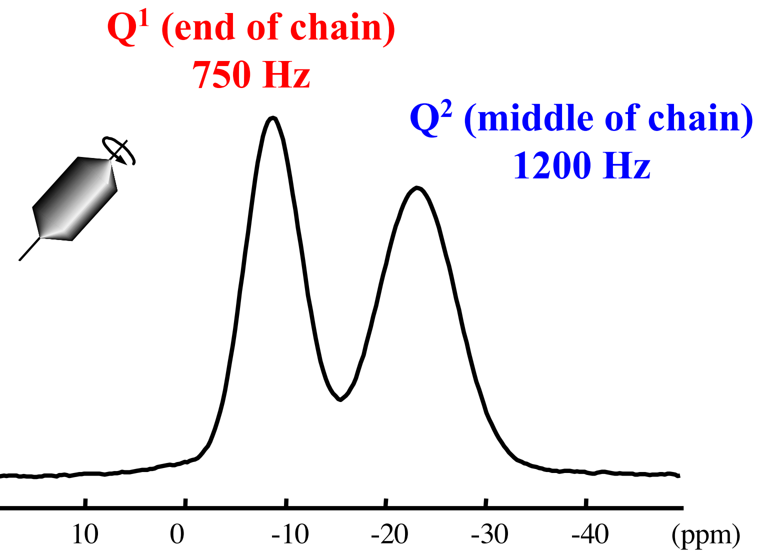

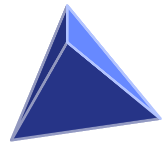

$[Q^1] = [Q^2]$

Average chain length
$N_{av.}$ ~ 4

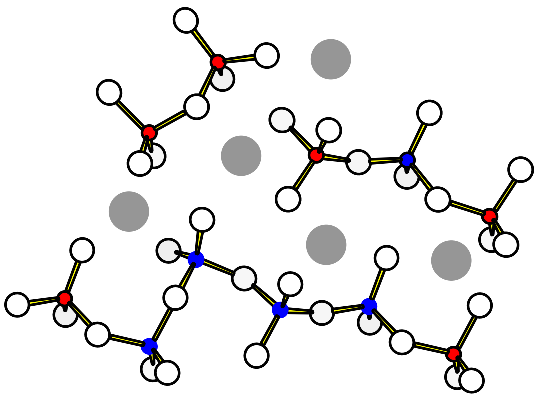

? Nature of disorder at the nanometric scale ?

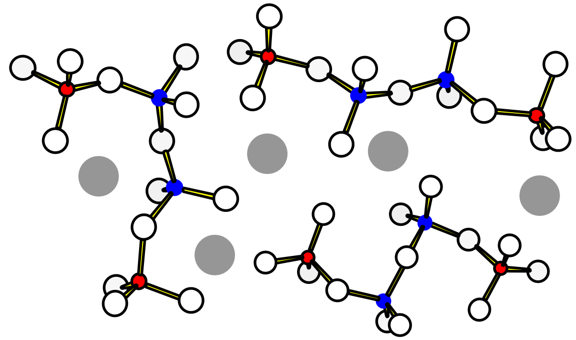

Chain length distribution?
Chemical disorder

Chain geometries?
Topological or geometrical disorder

P-O-P chemical bonds can be viewed from J based P-P experiments

^{31}P NMR in $PbO-P_2O_5$ glasses

Individual ^{31}P

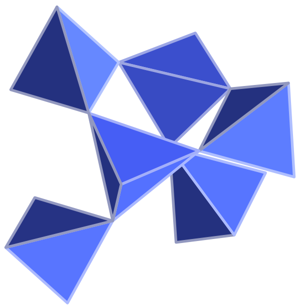

"Spin diffusion"
Spatial proximity

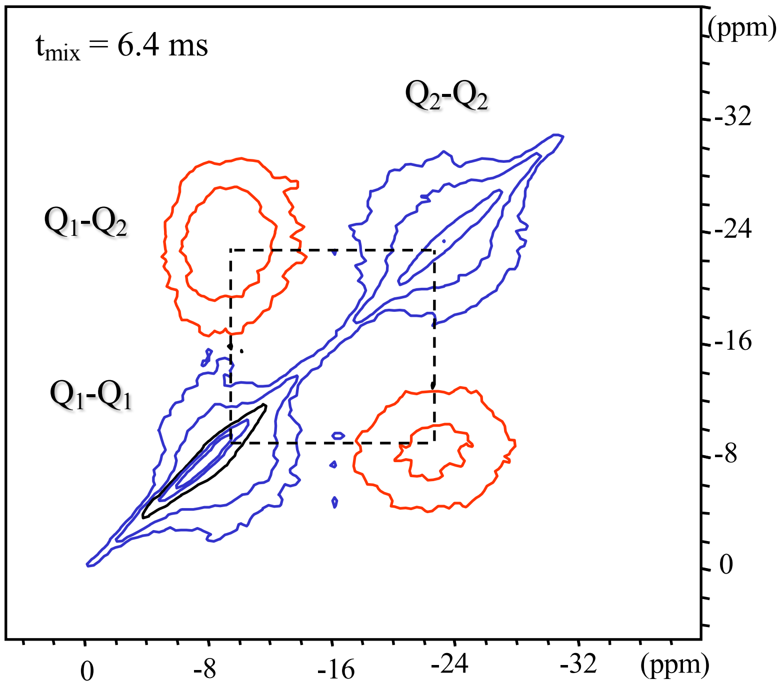

Pairs of ^{31}P

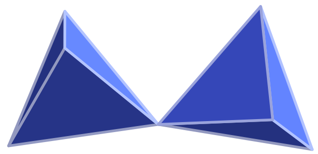

Double Quantum edition
Dipolar : spatial proximity
Jcoupling : chemical bond

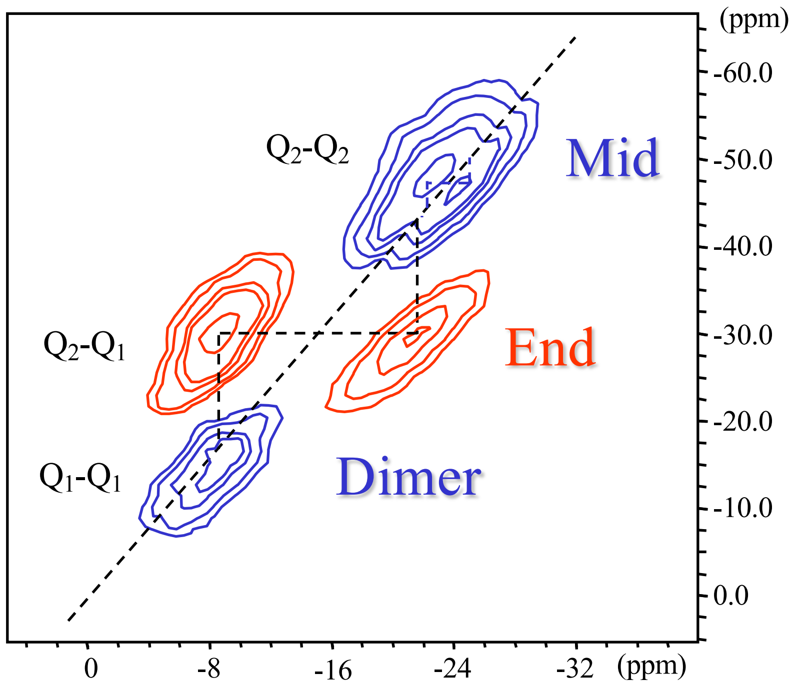

1 to 3 tetraedra – ^{31}P *J-couplings*

$(PbO)_{0.61}(P_2O_5)_{0.39}$ glass

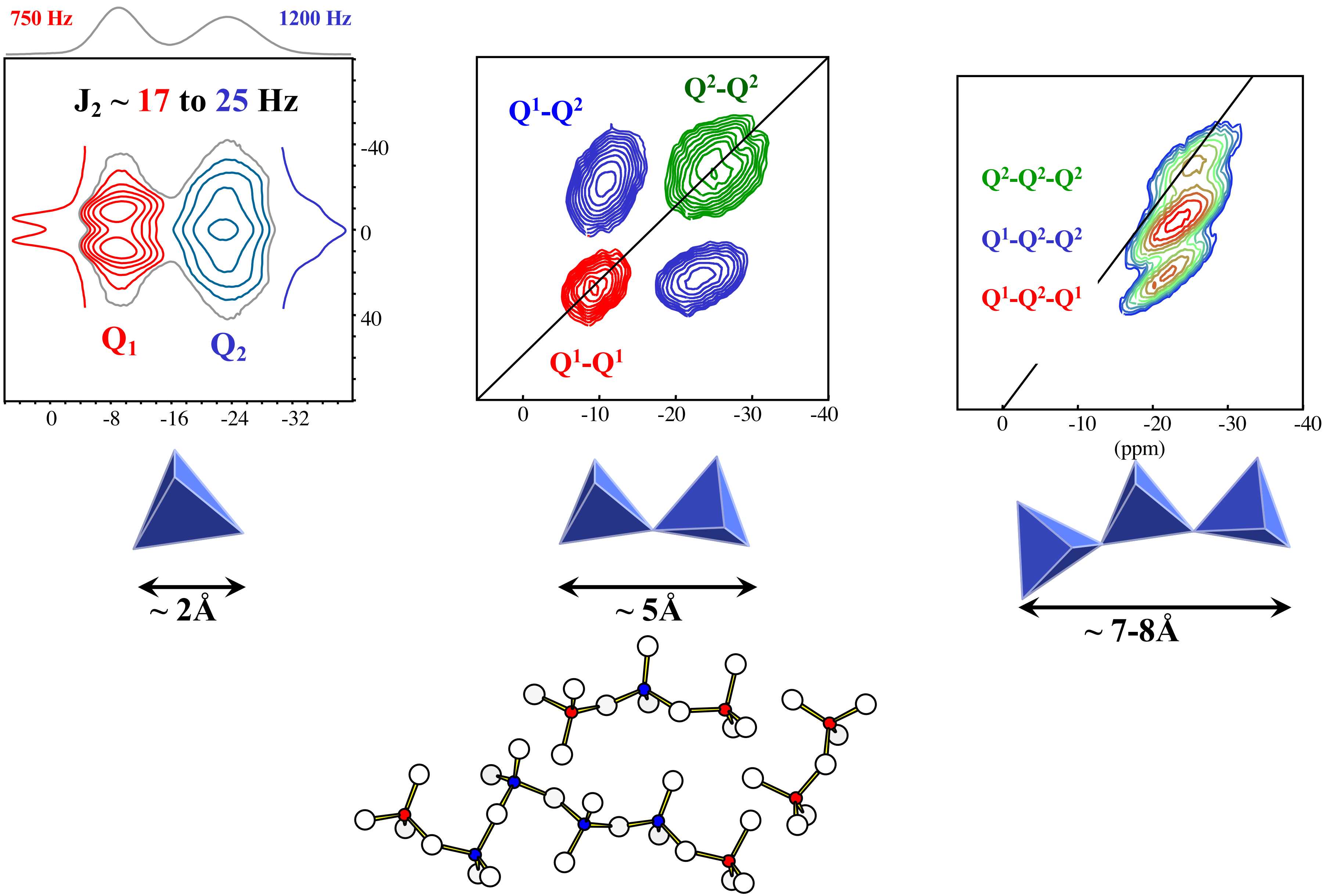

F. Fayon, I.J. King, R.K. Harris, J.S.O. Evans, D. Massiot Comptes Rendus de Chimie 7 351-361 (2004)
F.Fayon, C.Roiland, L.Emsley, D.Massiot, Journal of Magnetic Resonance 179 50-58 (2006)

1 to 3 tetraedra – ^{31}P *J-coupligs*

$(PbO)_{0.61}(P_2O_5)_{0.39}$ glass

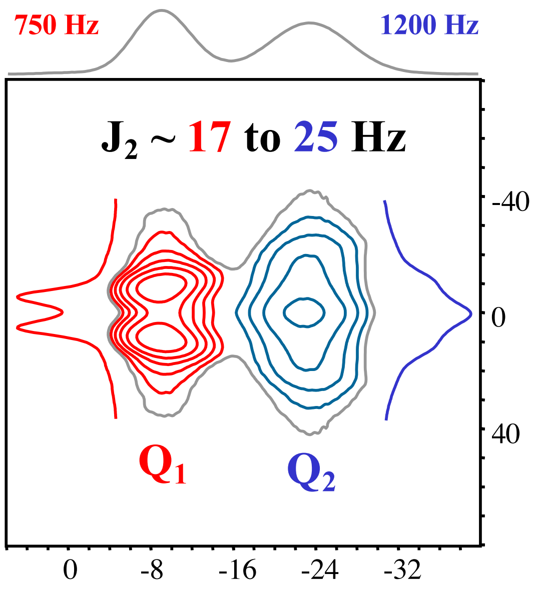

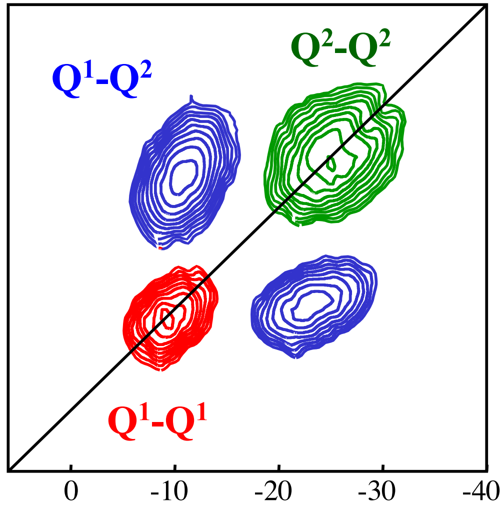

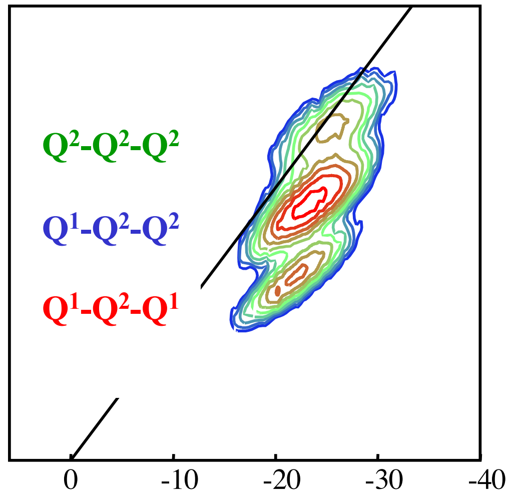

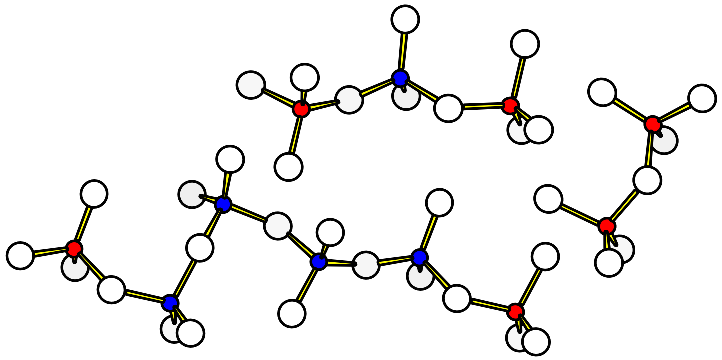

Topology

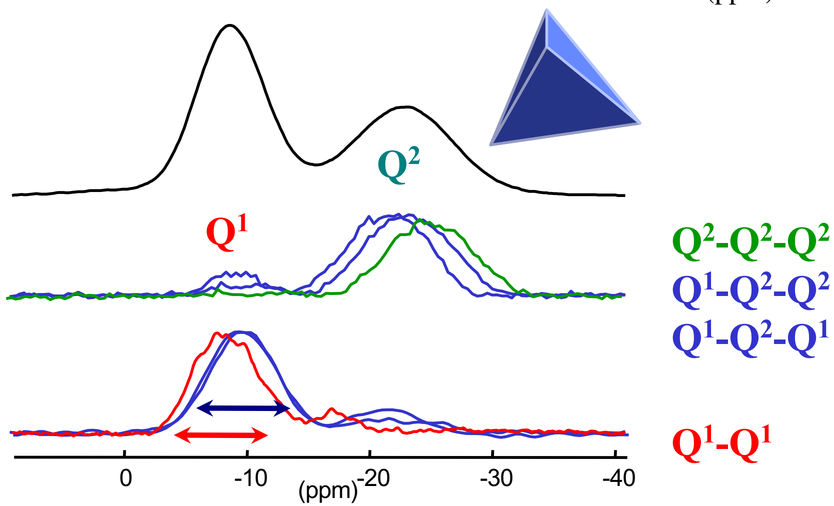

Geometry

"Chemistry"

F. Fayon, I.J. King, R.K. Harris, J.S.O. Evans, D. Massiot Comptes Rendus de Chimie 7 351-361 (2004)
F.Fayon, C.Roiland, L.Emsley, D.Massiot, Journal of Magnetic Resonance 179 50-58 (2006)

$\{^{27}Al\}\ ^{29}Si(O\text{-}^{29}Si)_{n?}$ Spin Counting

$CaO\text{-}Al_2O_3$ Glass

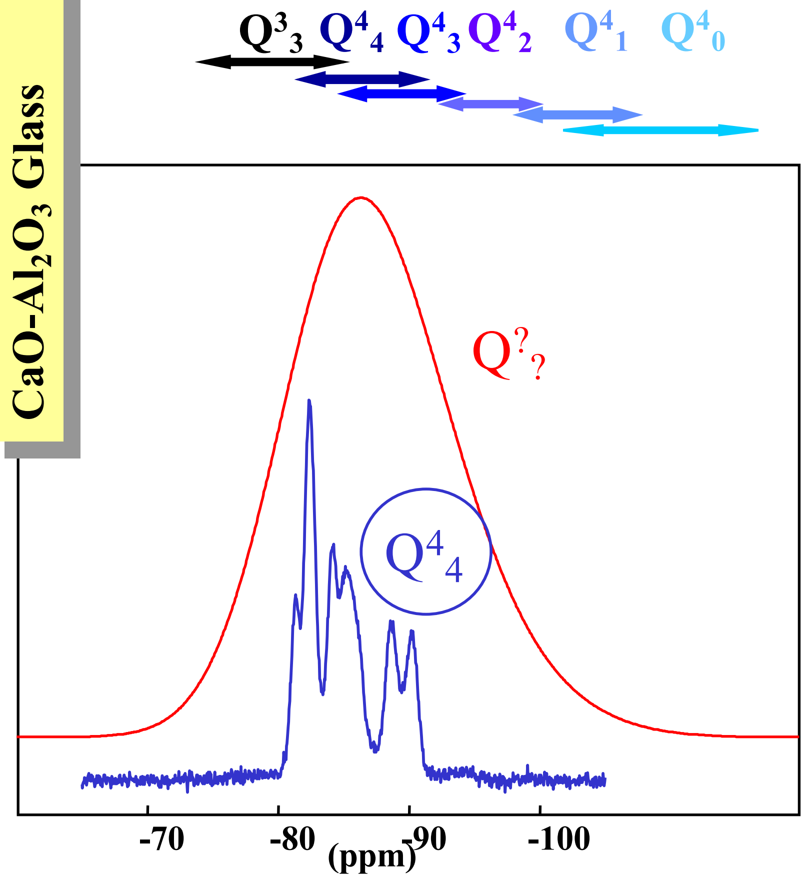

RMN ^{29}Si
Anorthite
Crystalline & Glass

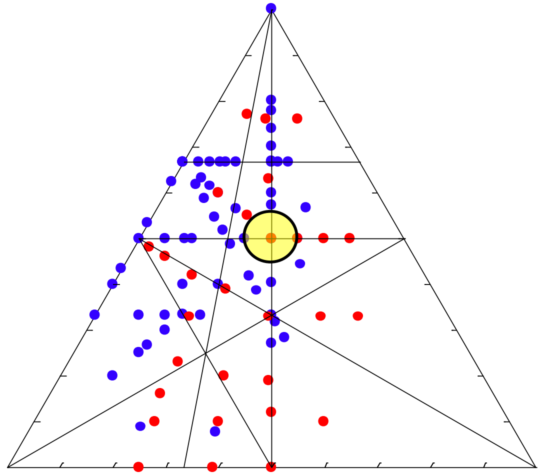

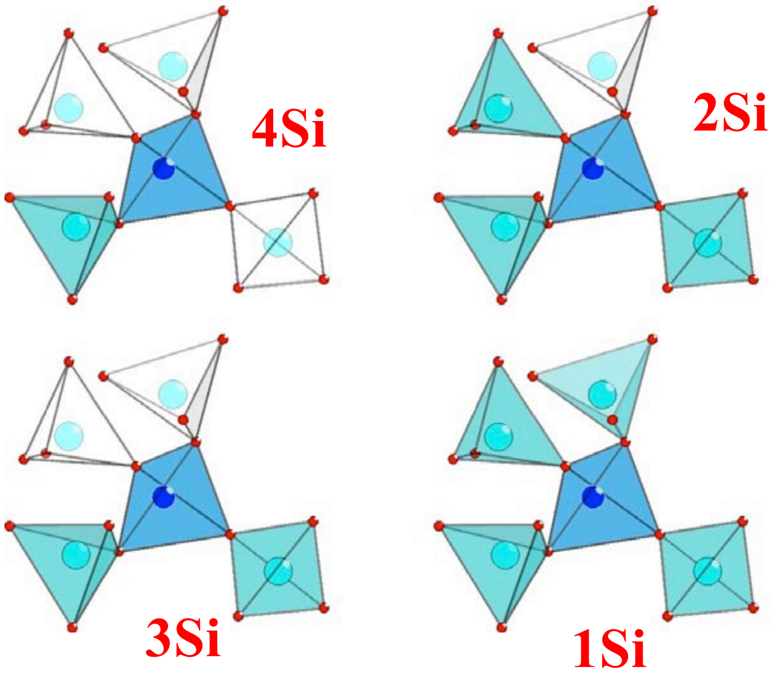

J.Hiet, M.Deschamps, N.Pellerin, F.Fayon, D.Massiot
"*Probing chemical disorder in glasses using silicon-29 NMR spectral editing*" *Phys. Chem. Chem. Phys.* 11 6935–6940 ***2009***

$\{^{27}Al\}\ ^{29}Si(O\text{-}^{29}Si)_{n?}$ Spin Counting

$CaO\text{-}Al_2O_3$ Glass

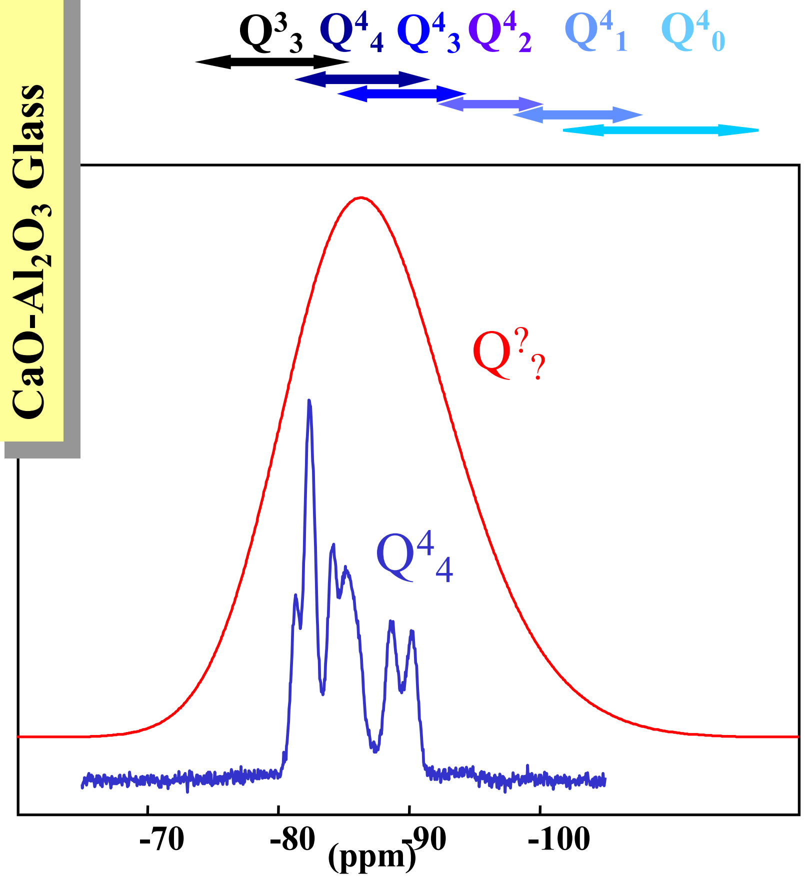

NMR^{29}Si
Anorthite
Crystalline & Glass

1Si

CaAlLaY Glass

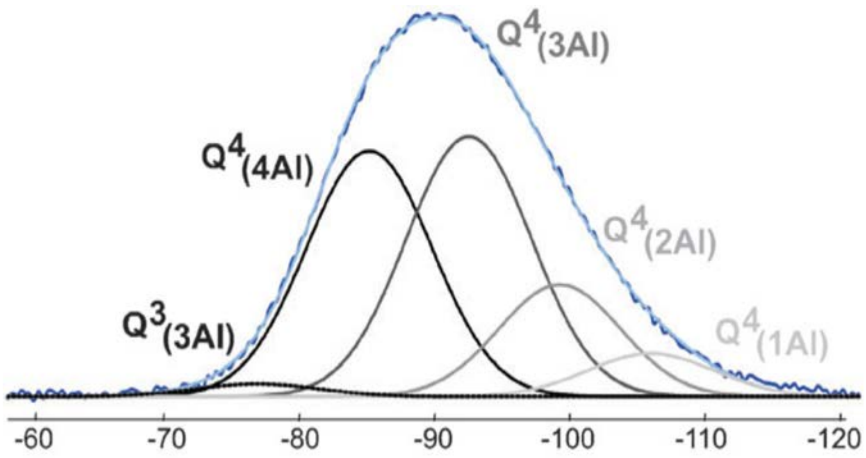

J.Hiet, M.Deschamps, N.Pellerin, F.Fayon, D.Massiot
"*Probing chemical disorder in glasses using silicon-29 NMR spectral editing*" *Phys. Chem. Chem. Phys.* 11 6935–6940 ***2009***

{^{27}Al} ^{29}Si(O-^{29}Si)$_{n?}$ Spin Counting

CaO-Al_2O_3 Glass

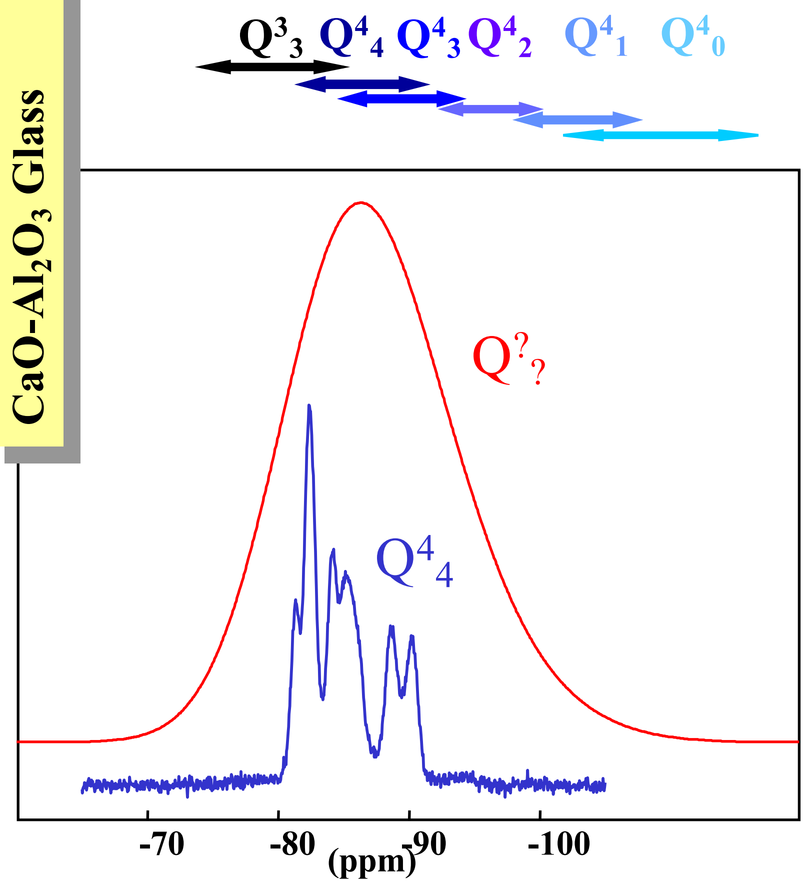

NMR ^{29}Si
Anorthite
Crystalline & Glass

CaAlLaY Glass

1Si

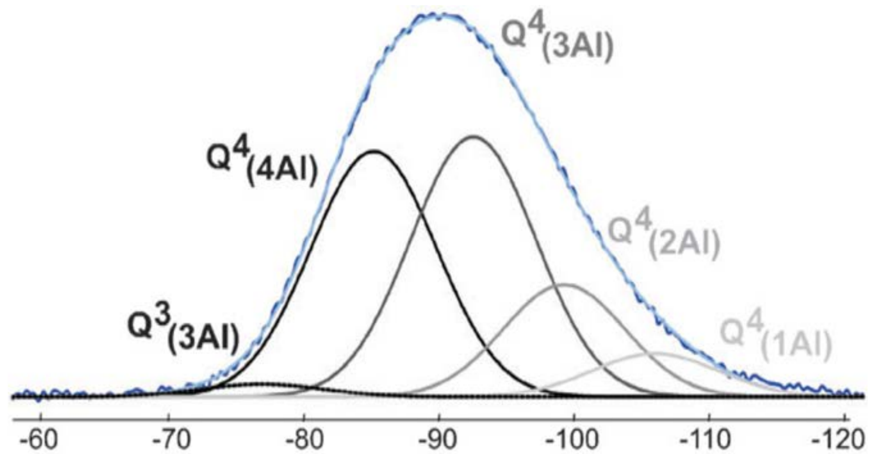

4Si

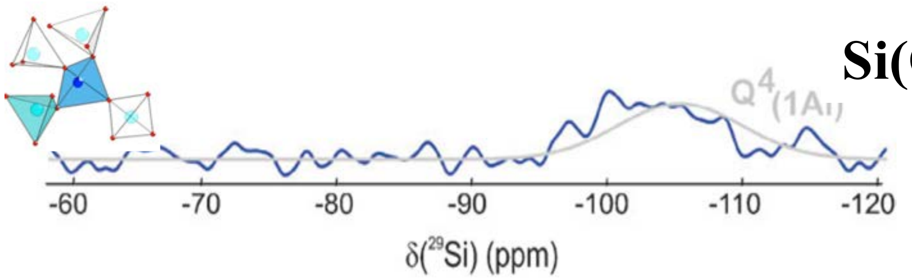

Si(OSi) $_{n\geq3}$

J.Hiet, M.Deschamps, N.Pellerin, F.Fayon, D.Massiot
"*Probing chemical disorder in glasses using silicon-29 NMR spectral editing*" *Phys. Chem. Chem. Phys.* 11 6935–6940 ***2009***

$\{^{27}Al\}\ ^{29}Si(O\text{-}^{29}Si)_{n?}$ Spin Counting

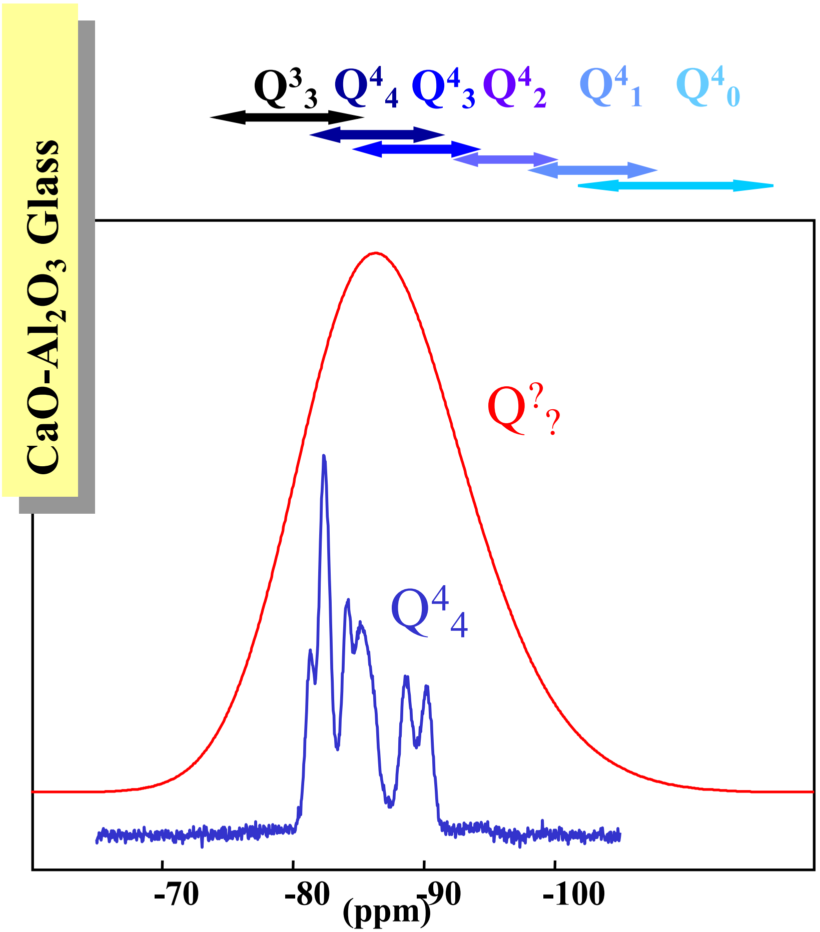

NMR 29Si
Anorthite
Crystalline & Glass

CaAlLaY Glass

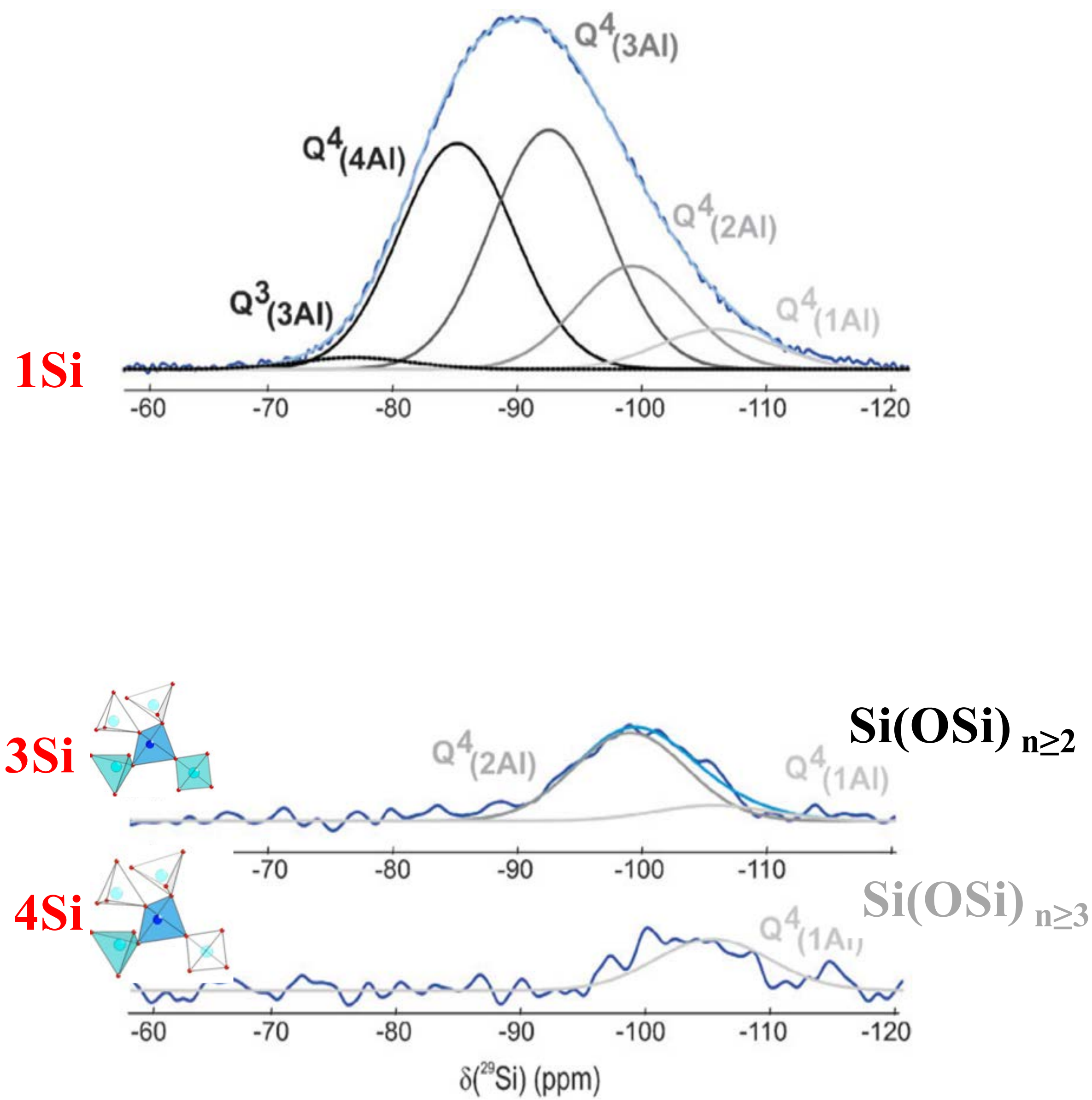

J.Hiet, M.Deschamps, N.Pellerin, F.Fayon, D.Massiot
"*Probing chemical disorder in glasses using silicon-29 NMR spectral editing*" *Phys. Chem. Chem. Phys.* 11 6935–6940 ***2009***

{^{27}Al} ^{29}Si(O-^{29}Si)$_{n?}$ Spin Counting

CaO-Al_2O_3 Glass

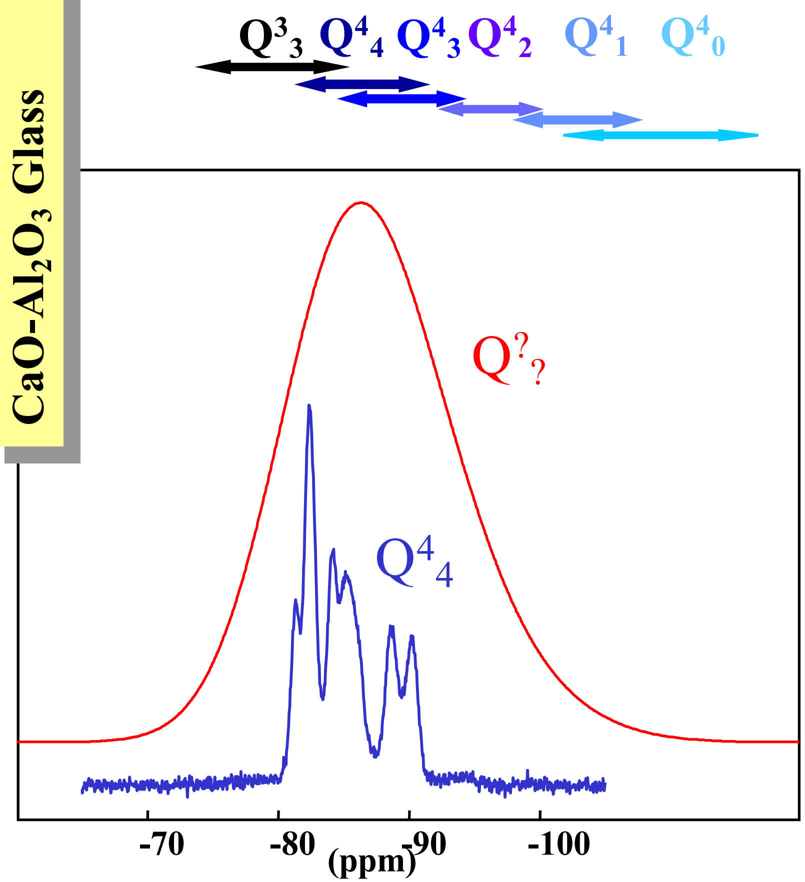

NMR^{29}Si
Anorthite
Crystalline & Glass

CaAlLaY Glass

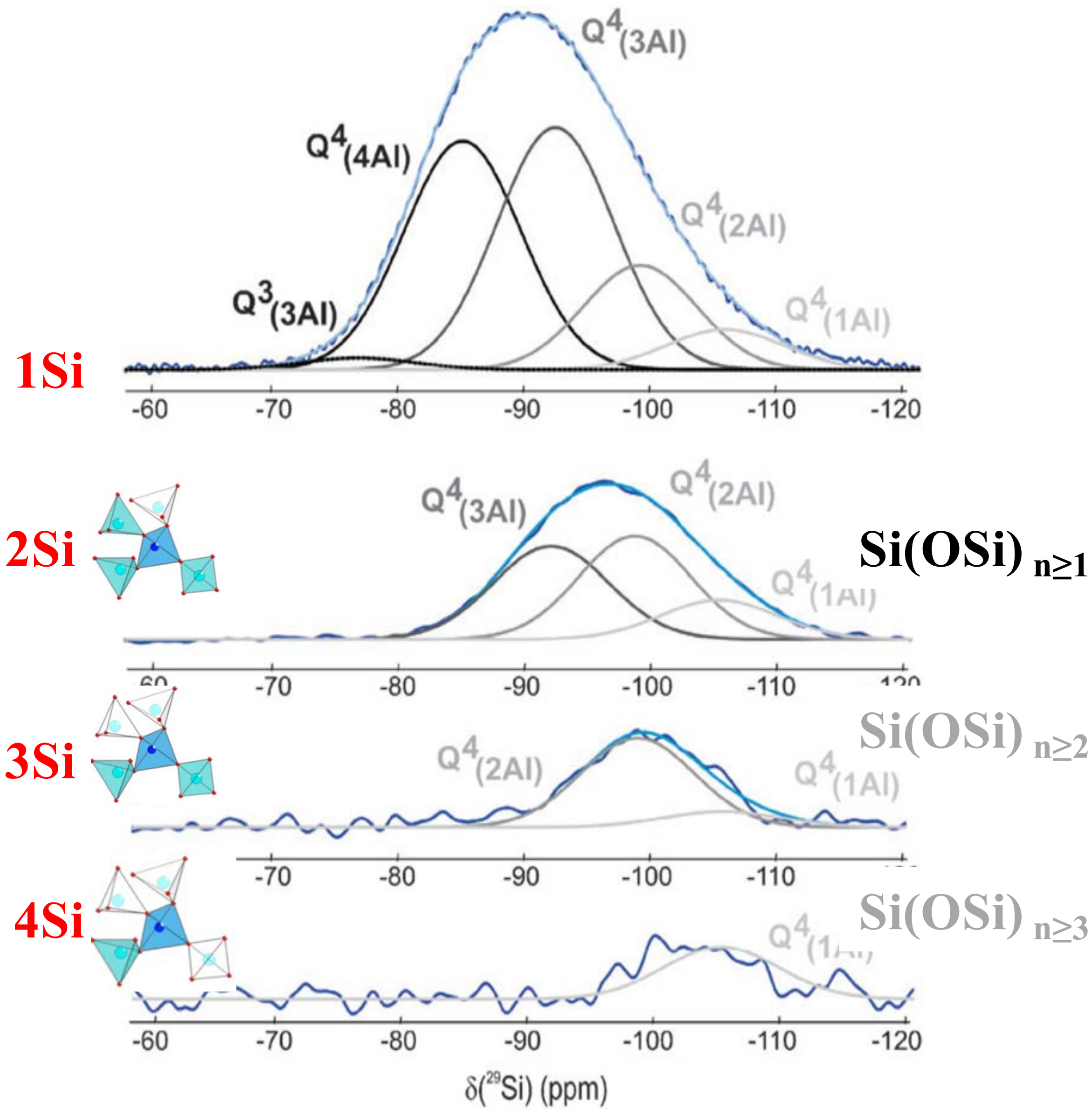

J.Hiet, M.Deschamps, N.Pellerin, F.Fayon, D.Massiot
"*Probing chemical disorder in glasses using silicon-29 NMR spectral editing*" *Phys. Chem. Chem. Phys.* 11 6935–6940 ***2009***

Chemical and Geometrical disorder

$CaO-Al_2O_3$ Glass

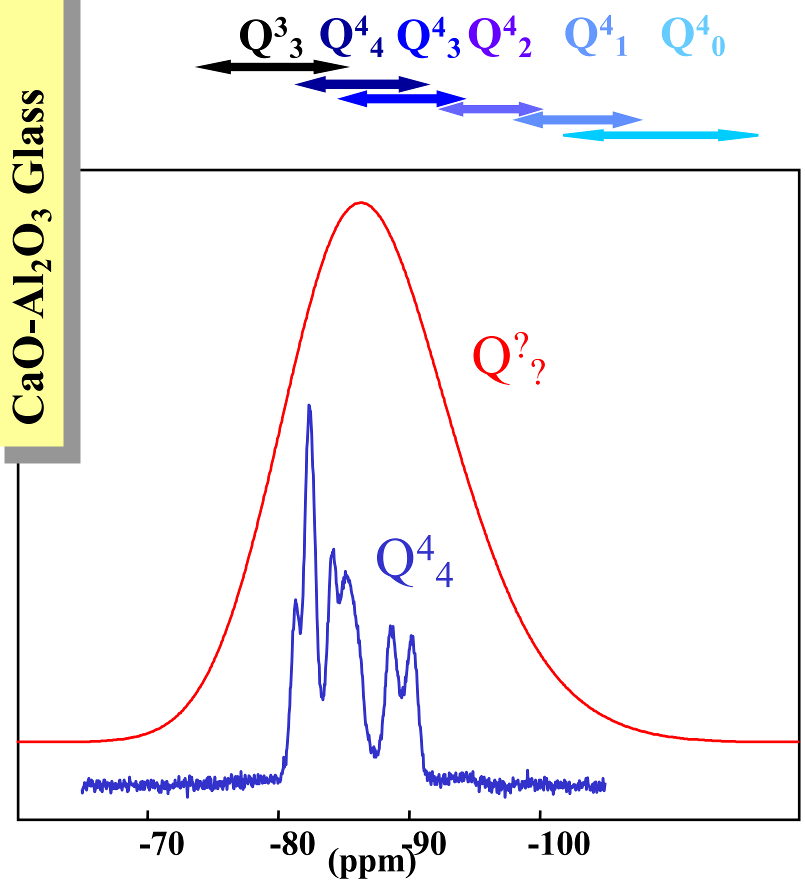

NMR^{29}Si
Anorthite
Crystalline & Glass

CaAlLaY Glass

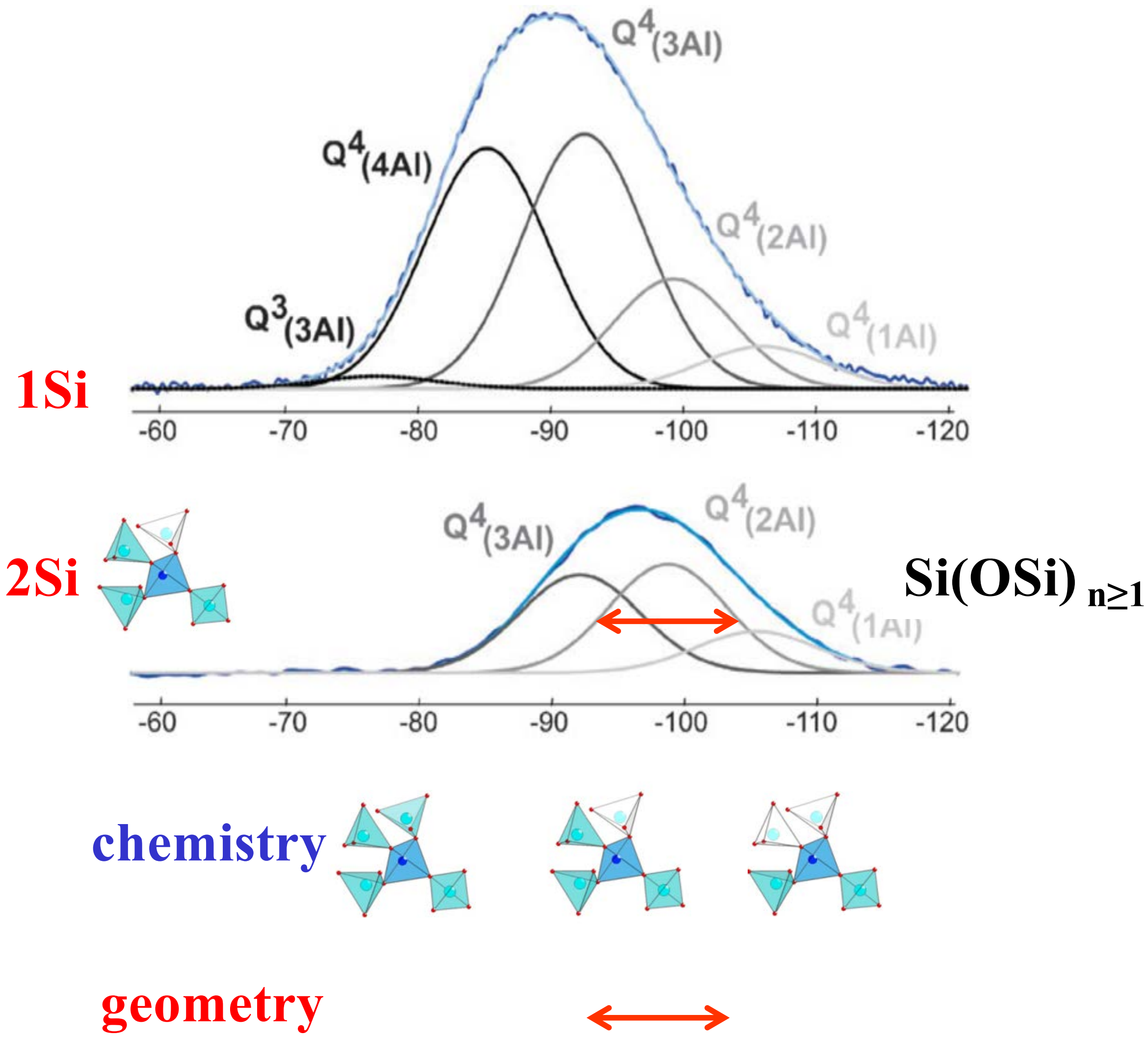

J.Hiet, M.Deschamps, N.Pellerin, F.Fayon, D.Massiot
"*Probing chemical disorder in glasses using silicon-29 NMR spectral editing*" *Phys. Chem. Chem. Phys.* 11 6935–6940 ***2009***

Verres : Ordre Chimique & Géomatrique

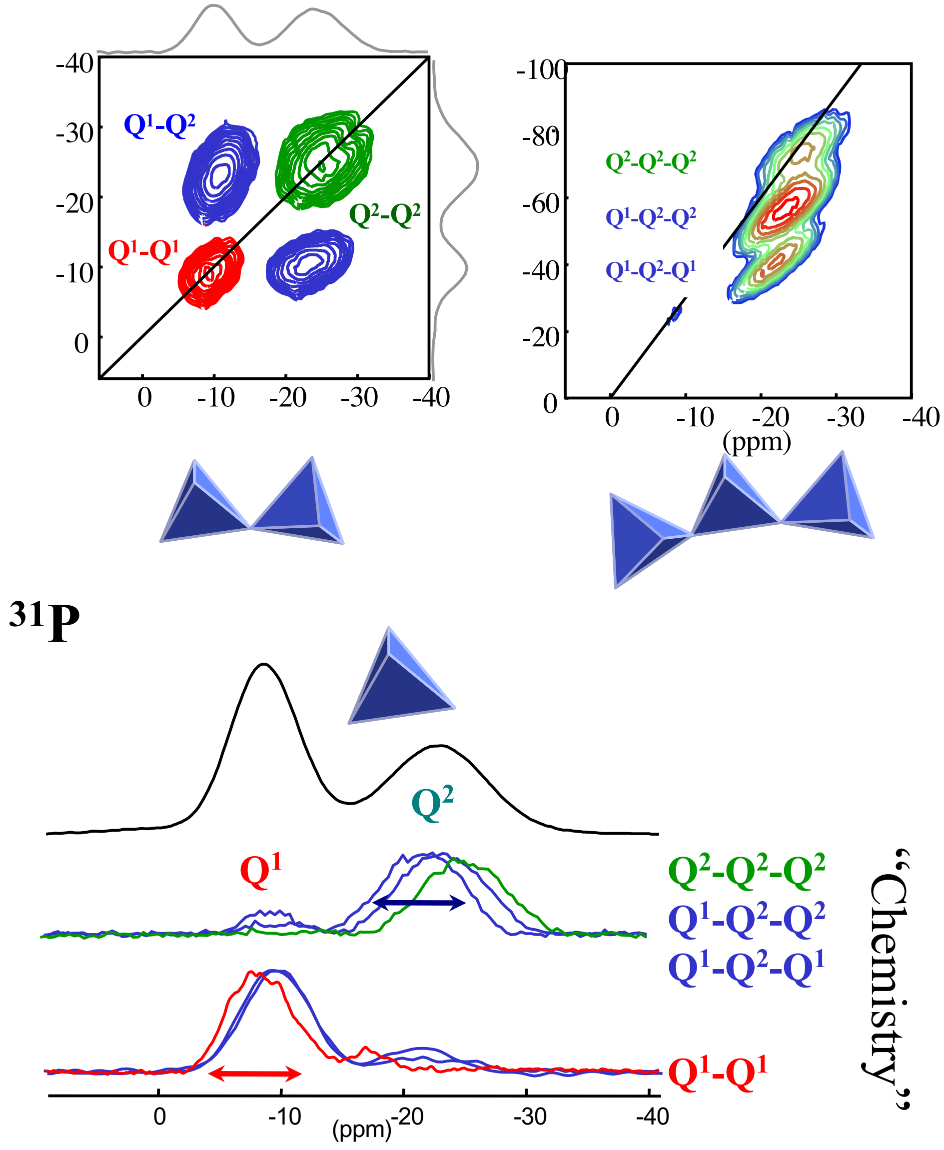

Lead Phosphate glasses

F.Fayon, *et al.* Journal of Magnetic Resonance 179 50-58 (2006)

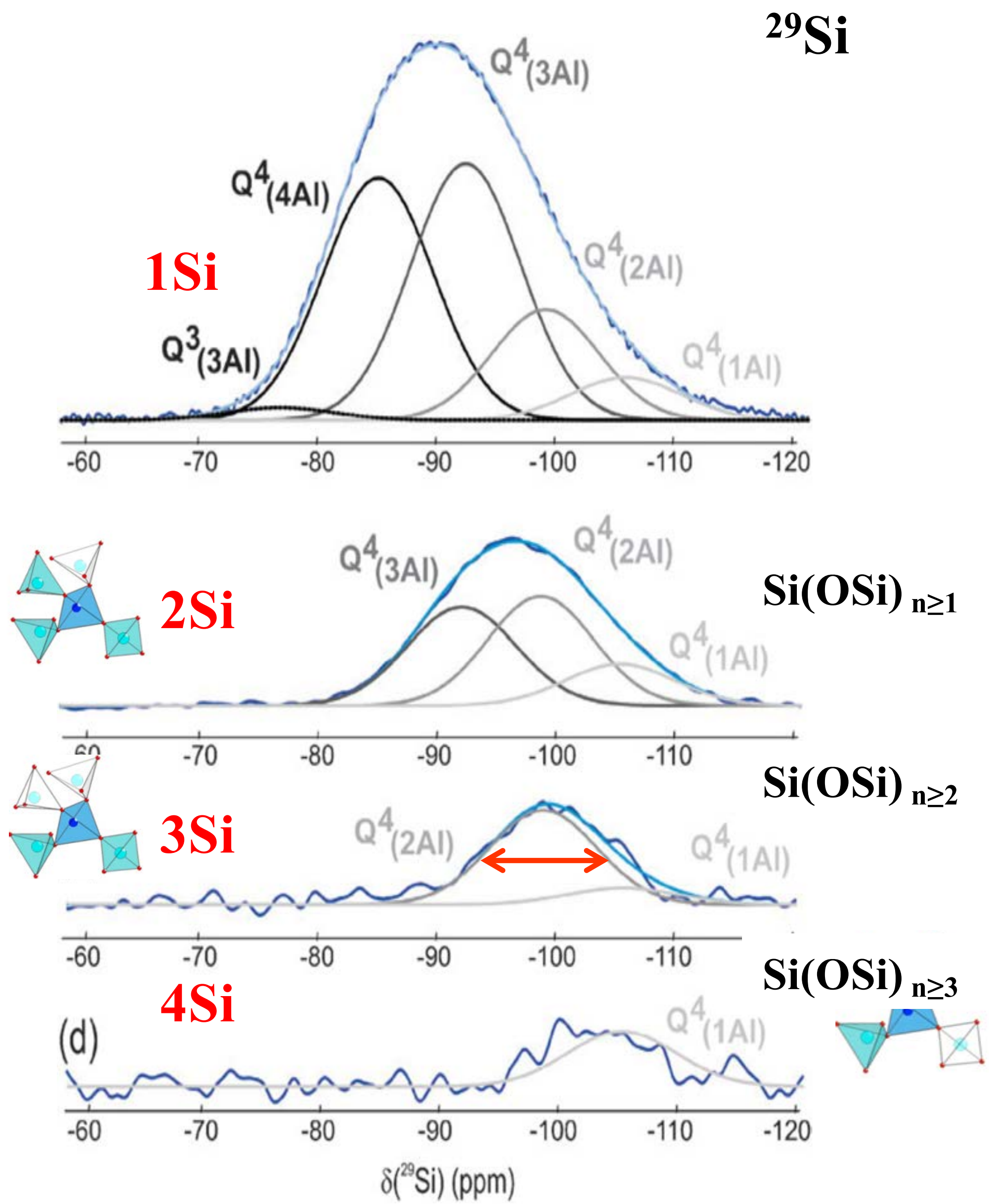

Calcium REE-Alumino-Silicate glasses

J.Hiet, et al. *Phys. Chem. Chem. Phys.* 11 6935–6940 ***2009***

MAS Quadrupolar nuclei

^{27}Al in YAG two sites Al_{IV} and Al_{VI}

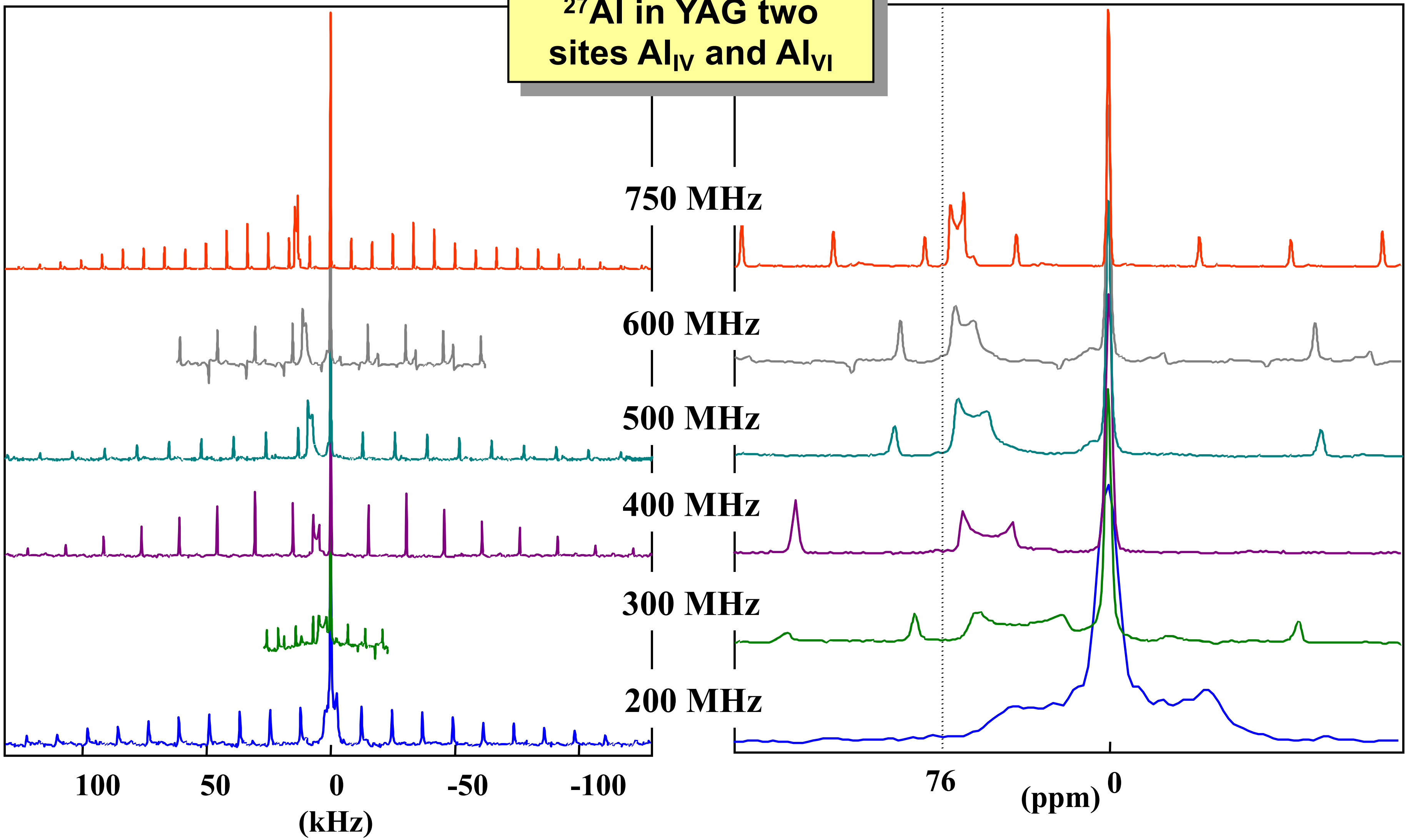

Second order shift and width goes with ν_Q^2/ν_0 (Hz)

2I+1 energy levels, 2I single quantum transitions

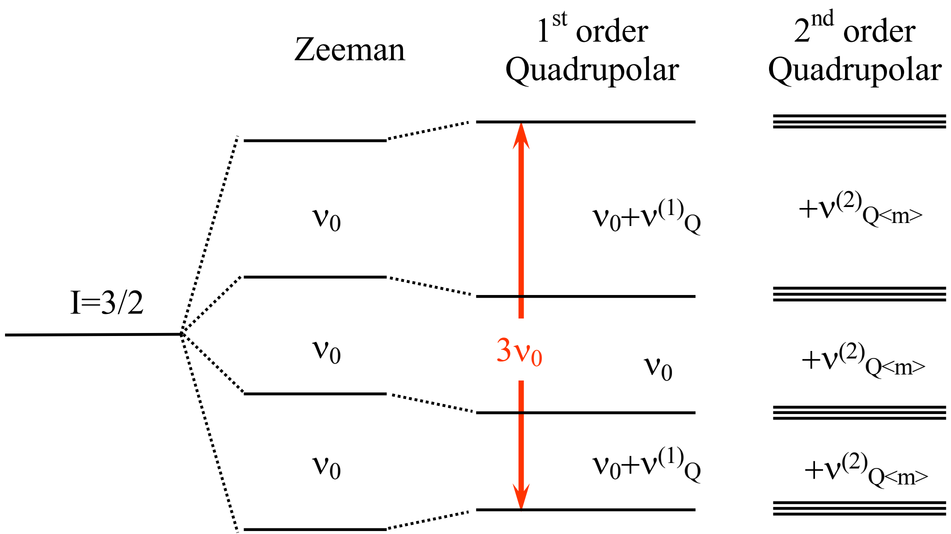

1st order quadrupolar interaction

$$H_Q^{(1)} = C_Q \sqrt{\frac{1}{6}} A_{20}^Q \left[3I_z^2 - I(I+1)\right]$$

2nd order quadrupolar interaction

$$H_Q^{(2)} = \frac{C_Q^2}{2\omega_0}\left[\begin{array}{l} A_{2-1}^Q A_{21}^Q \left\{4I(I+1) - 8I_z^2 - 1\right\} \\ + A_{2-2}^Q A_{22}^Q \left\{2I(I+1) - 2I_z^2 - 1\right\} \end{array}\right]$$

$$\nu_{<m,m-1>} = \nu_0 + \nu_{<m,m-1>}^{iso(2)} + \nu_{<m,m-1>}^{(2)}(\alpha,\beta,\gamma)$$

$$\nu_{<m,m-1>}^{iso(2)} = -\frac{I(I+1) - 3 - 9m(m-1)}{30}\frac{\nu_Q^2}{\nu_0}\sqrt{1 + \frac{\eta^2}{3}}$$

Magic Angle Spinning - 2nd order

First order $H_I \ll H_z$

$$\nu_{<m,m-1>} = \nu_0 + P_2(\mathrm{Cos}\theta)\frac{(1-2m)}{2}\nu_Q C_{\alpha,\beta} + \sum_{n=1}^{2} A_n e^{-i(n\omega_r t+\phi)}$$

Second order $H_I < H_z$

$$\nu_{<m,m-1>} = \nu_0 + \sum_{l=0,2,4} C^{l}_{m,I} B^{(2)}_{l} P_l(\mathrm{Cos}\theta) + \sum_{n=1}^{4} A^{(2)}_{n} e^{-i(n\omega_r t+\phi)}$$

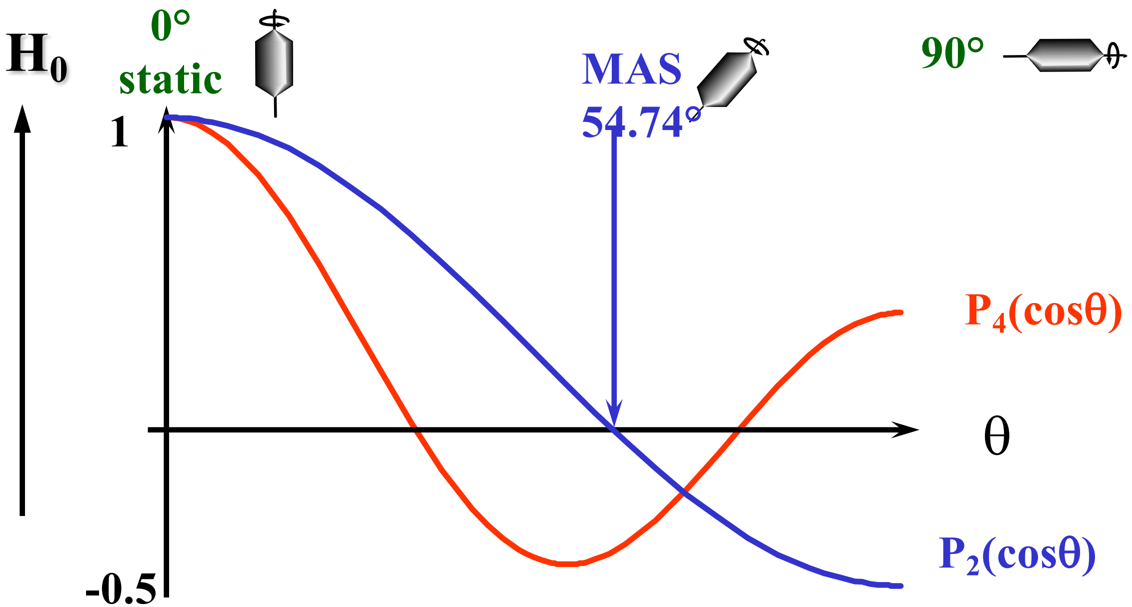

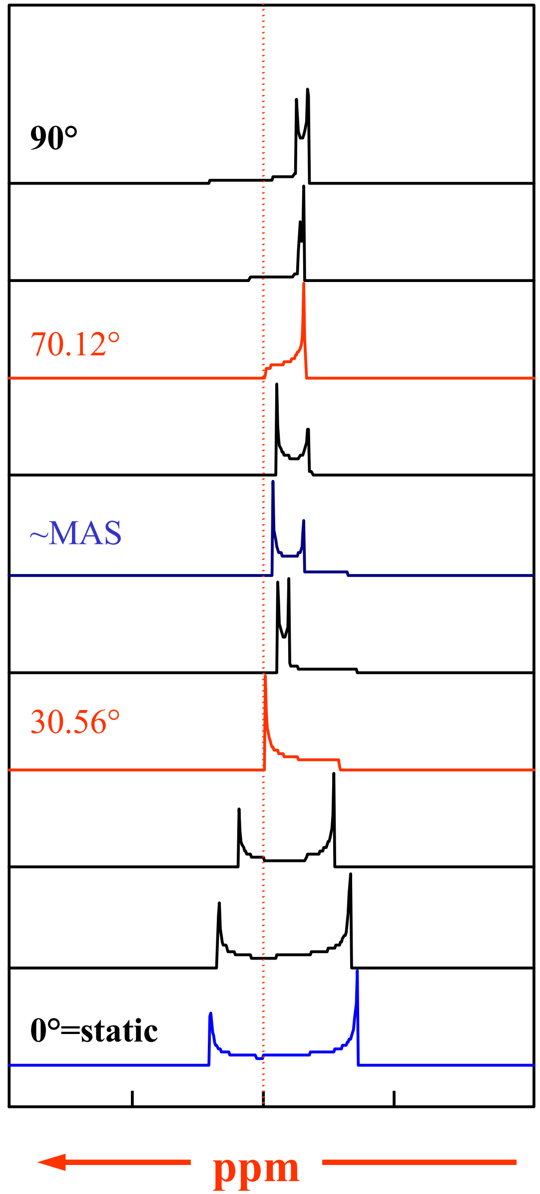

^{27}Al in A9B2 ($Al_{18}B_4O_{33}$) 750 MHz

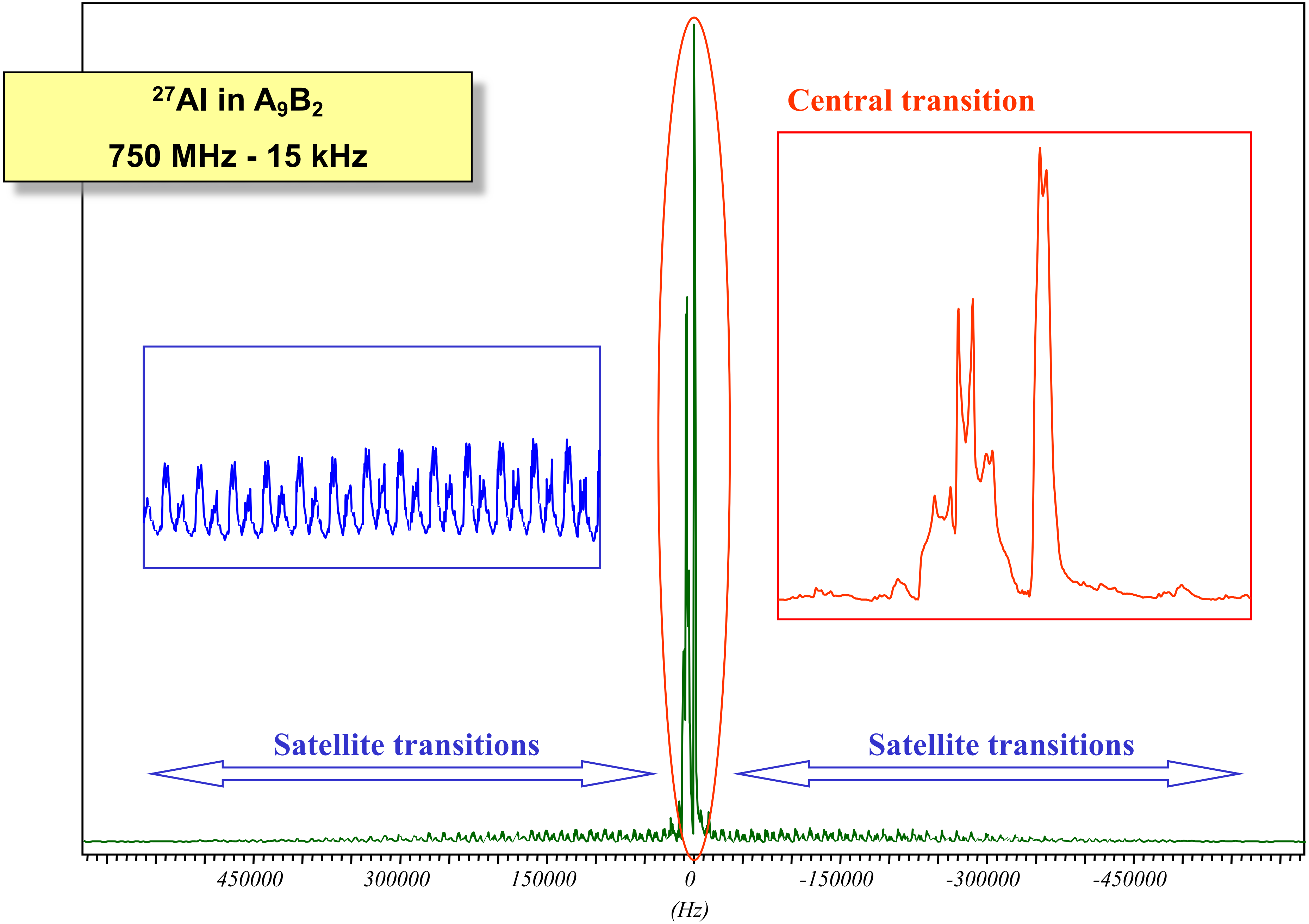

A9B2 – 750 MHz 31.25kHz

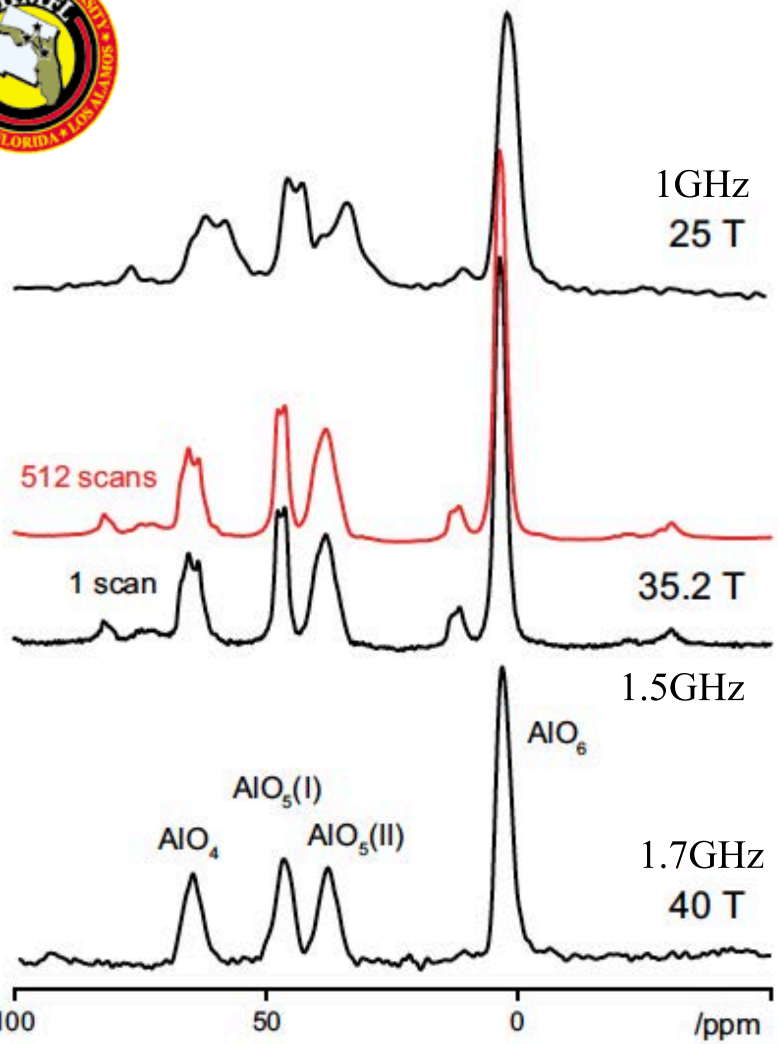

.. APM Kentgens.. Solid State NMR 5 175-180 ***1995***
.. Z. Gan .. J. Am. Chem. Soc. 124 5634-5635 ***2002***
Z.Gan... JMR ***2017***

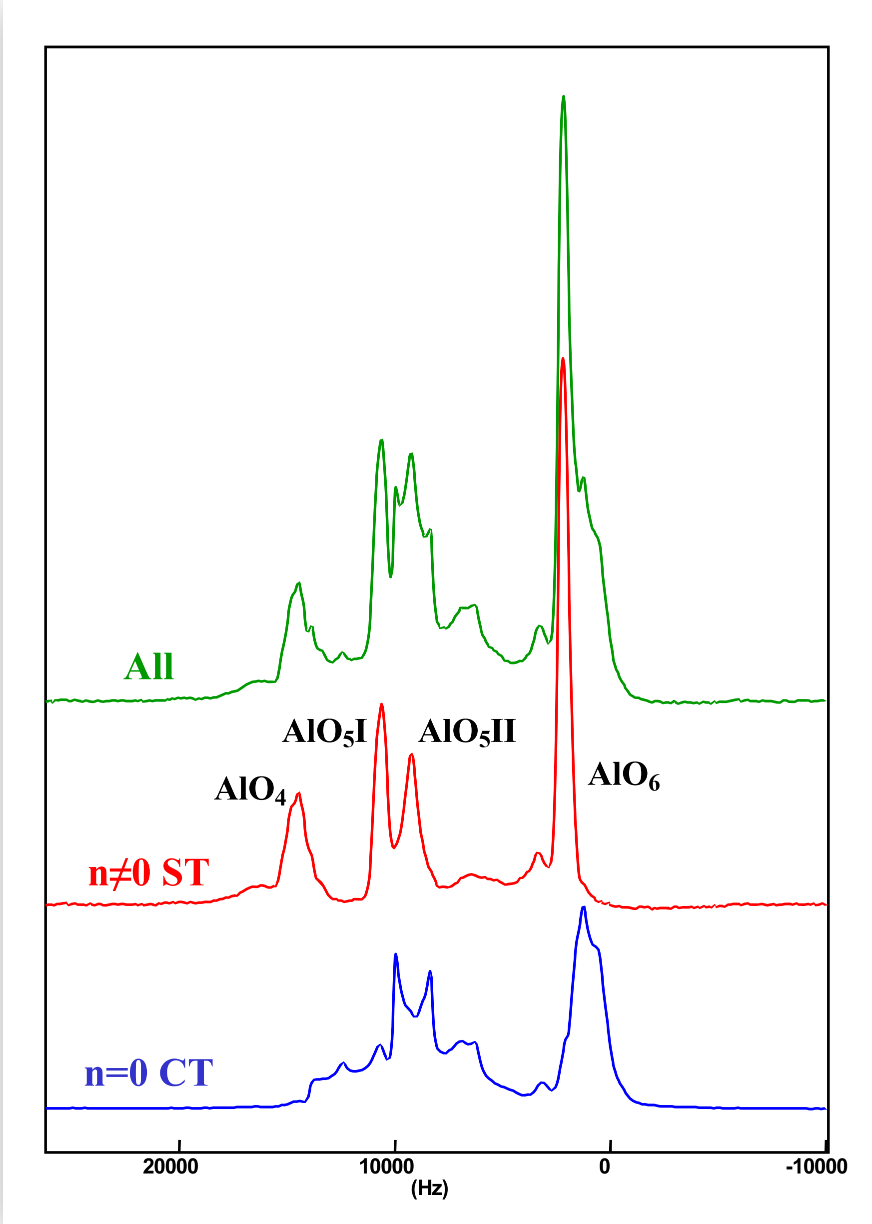

DAS, MQ-MAS & STMAS

DAS | MQ-MAS | STMAS

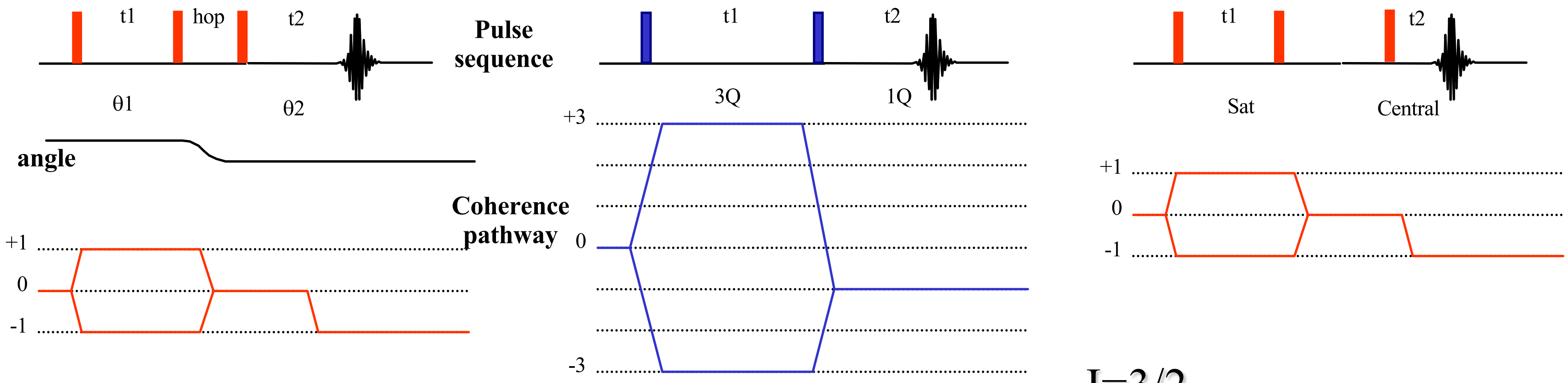

$$\Omega_p = -\sum_{l=0,2,4} C_l^p A_l\left(\theta,\varphi\right) P_l\left(\cos\beta\right)$$

I=3/2

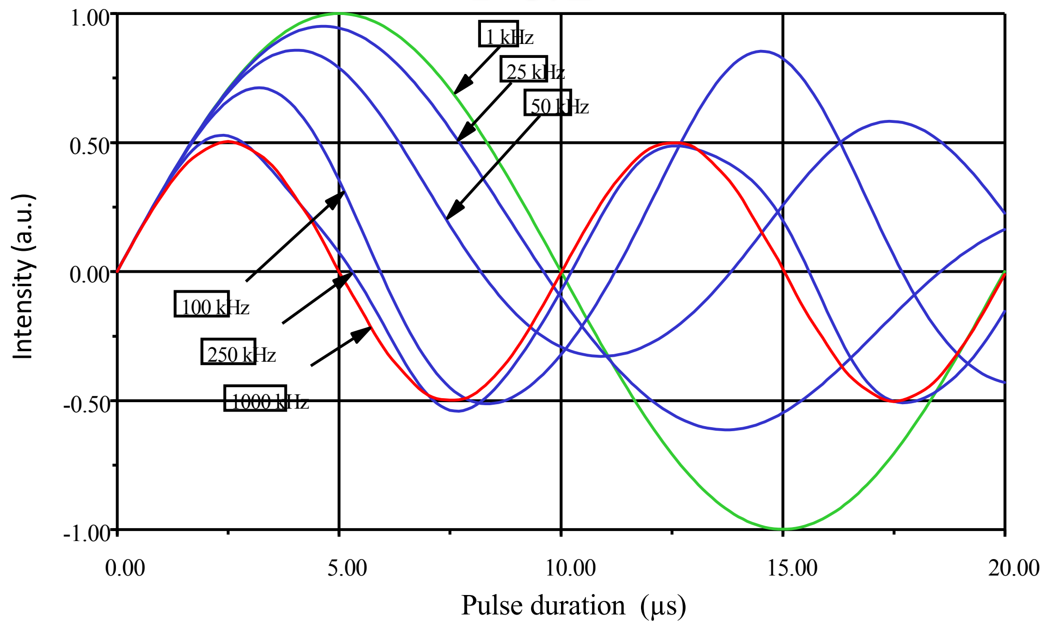

Ultimate resolution at ultra high field (40T)

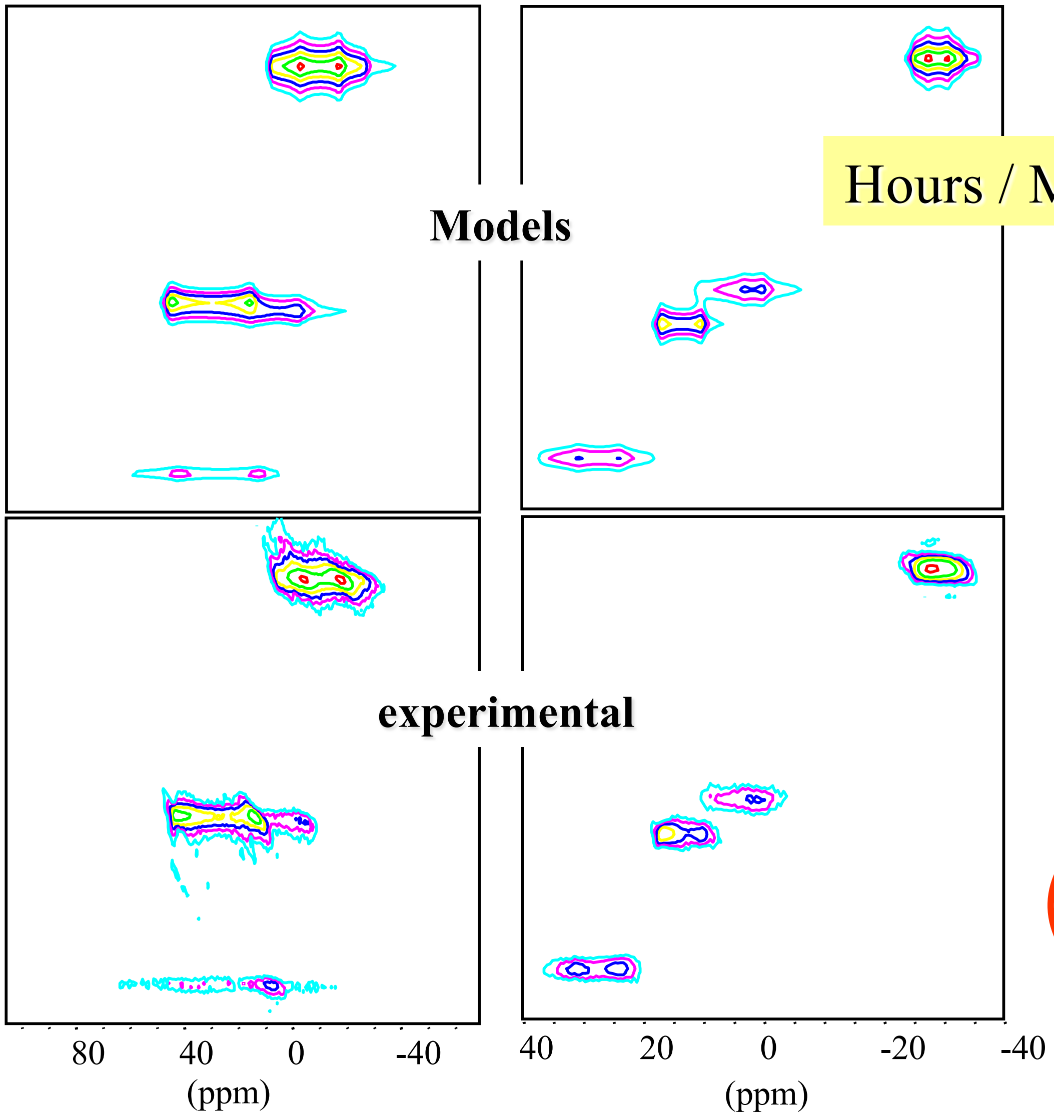

MQ-MAS 400 **STMAS 830**

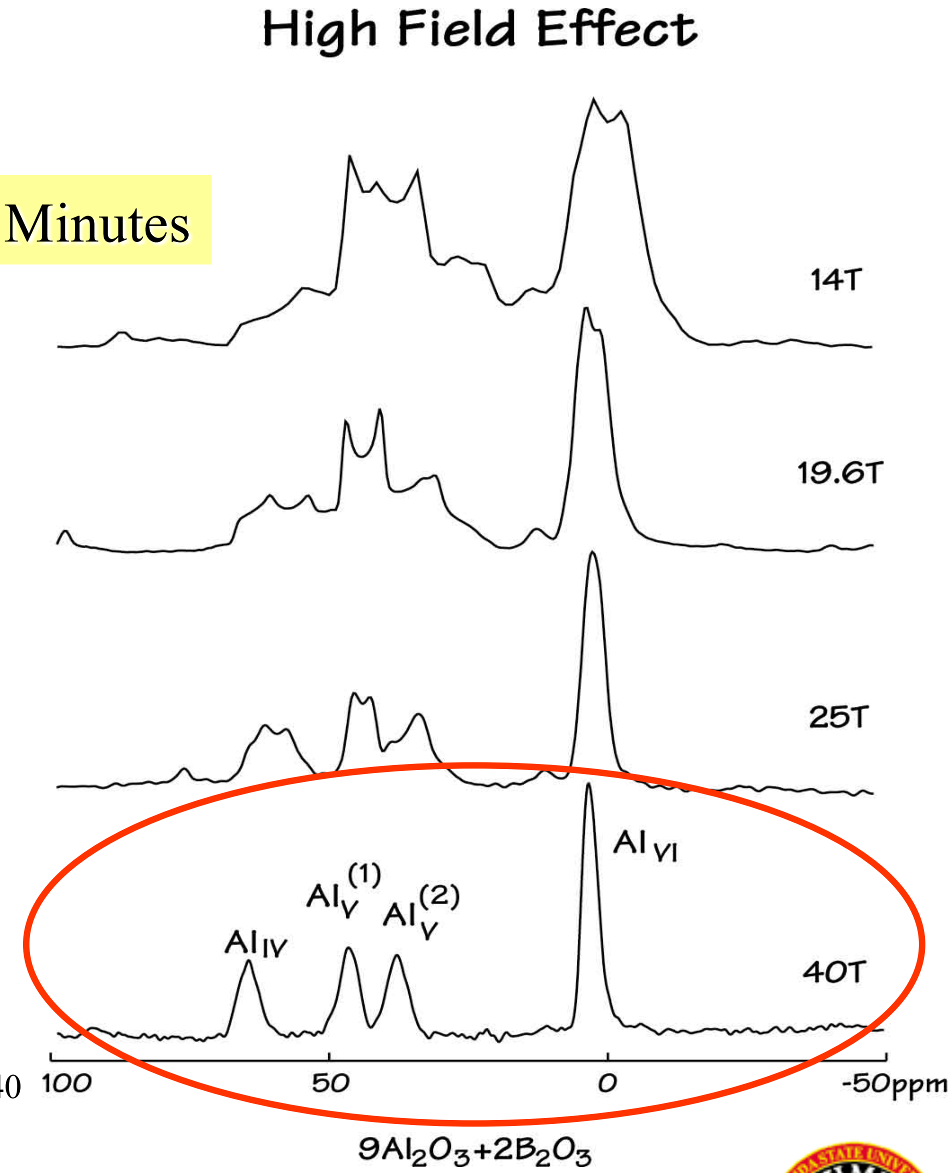

NHMFL – Z. Gan

Gan, Gor’kov, Cross, Samoson, Massiot, JACS **124** 5634-5635 (2002)

Ca 50_25 / 30 fit 1D & 2D 750/400 MHz

Glass (SiO_2, Al_2O_3, CaO)

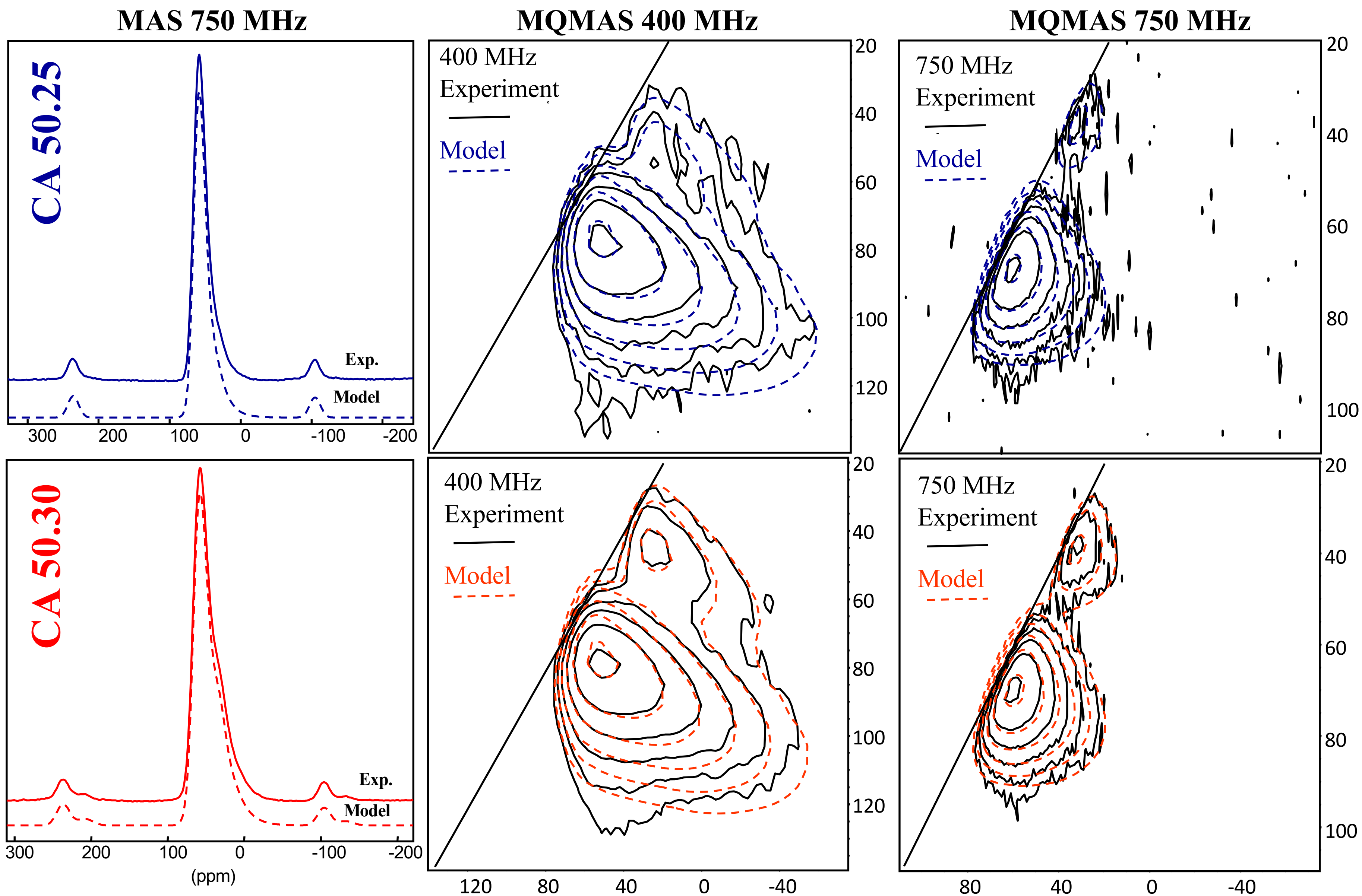

D.R.Neuville, L.Cormier, D.Massiot 'Al coordination and speciation in calcium aluminosilicate glasses : effects of composition determined by 27Al MQ-MAS NMR and Raman spectrocospy' Chem. Geol. 229 173-185 (2006)
D.R. Neuville, L. Cormier, D. Massiot 'Al environment in tectosilicate and peraluminous glasses: a NMR, Raman and XANES investigation' Geochim. Cosmochim. Acta 68 5071-5079 (2004)

^{27}Al - Ternary SiO_2-Al_2O_3-CaO

CaO-Al_2O_3 Glass

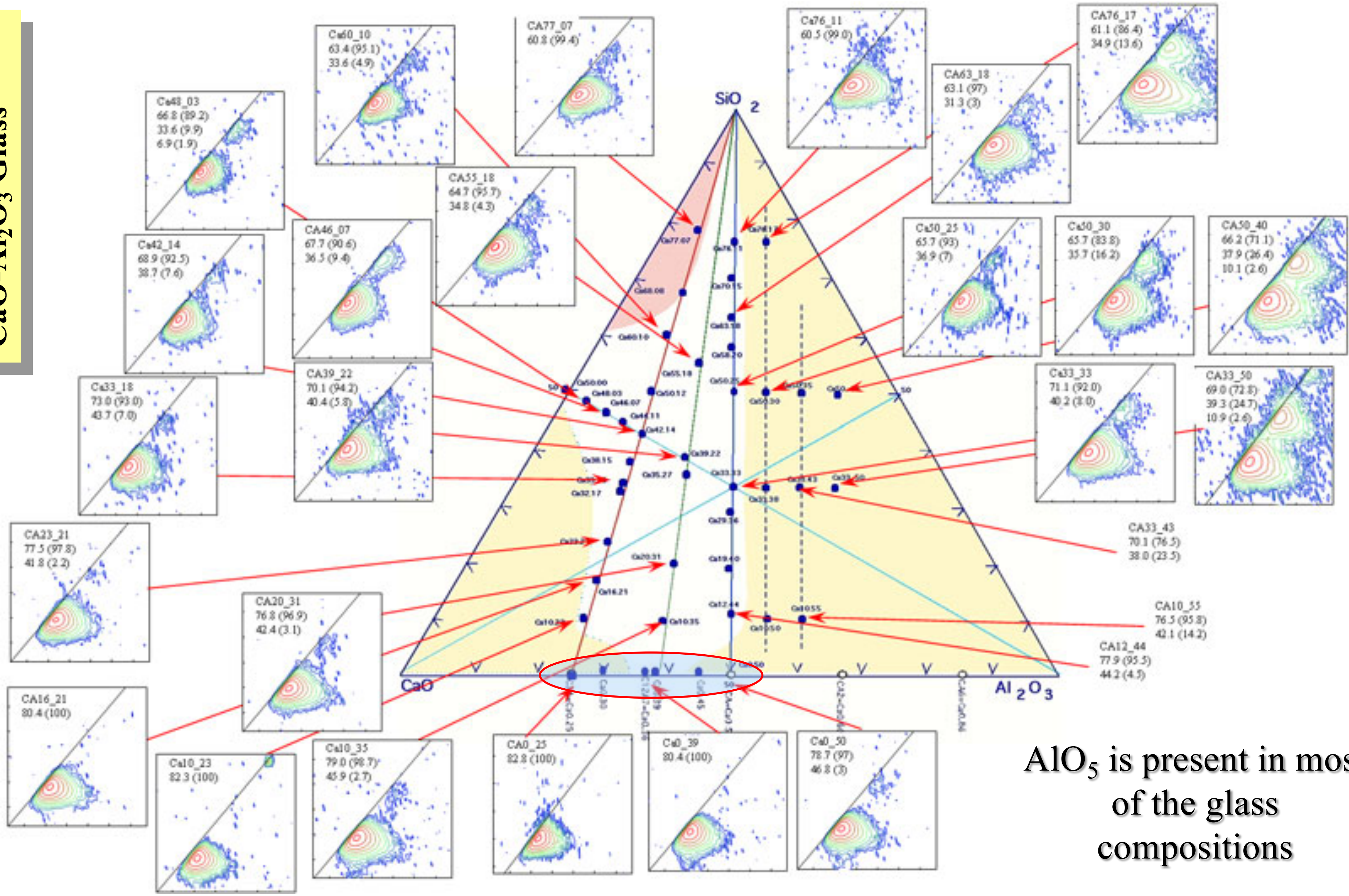

AlO$_5$ is present in most of the glass compositions

D.R.Neuville, L.Cormier, D.Massiot 'Al coordination and speciation in calcium aluminosilicate glasses : effects of composition determined by 27Al MQ-MAS NMR and Raman spectrocospy' Chem. Geol. 229 173-185 (2006)

"In silico" 2D colloidal glass simulation

1 particle size: crystallization

2 particle sizes: no long-range order
➔ *Glass*

Hexatic order in a 2D colloidal glass with two particle sizes :

Medium Range Crystalline Order
And
Locally Favored Structures LFS

Q_n^m, SiO_5, AlO_5, μ_3O, Al-O-Al…

From the model to the real glass?

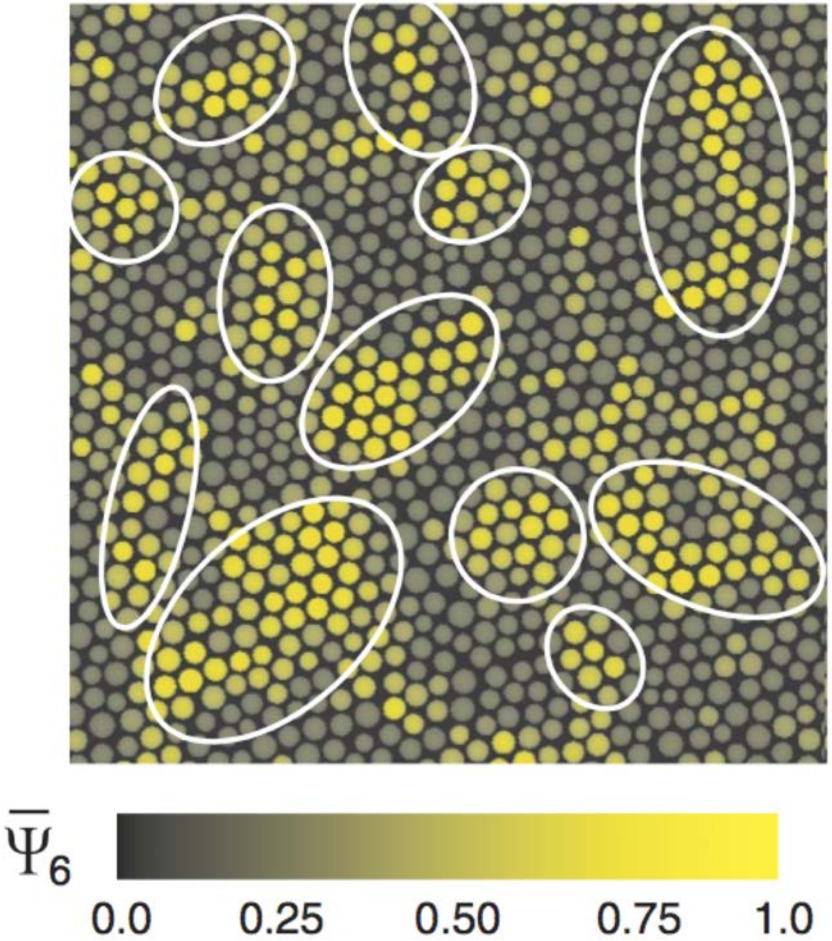

Similarity to Hexatic order

Correlation between Dynamic Heterogeneity and Medium-Range Order in Two-Dimensional Glass-Forming Liquids
Takeshi Kawasaki, Takeaki Araki, and Hajime Tanaka
PRL 99, 215701 (2007)

Chemical Disorder in a Structural Order

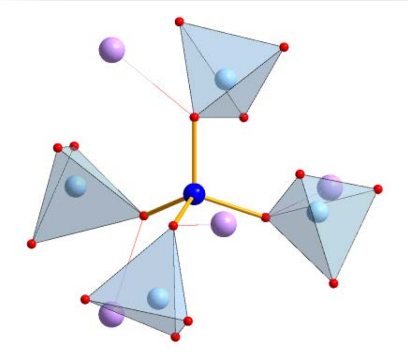

T_1 : Al only

5 configurations

Al-Al_4
Al-$SiAl_3$
Al-Si_2Al_2
Al-Si_3Al
Al-Si_4

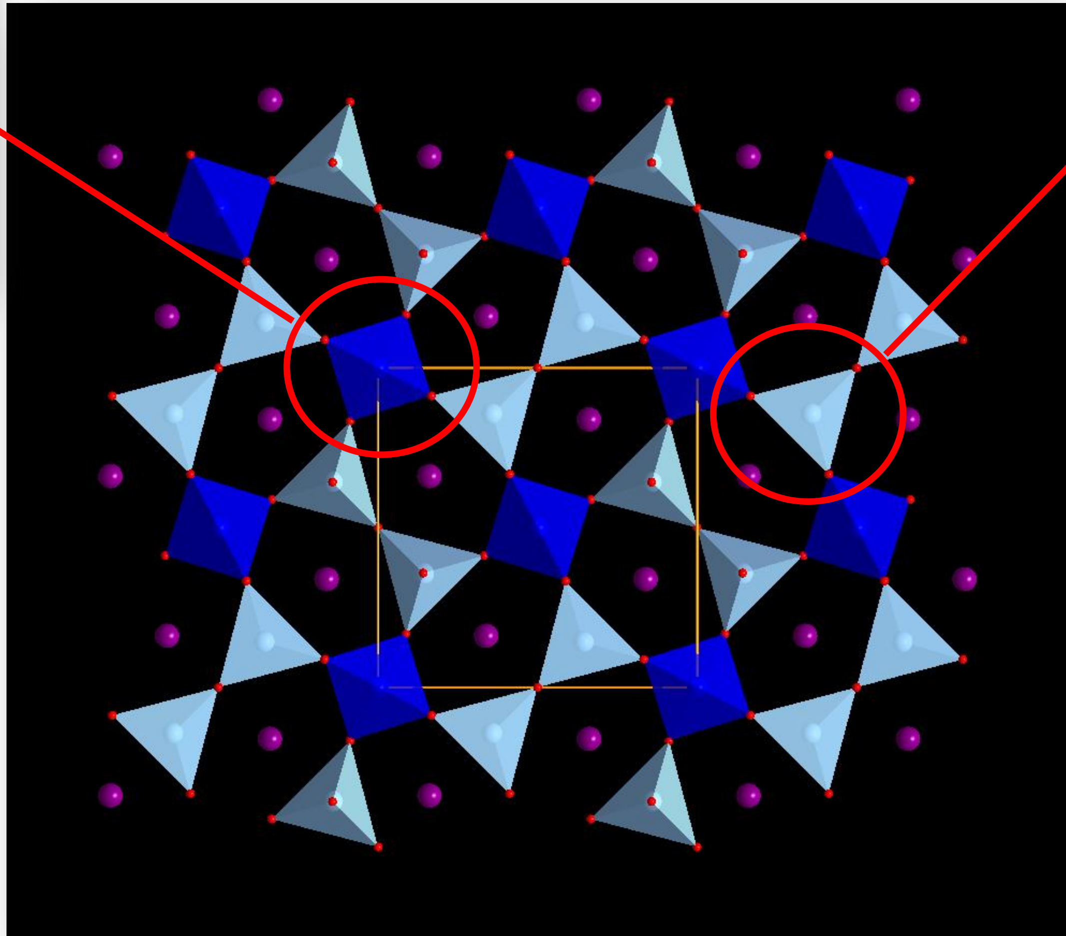

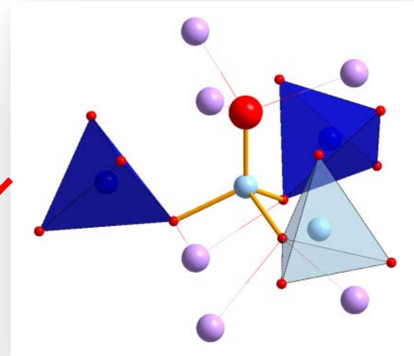

T_2 : $(Al_{0.5},Si_{0.5})$

2 configurations

Al-$SiAl_2$ Si-$SiAl_2$
Al-Al_3 Si-Al_3

Gehlenite $Ca_2Al_2SiO_7$

CHEMISTRY OF MATERIALS

P.Florian, E.Veron, T.F.G.Green, J.R.Yates, D.Massiot Chem. Mater. 24 4068–4079 **2012**

Chemical Disorder in a Structural Order

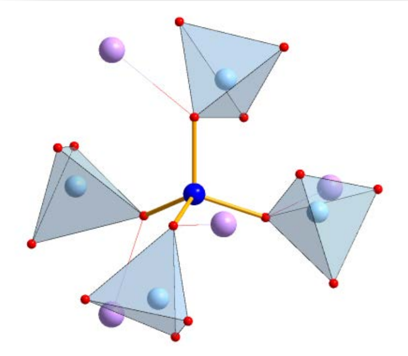

Gehlenite $Ca_2Al_2SiO_7$

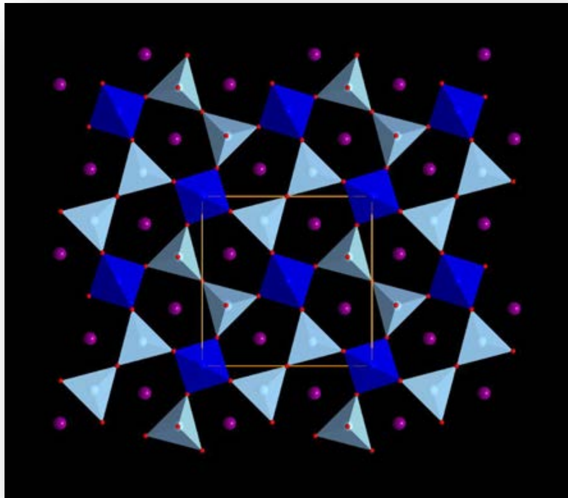

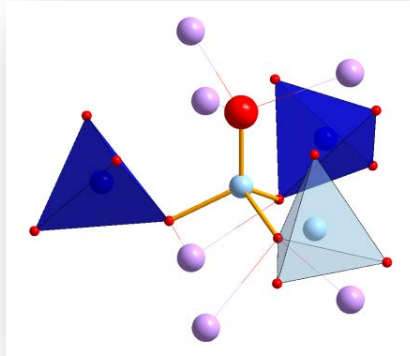

^{27}Al MAS @ 17.6T

T_1 & T_2 Al

Al-$SiAl_2$

Al-Al_3

Al-Si_2Al_2

Al-Al_4
Al-$SiAl_3$
Al-Si_3Al
Al-Si_4

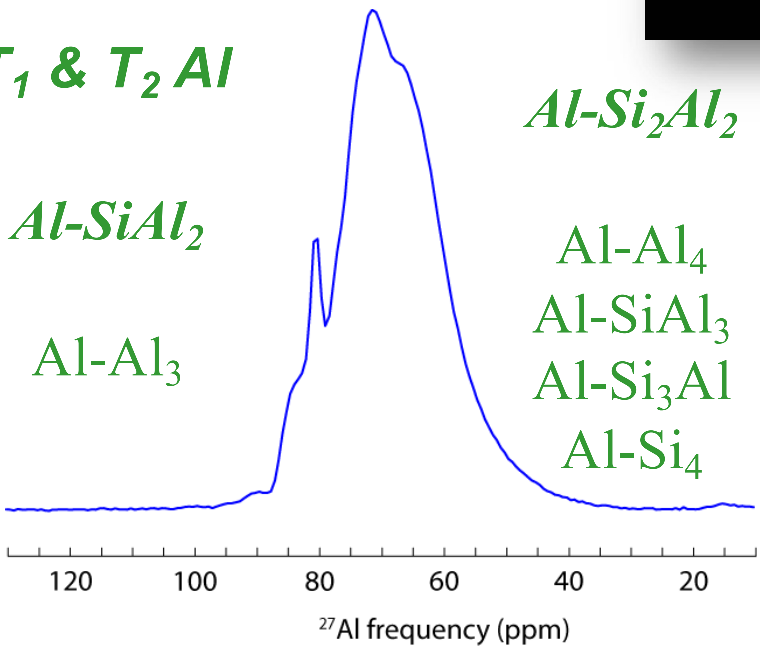

^{29}Si MAS

T_2 Si

Si-Al_3

Si-$SiAl_2$

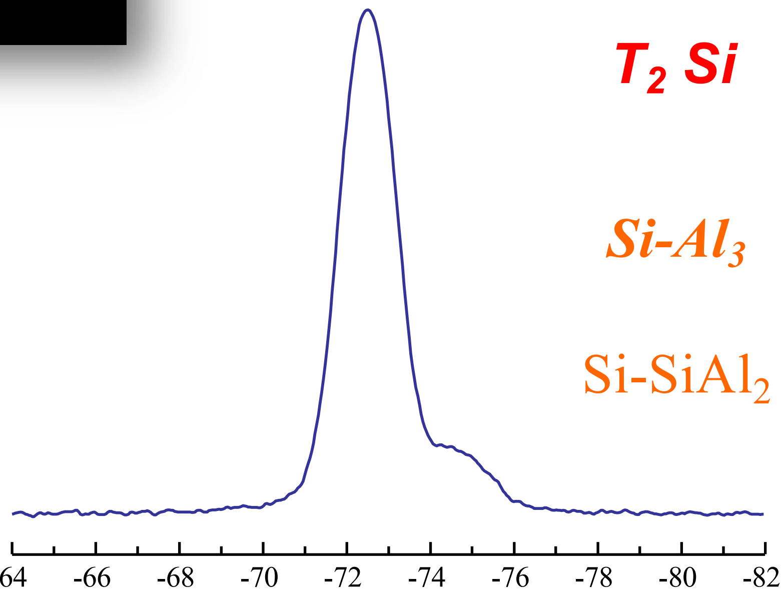

P.Florian, E.Veron, T.F.G.Green, J.R.Yates, D.Massiot Chem. Mater. 24 4068–4079 **2012**

Local Order in Gehlenite from ^{29}Si

Gehlenite
$Ca_2Al_2SiO_7$
T_f = 1590°C

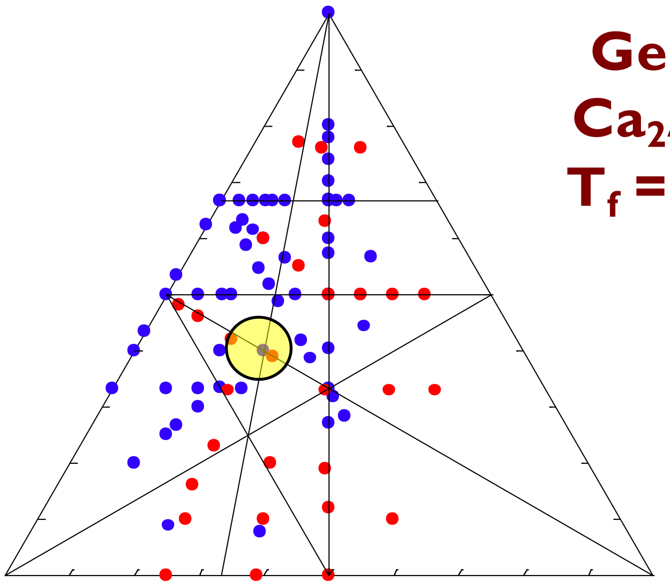

T1
100% Al

T2
Si 50% /Al 50%

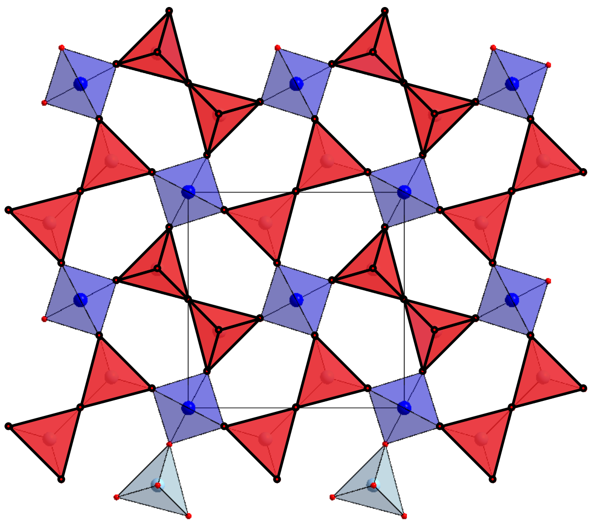

p(AlOAl) = p(SiOSi) = 0.11

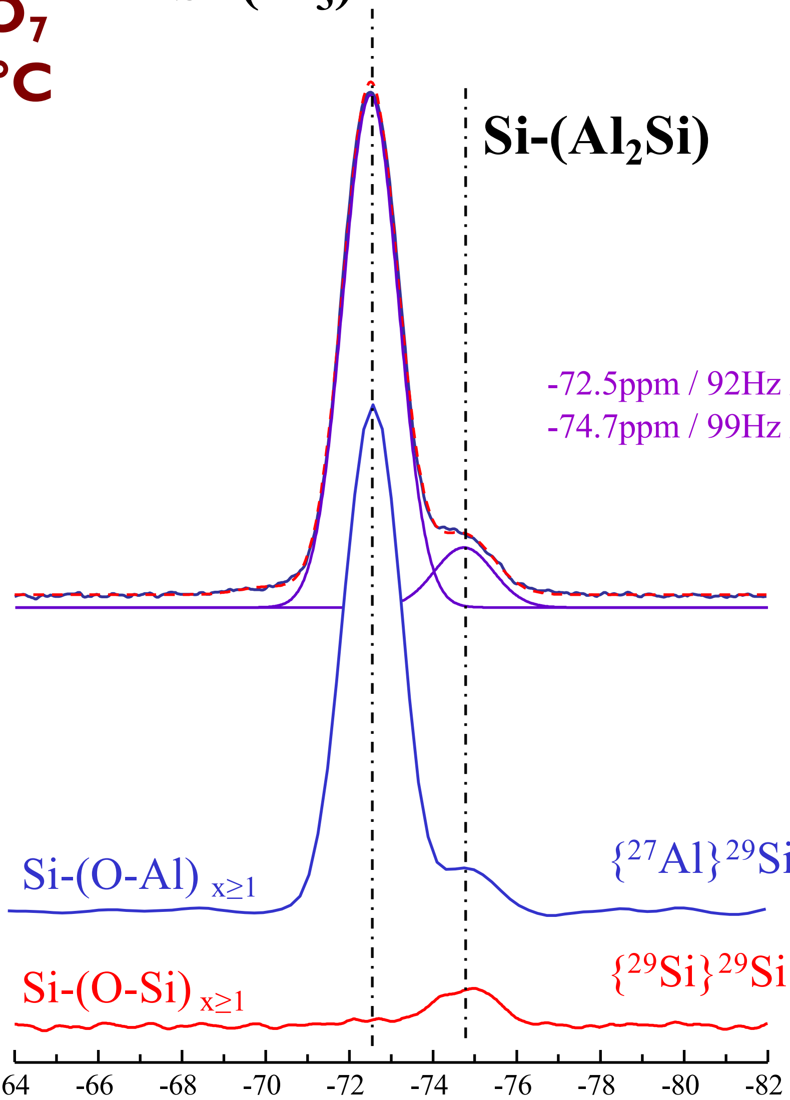

Si-$SiAl_2$
Si-Al_3

Si-$SiAl_2$

P.Florian, E.Veron, T.F.G.Green, J.R.Yates, D.Massiot Chem. Mater. 24 4068–4079 **2012**

Al spectra: how to decipher?

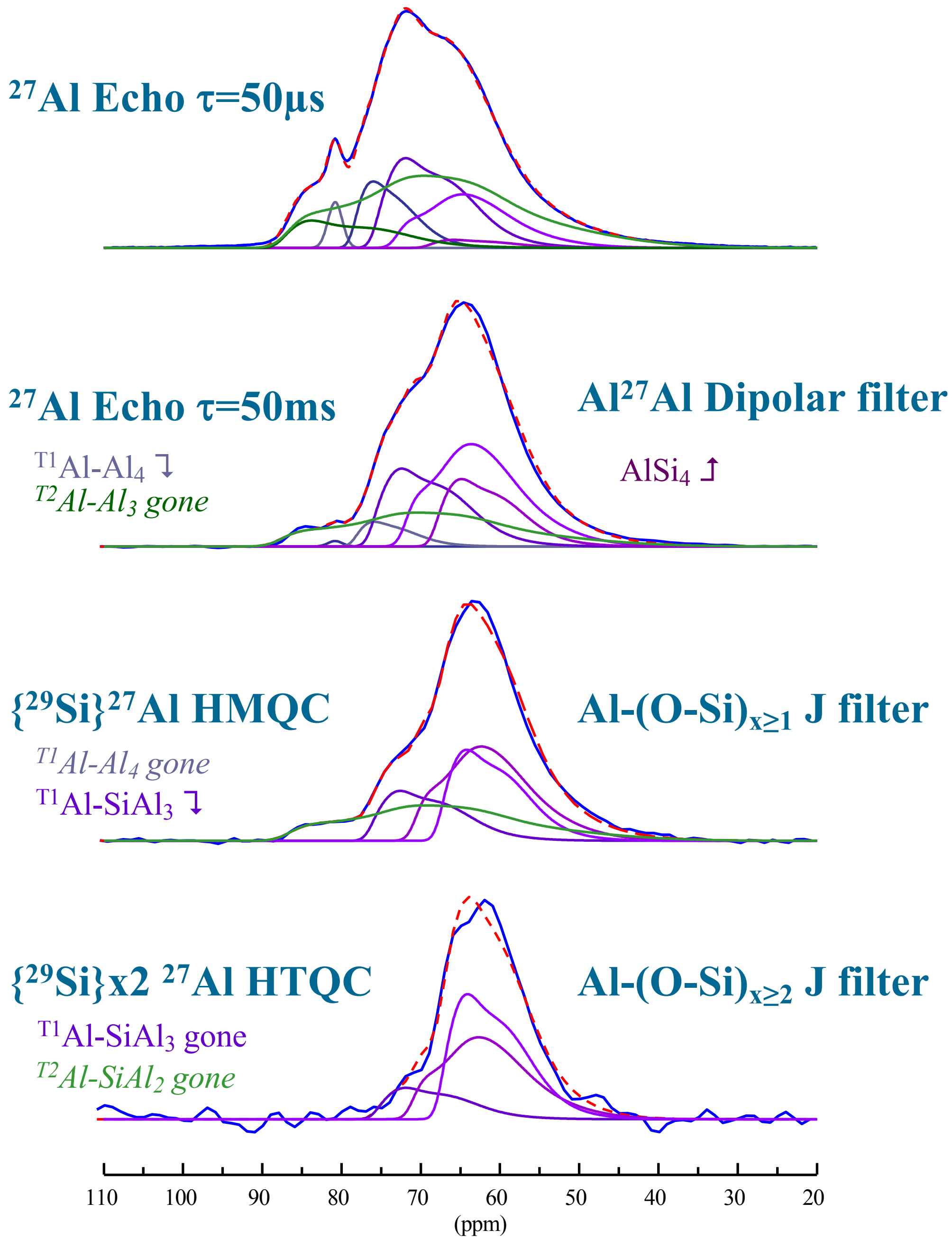

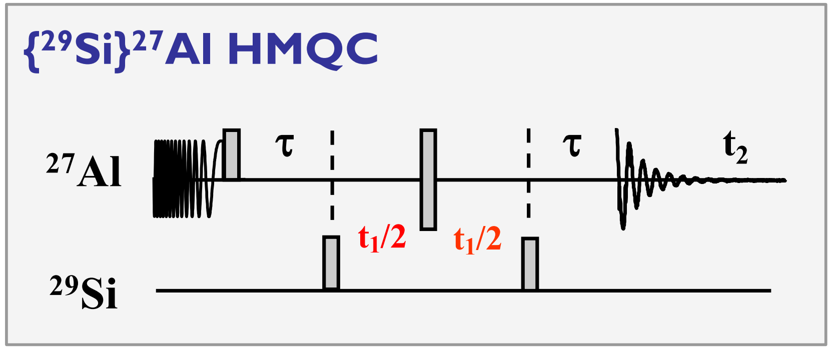

{^{29}Si}^{27}Al *J-coupling*
→ Bond angles from DFT

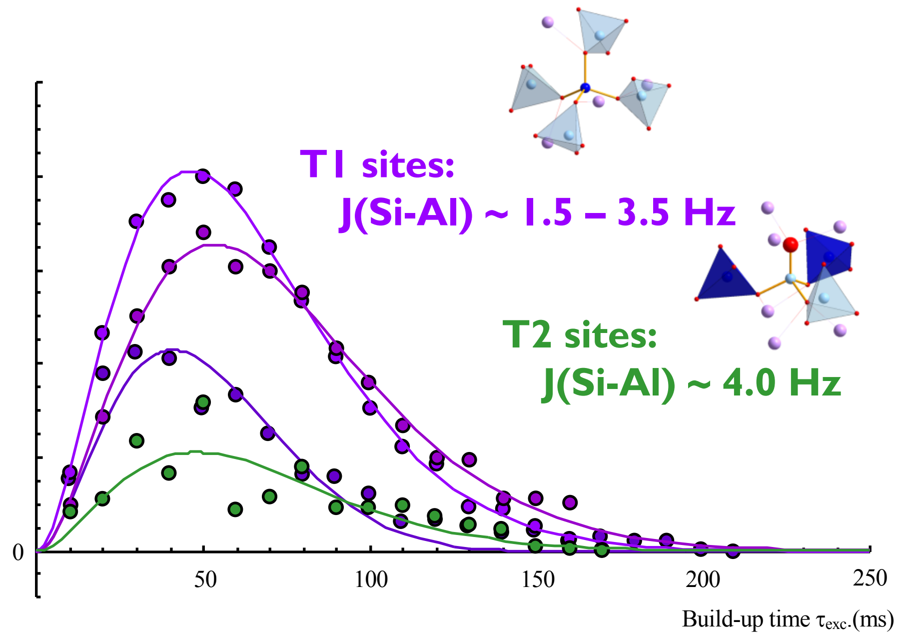

P.Florian, E.Veron, T.F.G.Green, J.R.Yates, D.Massiot Chem. Mater. 24 4068–4079 **2012**

The ^{27}Al point of view

		%	δ_{iso}(ppm)	$\Delta\delta_{iso}$	C_Q(MHz)	ΔC_Q	η_Q	T_2 (ms)
#1 - T1a	$AlAl_4$	3	82.5	n/a	1.75	n/a	n/a	9 (±1)
#2 - T1b	$AlAl_3Si_1$	11	79.2	*1.50*	5.82	*2.00*	*0.3*	21 (±1)
#3 - T1c	$AlAl_2Si_2$	24	76.7	*1.50*	7.27	*2.00*	*0.3*	28 (±1)
#4 - T1d	$AlAl_2Si_3$	16	73.4	*1.50*	7.59	*2.00*	*0.6*	47 (±2)
#5 - T1e	$AlSi_4$	3	70.2	*1.50*	6.89	*2.00*	*0.3*	86 (±12)
#6 - T2a	$AlAl_3$	7	89.4	1.48	8.31	2.20	0.24	12 (±2)
#7 - T2b	$AlAl_2Al_1$	36	87.7	1.49	10.7	1.84	0.61	38 (±2)

3 ppm shift per Si/Al substitution in T1 sites

^{27}Al quantitative MAS at 17.6T

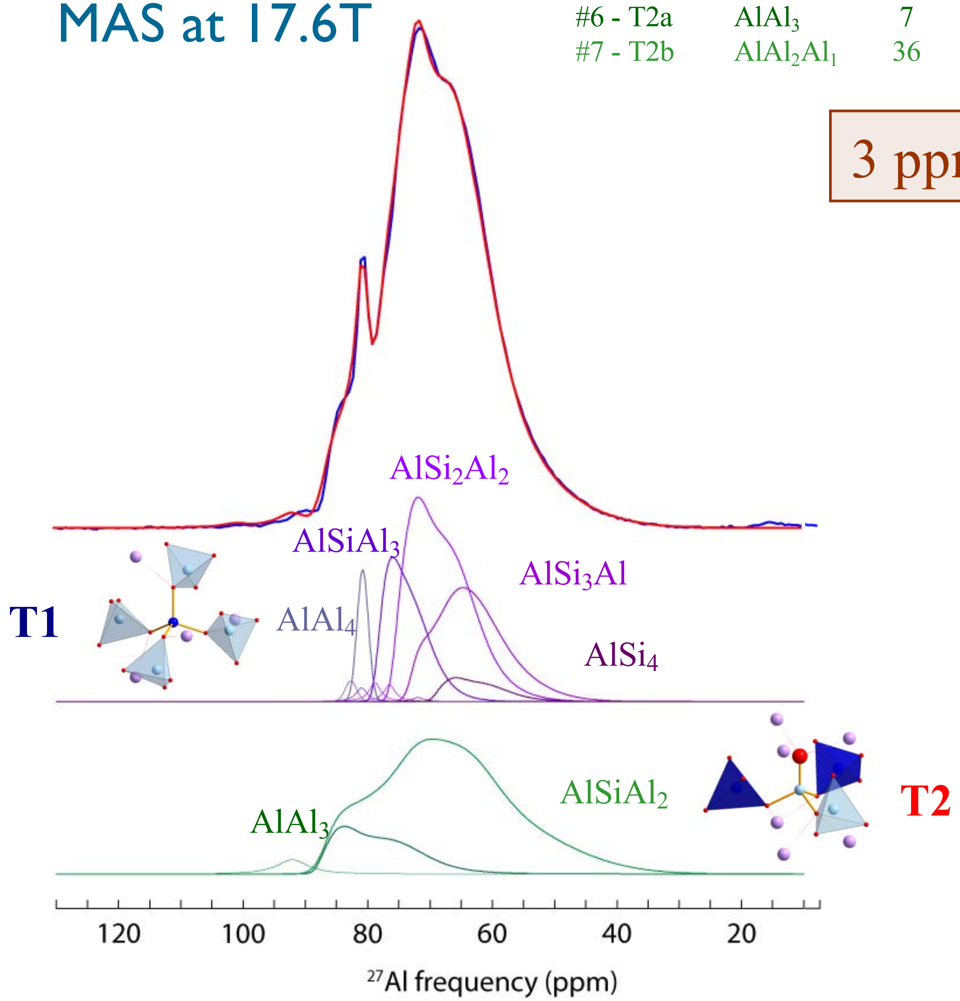

^{27}Al MQMAS @17T

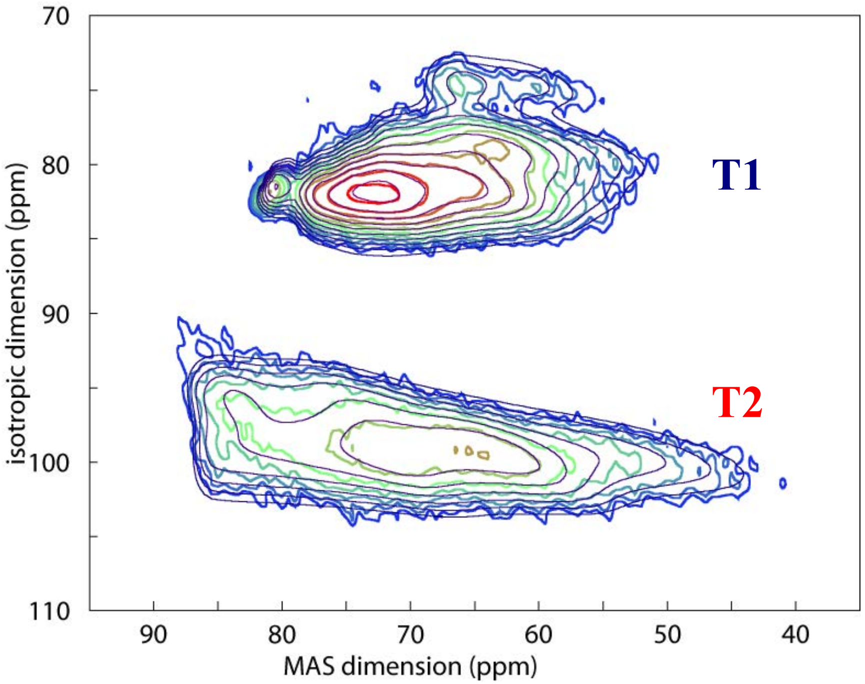

CHEMISTRY OF MATERIALS
P.Florian, E.Veron, T.F.G.Green, J.R.Yates, D.Massiot Chem. Mater. 24 4068–4079 **2012**

$CaO-Al_2O_3-SiO_2$ – the ^{17}O viewpoint

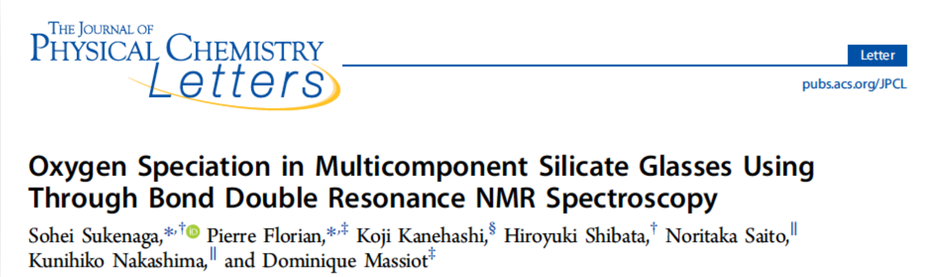
THE JOURNAL OF PHYSICAL CHEMISTRY Letters

Letter

pubs.acs.org/JPCL

Oxygen Speciation in Multicomponent Silicate Glasses Using Through Bond Double Resonance NMR Spectroscopy

Sohei Sukenaga,*,† Pierre Florian,*,‡ Koji Kanehashi,§ Hiroyuki Shibata,† Noritaka Saito,‖ Kunihiko Nakashima,‖ and Dominique Massiot‡

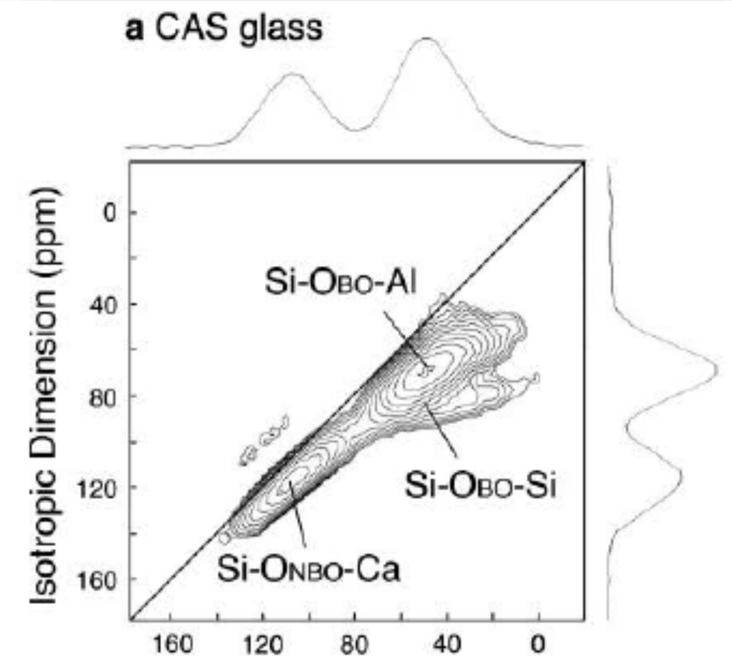

Lee et al., Geochim. Cosmochim. Acta ***70*** *4275-4286 (2006)*

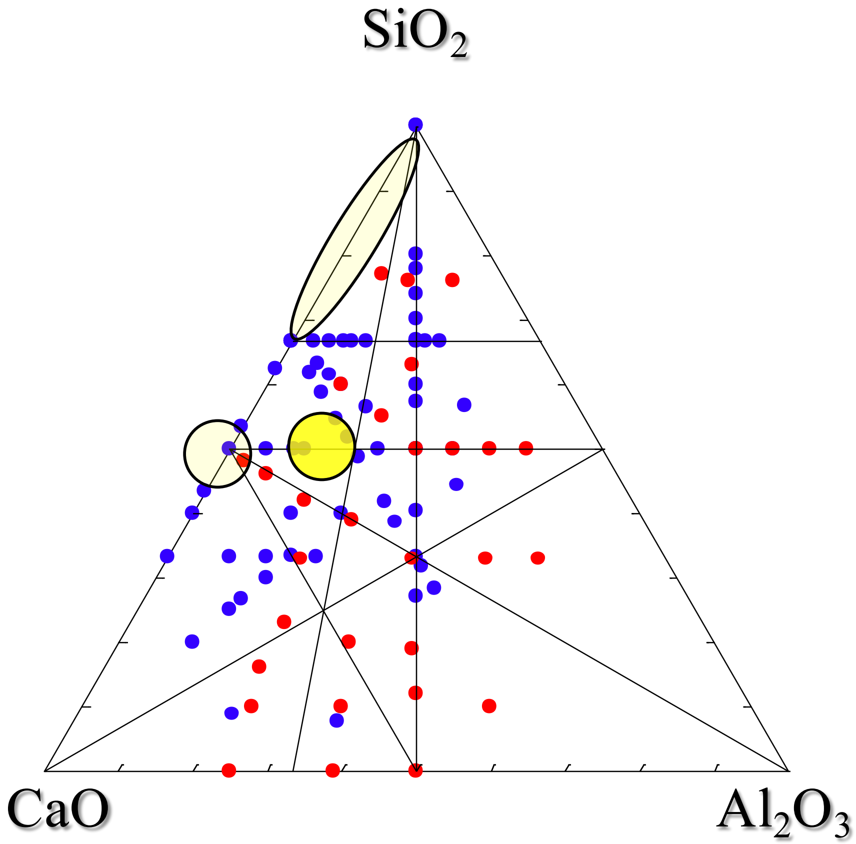

S.Sukenaga, P.Florian, K.Kanehashi, H.Shibata, N.Saito, K.Nakashima, D.Massiot – J.Phys.Chem. Lett. 8, 2274, **2017**

$CaO-Al_2O_3-SiO_2$ – the ^{17}O viewpoint

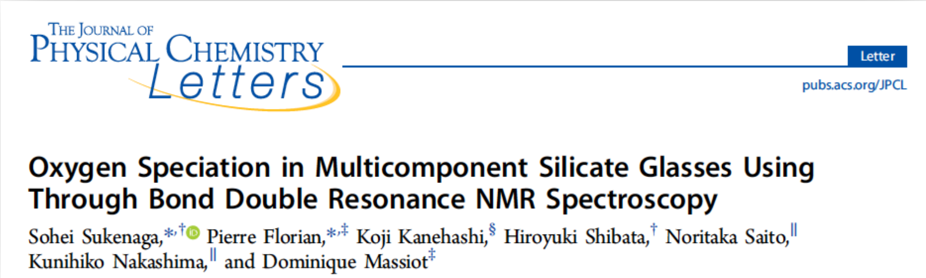
The Journal of Physical Chemistry Letters

Letter

pubs.acs.org/JPCL

Oxygen Speciation in Multicomponent Silicate Glasses Using Through Bond Double Resonance NMR Spectroscopy

Sohei Sukenaga,*,† Pierre Florian,*,‡ Koji Kanehashi,§ Hiroyuki Shibata,† Noritaka Saito,∥ Kunihiko Nakashima,∥ and Dominique Massiot‡

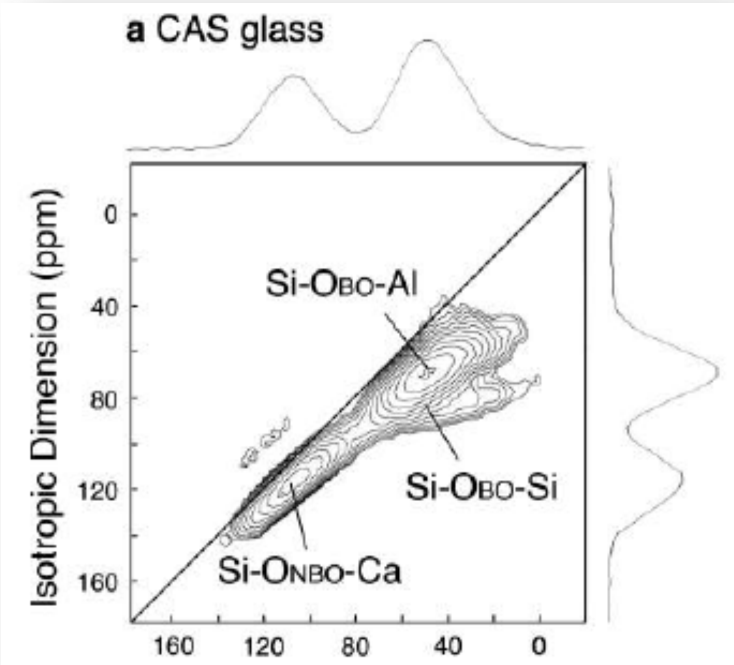

Lee et al., Geochim. Cosmochim. Acta **70** *4275-4286 (2006)*

36.5 CaO – 51 SiO_2 – 12.5 Al_2O_3

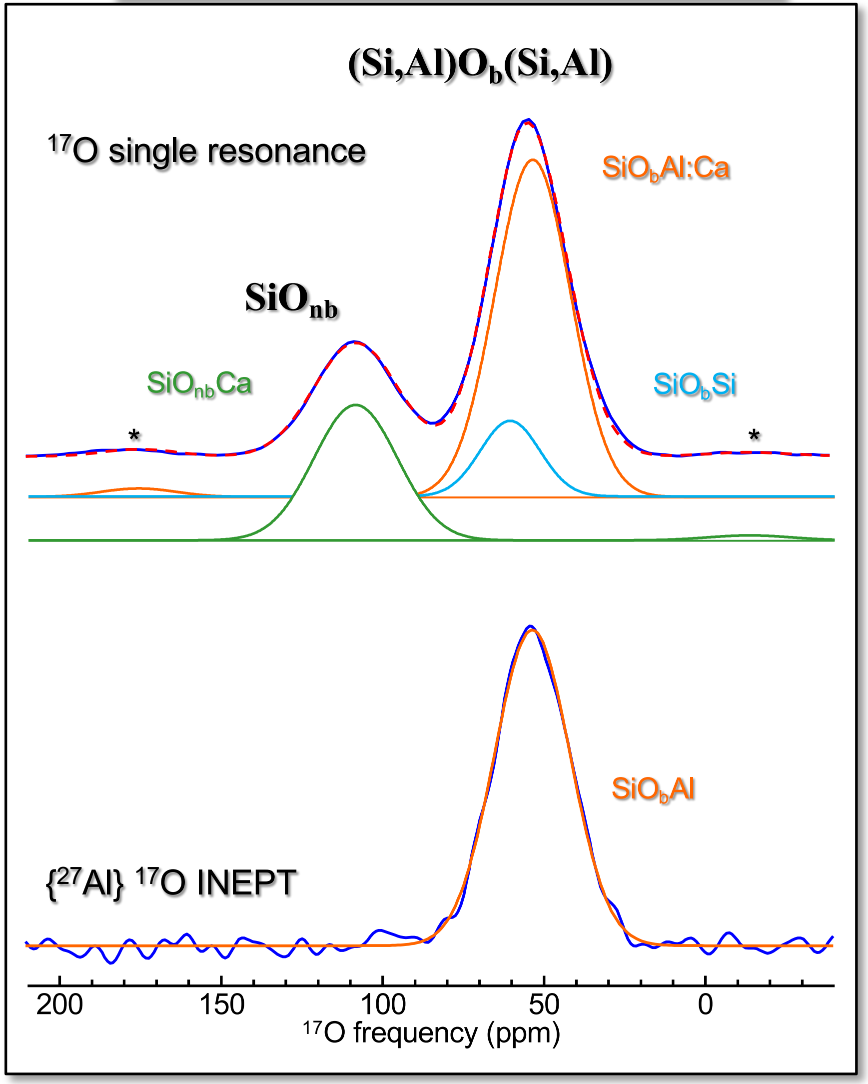

S.Sukenaga, P.Florian, K.Kanehashi, H.Shibata, N.Saito, K.Nakashima, D.Massiot – J.Phys.Chem. Lett. 8, 2274, **2017**

$CaO-Al_2O_3-SiO_2 + Na_2O$ – the ^{17}O viewpoint

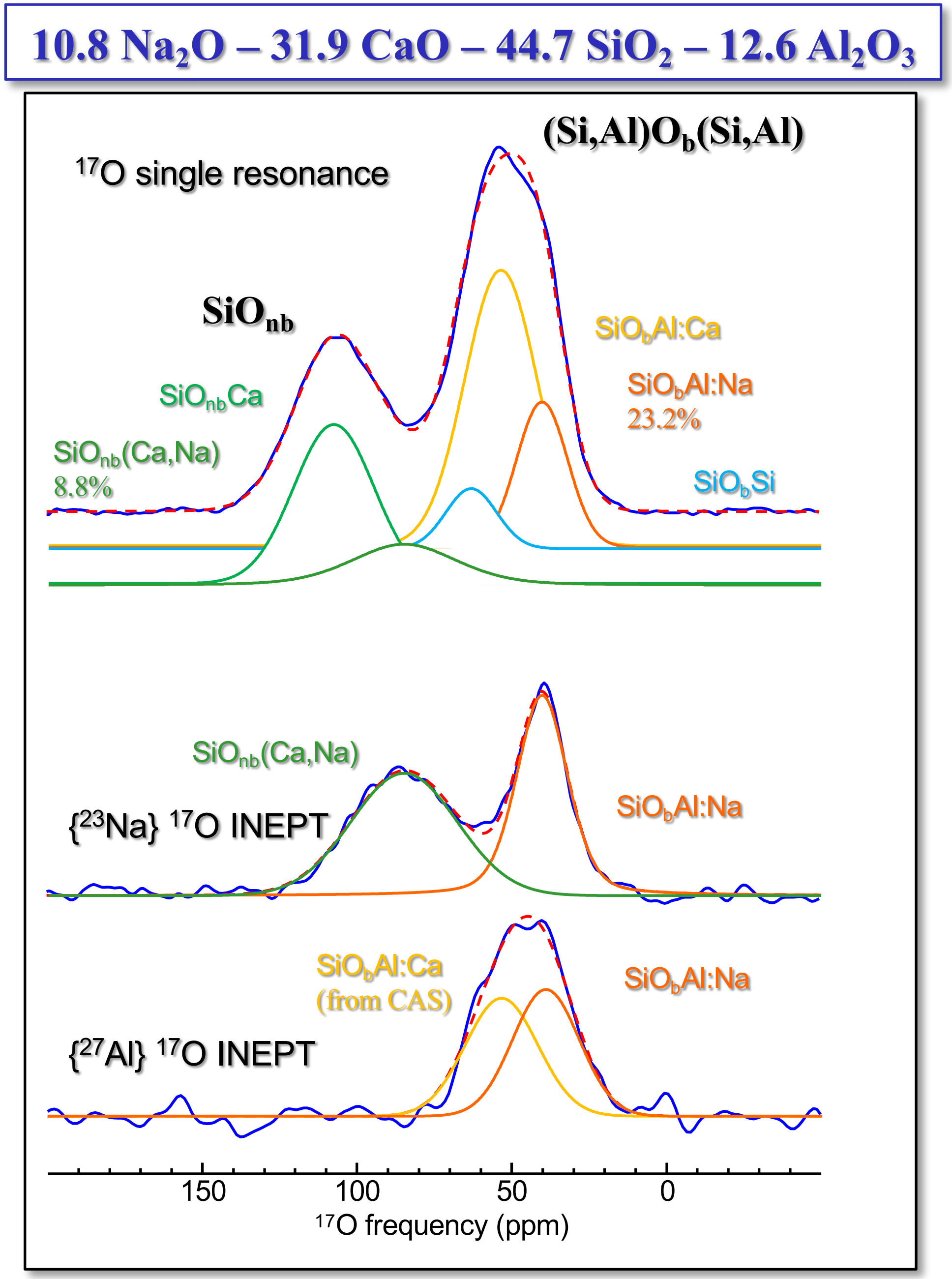

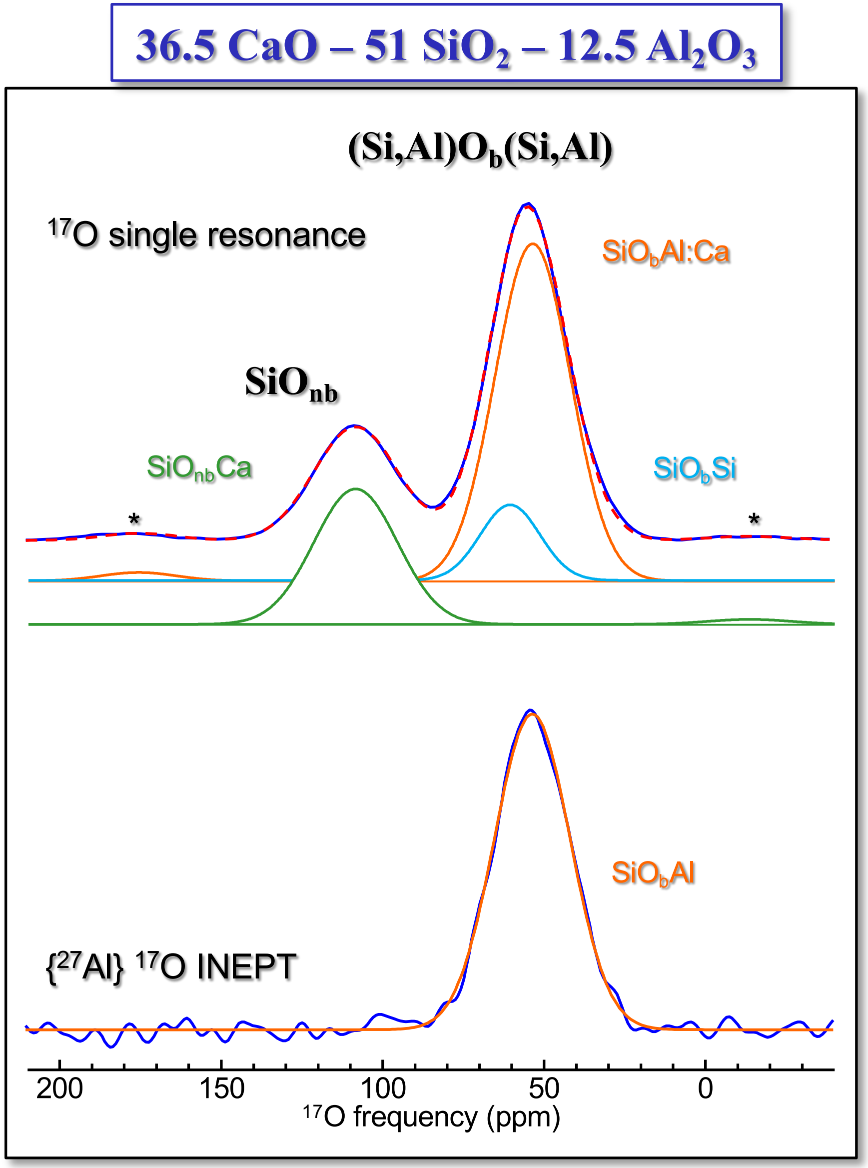

S.Sukenaga, P.Florian, K.Kanehashi, H.Shibata, N.Saito, K.Nakashima, D.Massiot – J.Phys.Chem. Lett. 8, 2274, **2017**

Separation, Simplification… and gains

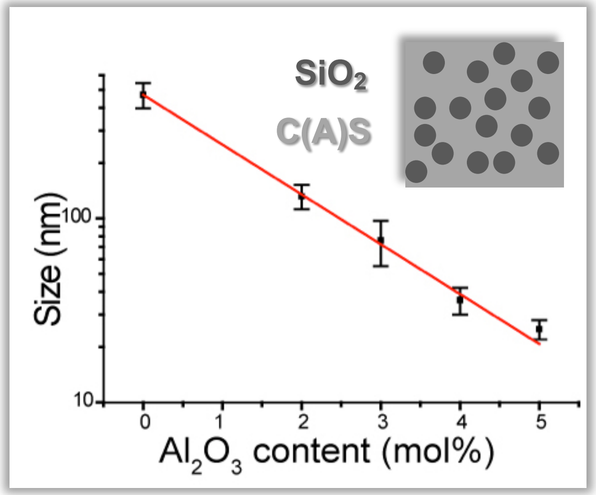

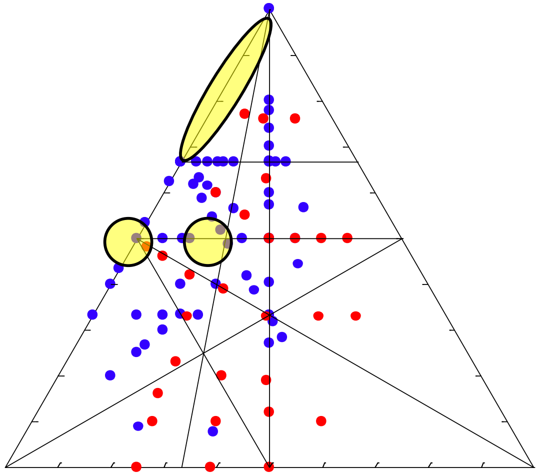

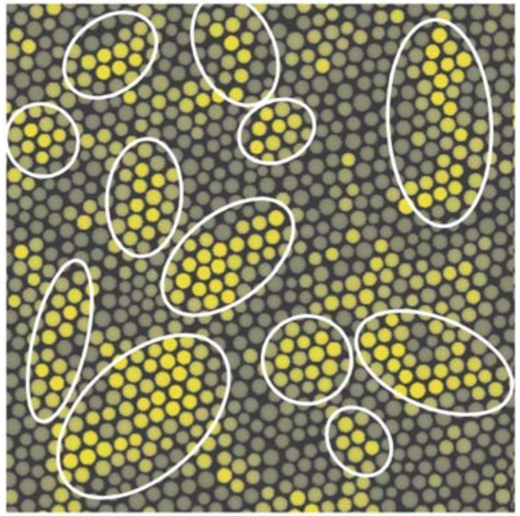

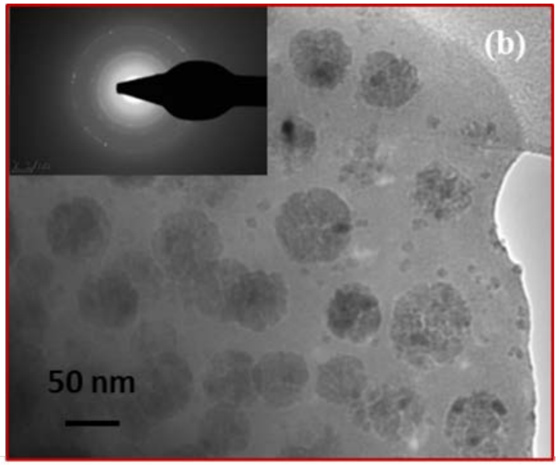

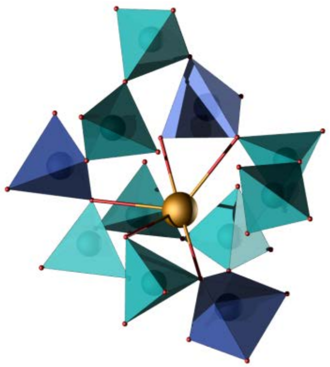

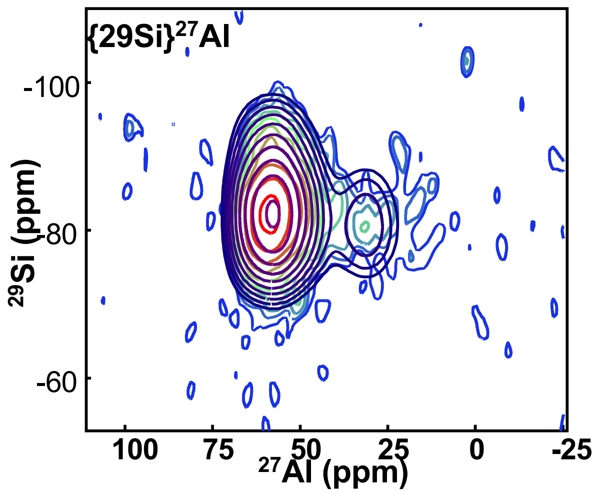

Phase separation

Network Topology

Local structures

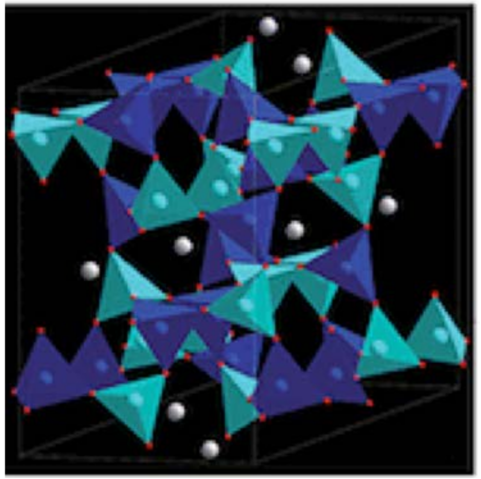

ACCOUNTS
of chemical research

Topological, Geometric, and Chemical Order in Materials: Insights from Solid-State NMR

DOMINIQUE MASSIOT,* ROBERT J. MESSINGER,
SYLVIAN CADARS, MICHAËL DESCHAMPS,
VALERIE MONTOUILLOUT, NADIA PELLERIN,
EMMANUEL VERON, MATHIEU ALLIX, PIERRE FLORIAN, AND
FRANCK FAYON

Accounts Chem. Res. **46** 1975–1984 (2013)

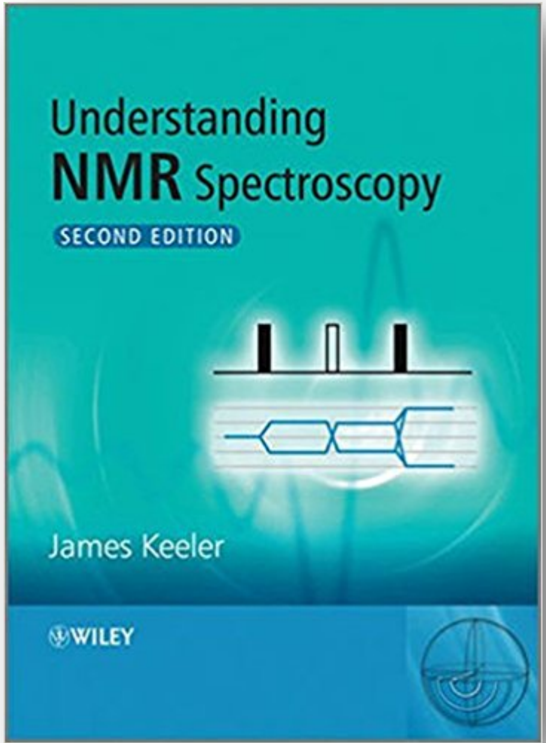

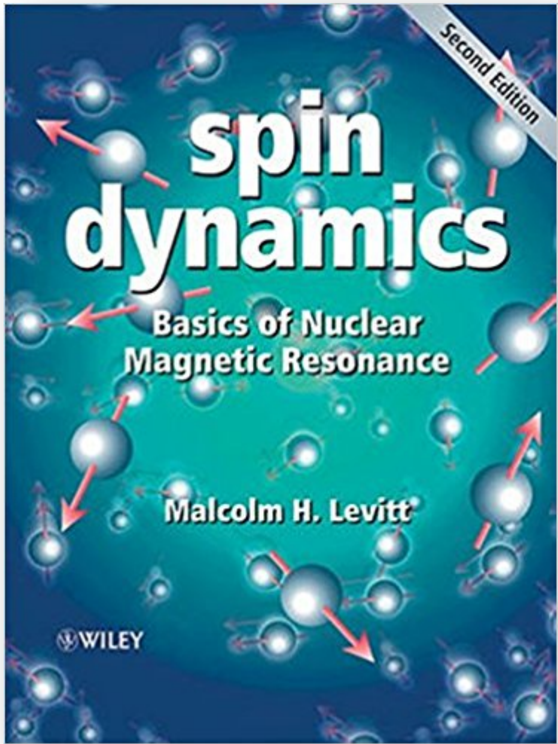

James Keeler – University of Cambridge
http://www-keeler.ch.cam.ac.uk/lectures/

Malcom Levitt – University of Southampton
http://www.spindynamica.soton.ac.uk/author/mhl/

Dmfit

~8700 reg. users

~2500 citations

Google

dmfit nmr

http://www.tgir-rmn.org/

Acknowledgements

Orléans
C.Bessada
F. Fayon
M. Allix
P. Florian
M. Deschamps
V. Montouillout
N. Pellerin
E. Véron
S. Cadars
V. Sarou-Kanian
J. Hiet
S. Chenu
L. Martel
S. Alahraché
M. Yon
R. Shakhovoy
A. Novikov
Ch. Martineau

France
F. Babonneau
C. Sanchez
Ch. Bonhomme…
D. Neuville
Ch. Le Losq
L. Cormier
B. Alonso
F. Taulelle
B. Bujoli
B. Bureau
T. Charpentier

Germany U. Scheler

Japan
S. Sukenaga
K. Kanehashi
N. Saito
K. Nakashima

UK
R.K. Harris
J.R. Yates
N. Greaves
M. Smith
R. Dupree
I. Farnan

Denmark T. Vosegaard

USA
P.J. Grandinetti
Z. Gan
B.F. Chmelka
R.J. Messinger

Australia T. Bastow

Spain M. Alba J Sanz

THC IRMN
Lyon
Grenoble
Lille
Orléans
Bordeaux
Paris
Gif sur Yvette

Dmfit
~8700 reg. users
~2500 citations

Bruker : D. Muller, H. Forster, S. Steurnagel, M. Ziliox, S. Wegner *et al.*